

Washington University in St. Louis
Washington University Open Scholarship

All Theses and Dissertations (ETDs)

Summer 9-1-2014

Dual Roles of Interferon Stimulated Gene-15 During Respiratory Virus Infection

David James Morales

Washington University in St. Louis

Follow this and additional works at: <https://openscholarship.wustl.edu/etd>

Recommended Citation

Morales, David James, "Dual Roles of Interferon Stimulated Gene-15 During Respiratory Virus Infection" (2014). *All Theses and Dissertations (ETDs)*. 1326.

<https://openscholarship.wustl.edu/etd/1326>

This Dissertation is brought to you for free and open access by Washington University Open Scholarship. It has been accepted for inclusion in All Theses and Dissertations (ETDs) by an authorized administrator of Washington University Open Scholarship. For more information, please contact digital@wumail.wustl.edu.

WASHINGTON UNIVERSITY IN ST. LOUIS
Division of Biology and Biomedical Sciences
Molecular Microbiology and Microbial Pathogenesis

Dissertation Examination Committee:
Deborah Lenschow, Chair
John Atkinson
Jacco Boon
Marco Colonna
Anthony French
Michael Holtzman
Thaddeus Stappenbeck

Dual Roles of Interferon Stimulated Gene-15 During Respiratory Virus Infection

by

David James Morales

A dissertation presented to the
Graduate School of Arts and Sciences
of Washington University in
partial fulfillment of the
requirements for the degree
of Doctor of Philosophy

August 2014

St. Louis, Missouri

TABLE OF CONTENTS

	<u>Page</u>
List of Figures	iii
Acknowledgements	v
Chapter 1: Introduction	1
References	27
Chapter 2: The Effects of Increased ISG15 Conjugation on Influenza B Virus Replication	33
References	63
Chapter 3: A Novel Mode of ISG15 Mediated Protection From Influenza A Virus and Sendai Virus in Mice.	65
References	99
Chapter 4: Conclusions and Future Directions	104
References	127

LIST OF FIGURES

<u>Chapter 1</u>		<u>Page</u>
Figure 1.1	A comparison between the ubiquitin and ISG15 conjugation pathways.	25
<u>Chapter 2</u>		
Figure 2.1	ISG15 restricts influenza B virus replication in mTEC	52
Figure 2.2	ISG15 heterozygous mice exhibit intermediate disease relative to WT and ISG15 ^{-/-} mice after influenza B virus infection	54
Figure 2.3	UBP43 ^{C61A/C61A} mice are viable, retain UBP43 inhibition of interferon signaling	55
Figure 2.4	UBP43c61a mutation increases protection from influenza B virus infection <i>in vivo</i> in an ISG15 dependent manner	57
Figure 2.5	UBP43c61a mutation increases the pool of ISG15 conjugates but also increases ISG protein levels in an ISG15 dependent manner	58
Figure 2.6	UBP43c61a mutation causes an elevation in ISG transcript levels in an ISG15 dependent manner	60
Figure 2.7	Increased protection against influenza B virus in UBP43c61a mTEC is dependent on ISG15	62
<u>Chapter 3</u>		
Figure 3.1	ISG15 protection against influenza A virus is conjugation dependent, but not anti-viral	90
Figure 3.2	ISG15 protects against Sendai virus induced lethality by a conjugation dependent mechanism, but has no major effect on virus loads	91
Figure 3.3	Influenza A and Sendai virus replication is not altered in primary trachea epithelial cultures lacking ISG15 or ISG15 conjugates	92
Figure 3.4	ISG15 does not affect cytokine production after influenza A virus or Sendai virus infection	94

		<u>Page</u>
Figure 3.5	Similar numbers and cell populations are recruited to the lungs during Sendai virus infection in the presence and absence of ISG15 conjugation	96
Figure 3.6	Infection with Sendai virus at a lower dose reveals increased weight loss and distal airway damage in ISG15 ^{-/-} mice	97
 <u>Chapter 4</u>		
Figure 4.1	Influenza virus proteins co-immunoprecipitate with ISG15 during infection in mTEC	119
Figure 4.2	Influenza virus nucleoprotein interacts with ISG15 in a conjugation dependent manner	121
Figure 4.3	ISG15 conjugation promotes cell survival in mTEC after Sendai virus infection	123
Figure 4.4	ISG15 ^{-/-} mice infected with sub-lethal dose of Sendai viruses exhibit no difference in weight loss compared to WT mice	125
Figure 4.5	ISG15 ^{-/-} mice exhibit ruffled fur after Sendai virus infection	126

ACKNOWLEDGMENTS

This thesis would not have been possible without the help and support of many people. First and foremost I would like to thank Debbie for taking me in under her mentorship and allowing me to pursue my Ph.D. research in her lab. She has allowed me the intellectual freedom to shape my thesis while always keeping me reined in and on track. Her door has always been open, and I am forever grateful for her mentorship. I am also indebted to the members of my thesis committee for their guidance over the years. Each has been exceedingly generous in sharing their time, expertise, and reagents, all of which have been essential to helping move my projects forward.

I also owe a debt of gratitude to the Lenschow lab members of past and present who have made lab enjoyable and whose advice and suggestions have been invaluable. In particular, this work would not have been possible without Kristen Monte who contributed greatly to this thesis both by maintaining the Lenschow lab mouse colony and by providing technical expertise with mouse experiments.

My work has also been assisted greatly by many collaborators that we have had outside of Washington University. In particular, I would like to thank Dr. Klaus-Peter Knobeloch (University of Freiburg) for providing us with the UBP43^{C61A/C61A} mouse, without which Chapter 2 would not have been possible.

Lastly, this work was made possible by generous tax-payer funding. These projects were partially funded by the NIH Cell and Molecular Biology training grant GM007067.

CHAPTER 1

Introduction

A large portion of this chapter was previously published in the following form:

Morales DJ, and D.J. Lenschow. 2013. The antiviral activities of ISG15. *Journal of molecular biology* **425:4995-5008**.

ISG15 Discovery

The study of ubiquitin conjugation has played a key role in furthering our understanding of the mechanisms by which proteins and biological pathways can be regulated at a post-translational level. Ubiquitin is an 8.5-kD protein originally named for the nearly universal cross-immunoreactivity between the ubiquitin homologs throughout eukaryotic species. Ubiquitin covalently conjugates to target proteins forming an isopeptide bond between its C-terminal glycine and the amine groups of lysine residues in target proteins. Ubiquitination occurs through an ATP dependent enzymatic pathway consisting of an E1 activating enzyme, an E2 conjugating enzyme, and an E3 ligase¹. One of the first functions ascribed to ubiquitin conjugation was the targeting of ubiquitinated proteins for proteasomal degradation². However ubiquitin has since been shown to affect many cellular processes independent of proteasomal degradation, including the regulation of vesicular trafficking, signaling pathways, and DNA damage repair³.

Following the discovery of ubiquitin, numerous other proteins were identified that also covalently conjugate to target proteins through an enzymatic pathway similar to that of ubiquitin conjugation⁴. These ubiquitin-like modifiers share limited sequence homology to ubiquitin but contain one or more domains that adopt a beta-grasp structure similar to that of ubiquitin. The first ubiquitin-like protein to be discovered was interferon stimulated gene 15 (ISG15). ISG15 was discovered independently by two different laboratories. Korant *et al.* identified ISG15 during a study characterizing proteins induced by type I interferons (IFN)⁵. Protein lysates from Daudi cells stimulated with IFN were analyzed by 2-D gel electrophoresis at different times after stimulation. ISG15 was found to be rapidly and robustly induced after IFN stimulation. ISG15

was also identified by a group evaluating how the pool of ubiquitin conjugates is affected by viral infection⁶. This study revealed that infecting A549 cells with encephalomyocarditis virus induced a 15-kD protein which cross-reacted with an antibody raised against ubiquitin. Consequently, ISG15 was originally named *ubiquitin cross-reactive protein* by this group. Subsequent cloning and characterization of ISG15 revealed that it contained two ubiquitin-like domains, each with approximately 30% amino acid sequence homology to ubiquitin^{6; 7; 8}. The structural similarity of ubiquitin and the ubiquitin-like domains of ISG15 was later confirmed when the crystal structure of ISG15 was solved⁹. Given the known regulatory potential of ubiquitin-like modifiers and the importance of type I IFN during viral infection, there has been great interest in understanding how ISG15 might regulate the immune response and virus replication.

ISG15 Conjugation

ISG15 forms conjugates with a diverse pool of target proteins in a process referred to as ISGylation. ISGylation occurs through a series enzymatic reactions similar to the ubiquitin conjugation pathway (Figure 1.1). ISG15 is encoded and expressed as a 17-kD precursor protein that is immediately proteolytically processed at its C-terminus to expose a C-terminal LRLRGG amino acid sequence, identical to the C-terminal sequence of ubiquitin¹⁰. The cognate ISG15 E1 activating enzyme, UBE1L, initiates the ISG15 conjugation enzymatic pathway by forming a thioester bond between the C-terminal glycine of ISG15 and a cysteine residue of UBE1L^{11; 12}. UBE1L is the only known E1 enzyme for ISG15, and it appears to be specific for ISG15 as it has not formed thioester bonds with other tested ubiquitin-like modifiers^{11; 13}. Confirmation of the

importance of Ube1L in this pathway has come from the analysis of mice deficient in Ube1L. These mice express unconjugated ISG15 but do not form ISG15 conjugates¹⁴. Once primed by Ube1L, ISG15 is then transferred to a cysteine residue of an E2 conjugating enzyme. siRNA knockdown of UbcH8 in human cells, and UbcM8 in mouse cells, results in nearly complete loss of ISG15 conjugate formation, suggesting that UbcH8 and UbcM8 serve as the predominant E2 enzymes in the ISG15 conjugation system^{15; 16}. Additional experiments evaluating whether other proteins may serve as ISG15 E2 enzymes have found the transfer of ISG15 to UbcH5 and to UbcH7, the closest homologs of UbcH8, to be highly unfavorable^{12; 17}. Finally, an E3 ligase facilitates the conjugation of ISG15 to target proteins. HERC5, HHARI, and Efp (TRIM25) have all been demonstrated capable of acting as E3 ligases for ISG15^{18; 19; 20; 21}. However, while HHARI and Efp have been shown to act as E3 ligases for specific target proteins, siRNA knockdown of the HECT E3 ligase HERC5 was shown to abrogate nearly all ISG15 conjugate formation, suggesting that it is the predominant E3 ligase for ISG15. Knockdown studies in mouse cells have similarly demonstrated that HERC6 is the predominant ISG15 E3 ligase in mice^{22; 23; 24}.

In an elegant study of ISG15 conjugation specificity, it was shown that almost any protein inserted into an expression vector can be ISGylated in a manner that appears to require little sequence specificity²⁵. Truncation of target proteins leads to alteration in the ISGylation profile of the protein, further suggesting that the specificity of ISG15 conjugation is not strictly determined by the local amino acid sequence environment of its lysine residues. This study showed that ISGylation targets newly translated proteins, and this appears to be mediated in part by the interaction of HERC5 with polysomes. Thus the specificity of ISG15 is in part derived

from the temporal expression of target proteins. How, or if, ISG15 might discriminate between proteins within the pool of actively translated proteins is unclear.

Enzymes capable of deconjugating ISG15 have also been identified. UBP43, also known as USP18, has been shown to deconjugate ISG15 from ISGylated target proteins²⁶. The biological function of UBP43 and the effect of increasing ISG15 conjugation were initially evaluated both *in vitro* and in UBP43 deficient mice^{26; 27; 28}. However, the interpretations of these studies have been complicated by the fact that UBP43 has been found to bind to the interferon α/β receptor (IFNAR) 2 and inhibit IFN signaling independent of its deconjugating activity^{29; 30}. USP2, USP5, USP13, USP14 have also been shown to cleave peptide fused to the C-terminus of ISG15, however, further studies are needed to determine whether they can deconjugate ISG15 from ISGylated proteins and to understand what biological roles they may play in the regulation of ISGylation³¹. Characterization of these ISG15 deconjugases could advance our understanding of ISGylation, as deubiquitinating enzymes have been found to play an important role in ubiquitin mediated regulation³².

Proteomic studies have identified hundreds of proteins that are either ISGylated or interact with ISG15 after IFN stimulation^{33; 34}. These potential target proteins are involved in all aspects of cellular biology. The functional consequence of ISGylation is still not well understood. Proteasome inhibition has been reported to increase the pool of ISG15 conjugates but does so by means of *de novo* conjugate formation, not inhibition of conjugate degradation³⁵. In fact, there is no evidence that ISGylation results in the proteasome mediated degradation of target proteins. One of the challenges of studying ISG15 has been that for every target protein studied, only a small fraction of the total pool of target protein is actually modified by ISG15. This phenomenon is also observed with the small ubiquitin-like modifier (SUMO). SUMO

modification is thought to be highly dynamic, but transient modification of transcription factors can lead to long lasting downstream consequences through chromatin remodeling or recruitment of inhibitory complexes³⁶. Whether a similar dynamic effect might mediate the functionality of ISGylation has yet to be determined.

Though the biochemical conjugation of ISG15 parallels that of ubiquitination, there are several notable differences between the conjugation systems (Figure 1.1). Firstly, like ISG15 itself, the predominant ISG15 conjugation and deconjugation enzymes, Ube1L, UbcH8/UbcM8, HERC5/HERC6, and UBP43/USP18 are all induced by type I IFN stimulation. Secondly, the ubiquitin conjugation system is constituted by many E2 and E3 proteins¹. It is the binding specificity of E2 to E3 and E3 to target proteins that allows for ubiquitin to affect such a vast number of biological processes with such specificity. In contrast, it seems that formation of the overwhelming majority of ISG15 conjugates occurs through one E2 enzyme and one E3 enzyme. Finally, there is no evidence that ISG15 conjugates to itself and forms ISG15 chains in the manner of poly-ubiquitin modification. While not fully understood, these differences between the ISG15 and ubiquitin pathways most likely reflect the specific function of ISG15 conjugation.

ISG15 has been implicated in regulating numerous biochemical pathways, and the generation and study of ISG15 deficient mice have revealed that it plays an important role during viral infection. Data collected to date has demonstrated that ISG15 can protect against a wide gamut of viruses, and the mechanisms by which it mediates this protection are varied. Here we will review the progress that has been made in the identification of viruses that are regulated by ISG15 and the mechanisms by which ISG15 mediates this protection.

Antiviral Activity of ISG15

The antiviral activity of ISG15 was first observed in a screen designed to identify antiviral interferon stimulated genes (ISG) important during Sindbis virus infection³⁷. Recombinant Sindbis viruses were engineered to express ISGs, and these ISGs were then evaluated for their ability to protect IFNAR^{-/-} mice from lethality after infection. Mice infected with a Sindbis virus expressing ISG15 but not a control virus were protected from virus induced lethality. This discovery was followed by numerous reports of ISG15 antiviral activity observed in tissue culture under conditions of ISG15 overexpression and siRNA knockdown. Influenza virus, vaccinia virus, vesicular stomatitis virus (VSV), Sendai virus (SeV), Japanese encephalitis virus (JEV), Newcastle disease virus (NDV), avian sarcoma leucosis virus (ASLV), human papilloma virus (HPV), human immunodeficiency virus 1 (HIV-1), Ebola virus-like particles (VLPs), dengue virus, and West Nile virus (WNV) have all been reported to be modestly inhibited by ISG15 *in vitro*. For several viruses contradictory results have been reported with regards to whether ISG15 antagonizes virus replication. These discrepancies are likely a result of different experimental conditions. In the case of influenza A virus it has been reported that inhibition of replication by ISG15 is species and/or cell type specific³⁸.

Importantly, the generation of ISG15 deficient mice has allowed for the verification of the antiviral activity of ISG15 *in vivo*³⁹. As predicted, ISG15^{-/-} mice infected with Sindbis virus were found to be more susceptible to lethality than WT mice⁴⁰. The increased lethality observed in the ISG15^{-/-} mice could be rescued when the mice were infected with a recombinant virus

expressing wild type (WT) ISG15, but not when infected with a recombinant virus expressing an ISG15(LRLRAA) mutant incapable of forming conjugates⁴⁰. This suggested that in this viral model the antiviral activity of ISG15 was dependent upon its ability to ISGylate proteins. A subsequent study confirmed the conjugation dependence of this protection by showing that Ube1L^{-/-} mice are also more susceptible than WT mice to Sindbis virus infection⁴¹.

Increased mortality was also observed in ISG15^{-/-} mice after infection with influenza A and influenza B viruses^{40; 42}. During influenza B virus infection, viral loads in WT mice remained very low over the course of infection and the mice experienced minimal weight loss or other clinical signs of illness. In contrast, ISG15^{-/-} mice experienced dramatic weight loss and viral loads reached levels up to 1000 fold higher than in WT mice at late time points. These observations were found to be true for both the mouse-adapted influenza B/Lee/40 strain, and a non-mouse-adapted influenza B/Yamagata/88 strain, indicating that ISG15 may contribute to the species tropism barrier for influenza B virus infection. Ube1L^{-/-} mice infected with influenza B virus similarly exhibited increased lethality and increased viral burden compared to WT mice, suggesting that ISG15 mediated protection from influenza B virus is also dependent on the ability of ISG15 to form conjugates⁴². Bone marrow chimera studies suggest that the expression of ISG15 in a radioresistant cell line is responsible for mediating this protection, however, it remains unclear as to how ISG15 conjugation is affecting influenza B virus replication⁴².

These initial studies established the precedent of ISG15 antiviral activity *in vivo*. Subsequent studies have identified additional viruses that ISG15 mediates protection against *in vivo*. Increased susceptibility has been seen with Chikungunya virus (CHIKV), herpes simplex virus-1 (HSV-1), gamma herpes virus 68 (γ HV68), and vaccinia virus infections. However, despite this diverse array of viruses that appear to be affected by ISG15, ISG15^{-/-} mice have not

displayed increased susceptibility to all viruses tested. No phenotype was observed following infection of ISG15^{-/-} mice with lymphocytic choriomeningitis virus (LCMV) or VSV³⁹. Our lab also has not observed increased susceptibility in ISG15^{-/-} mice after WNV infection (D. Lenschow, unpublished observations).

After the discovery of ISG15, much attention was invested in studying ISG15 conjugation. The initial discoveries of conjugation mediated protection against Sindbis virus and influenza B virus seemed to corroborate the importance of ISGylation. Recently, however, it has been reported that while ISG15^{-/-} mice are more susceptible to CHIKV infection, UbE1L^{-/-} mice display similar susceptibility to CHIKV as WT mice, suggesting a conjugation independent role for ISG15 during virus infection⁴³. This phenomenon has also been observed with Ross River virus infection (D. Lenschow, unpublished observations). *In vitro* and *in vivo* studies have shown that the antiviral activity of ISG15 targets viruses from diverse families ranging from retroviruses (HIV-1, ASLV), to large DNA viruses (vaccinia virus, HSV-1), to both positive and negative sense RNA viruses (Sindbis virus, Influenza A virus respectively)^{40; 44; 45; 46}. The mechanisms through which ISG15 mediates protection are likely to be just as diverse. Below we will cover what is currently known about the mechanisms through which ISG15 exerts its protective effects.

Mechanisms of ISG15 Activity

Inhibition of virus release:

Several studies have found that ISG15 can impact the viral life cycle at the stage of virus release. This has been seen with the retroviruses HIV-1 and ASLV, and also with Ebola virus.

Despite impacting the release of all of these viruses, detailed studies have identified different mechanisms through which ISG15 is acting. The first evidence of ISG15 inhibiting virus release was observed when characterizing the effect of ISG15 on HIV-1 replication. The replication of HIV-1 in 293T cells transfected with HIV-1 proviral DNA was found to be inhibited when cotransfected with a plasmid expressing ISG15⁴⁴. While ISG15 inhibited HIV-1 release into the supernatant, it did not affect HIV-1 protein production. Expression of ISG15 was shown to inhibit the ubiquitination of the HIV-1 Gag protein and the interaction between Gag and Tsg101. Both of these events are important for mediating HIV-1 budding and release⁴⁷. Interestingly, while cotransfection of UBE1L enhanced HIV-1 inhibition, the ectopic expression of ISG15 alone could inhibit the Gag-Tsg101 interaction, raising the possibility that the unconjugated form of ISG15 may be partly mediating this inhibition. A subsequent study has shown that HERC5 mediated ISG15 conjugation can inhibit HIV-1 budding from the plasma membrane⁴⁸. Unlike the initial HIV-1 study, this group found that the HIV-1 Gag protein is ISGylated by HERC5. It was also shown that overexpression of ISG15 without HERC5 resulted in an accumulation of Gag in cytoplasmic clusters, whereas co-expression of ISG15 with HERC5 resulted in an accumulation of Gag at the plasma membrane. These results suggest that unconjugated ISG15 and ISGylation may act to block HIV-1 budding by two distinct mechanisms.

ISG15 was also shown to inhibit Ebola VLP budding by a similar mechanism. Expression of the Ebola matrix protein, VP40, alone is sufficient to produce budding and release of VP40 VLPs⁴⁹. This release is regulated by the ubiquitin E3 ligase Nedd4 through a mechanism dependent on its ligase activity⁵⁰. Two studies demonstrated that the coexpression of ISG15 with VP40 can inhibit VP40 VLP release by inhibiting Nedd4 ligase activity, and thus inhibiting ubiquitination of VP40^{51; 52}. Like the HIV-1 studies, overexpression of ISG15 alone

was able to disrupt Ebola VLP release, suggesting that unconjugated ISG15 may be capable of inhibiting Nedd4 ligase activity⁵². Malakhova *et al.* was able to show that purified ISG15 protein was able to disrupt the ability of Nedd4 to bind to ubiquitin E2 conjugating enzymes, thus preventing ubiquitin from being transferred to the catalytic cysteine residue of Nedd4⁵¹. This study further showed that ISG15 could inhibit other Nedd4-like E3 ligases from augmenting VP40 VLP release. The ISG15 disruption of ubiquitin-mediated regulation during both Ebola virus and HIV-1 release raises an intriguing model for general ISG15 regulation through ubiquitin antagonism. It is possible that unconjugated ISG15 could compete with ubiquitin by binding to ubiquitin interacting domains in proteins or by forming thioester bonds with ubiquitin E2 or E3 enzymes. Additionally, ISG15 conjugation to Ubc13 on a lysine residue that is normally ubiquitinated has been reported to inhibit the E2 conjugating activity of Ubc13^{53; 54}. Thus competing for target lysine residues is yet another mechanism by which ISG15 can antagonize ubiquitin.

Studies of the retrovirus ASLV revealed yet another mechanism by which ISG15 can inhibit virus budding^{45; 55}. ASLV budding and release is dependent upon Gag binding to Nedd4⁴⁷. Despite the observed effects of ISG15 on Nedd4 in the Ebola studies, co-transfection of ISG15 with the ASLV Gag protein inhibited ASLV VLP release without disrupting the interaction between Gag and Nedd4. The disruption of Gag-Tsg101 interaction in the HIV-1 study suggested that ISG15 is disrupting an early stage in the endosomal sorting complexes required for transport (ESCRT) pathway. Chimeric HIV-1 or ASLV Gag proteins fused to downstream ESCRT proteins can bypass early stages of the ESCRT pathway to facilitate VLP release⁴⁷. However, in a study by Pincetic *et al.* it was found that ASLV Gag-ESCRT chimeras were still sensitive to ISG15 mediated inhibition⁴⁵. ISG15 was found to prevent VLP release by

inhibiting the recruitment of the AAA-ATPase Vps4 to the ESCRT pathway. This inhibition of Vps4 recruitment was dependent on charged multivesicular body protein (CHMP) 5 and correlated with ISGylation of CHMP5. However, other CHMP proteins were also found to be ISGylated in this study, and the mechanism by which ISG15 mediates this modulation of the ESCRT pathway was not conclusively shown.

It is not clear whether the ISG15 manipulation of the ESCRT pathway represents a general strategy for the inhibition virus propagation. Notably, both LCMV and HSV-1 have been shown to utilize the ESCRT pathway for virus budding, yet ISG15 has not been found to affect LCMV pathogenesis *in vivo* or inhibit HSV-1 replication *in vitro*^{39; 40; 56; 57; 58}. It is possible that these viruses are capable of antagonizing ISG15 and its effects on the ESCRT pathway. More studies will be needed to more precisely define the mechanisms by which ISG15 regulates viral budding. It will also be interesting to determine if ISG15 alteration of the ESCRT pathway represents specific strategy for targeting viruses, or if this might be reflective of a broader role that ISG15 plays in vesicular trafficking after IFN stimulation.

ISGylation of Viral proteins

The recombinant Sindbis virus studies not only demonstrated that ISG15 could act as an antiviral molecule, but also showed that it could do so when expressed only from within the virus genome, exerting its activity from within a virally infected cell^{37; 40}. Similarly, knock-down of ISG15 in human cells was shown to increase influenza A virus replication, further suggesting that ISG15 can directly antagonize virus replication and sparking subsequent studies exploring the possibility of ISG15 acting by directly conjugating to viral proteins³⁸. Indeed, there now is

evidence that during some infections viral proteins are targeted for ISGylation and this contributes to the type I IFN mediated inhibition of virus replication.

The first viral protein shown to be modified by ISG15 was the NS1 protein of influenza A virus. Two studies have been published showing that influenza A virus NS1 protein can be ISGylated by HERC5, and different functional consequences have been attributed to this modification^{59;60}. Both studies found that NS1 is ISGylated on more than one lysine residue. Zhao *et al.* found that the lysine residue at position K41 was the dominant site for ISGylation⁵⁹. Modification at this site was shown to have no impact on the ability of NS1 to bind to double stranded RNA but did inhibit its ability to interact with importin alpha, an interaction involved in the nuclear translocation of NS1. A recombinant influenza A virus containing the K41A mutation in its NS1 protein to reduce ISGylation of NS1 was less susceptible to inhibition of replication by IFN as compared to a WT virus. Tang *et al.* found that seven lysines in NS1 had to be mutated to generate a non-ISGylated NS1⁶⁰. This study found that ISGylated NS1 could not interact with the N-terminus of PKR, the RNA binding domain of NS1, U6snRNA, or dsRNA. On a functional level, ISGylation of NS1 inhibited the ability of NS1 to antagonize the induction of ISGs by SeV infection, suggesting that ISGylation of NS1 would render influenza A virus more susceptible to the antiviral response. Differences in the findings of these two studies could be due to the different strains of influenza A virus that were used in each study. However, both studies further support the hypothesis that by modifying viral proteins ISG15 can directly antagonize virus replication.

The HPV capsid protein has also been shown to be ISGylated by HERC5²⁵. Using a HPV pseudovirus packaging system, Durfee *et al.* demonstrated that the expression of the ISG15 conjugation system led to the ISGylation of the HPV capsid protein, which then incorporated

into released virus. ISGylation of HPV capsid protein correlated with a decrease both in the amount of virus released and in the subsequent infectivity of the virus produced in the presence of ISG15. This observation led to a model in which ISGylated capsid protein is incorporated into virions but results in an alteration of the geometry of the viral capsid. It is hypothesized that this change in the capsid structure then inhibits the infectivity of the released virus. As mentioned previously, Woods *et al.* also found that HIV-1 Gag protein can also be ISGylated by HERC5⁴⁸. It is important to note that direct causality of virus replication inhibition through viral protein ISGylation, as opposed to ISGylation of host proteins, was not verified with non-ISGylatable HPV capsid or HIV-1 Gag mutants. Nonetheless, these observations help to further an attractive model for ISG15 function that could help to explain how ISGylation of a small fraction of the total pool of a protein could lead to a large downstream effect on virus fitness. Homooligomerization of viral proteins is a universal necessity in viral genomes to facilitate virion formation and genome packaging. Future studies will be needed to determine if this model can be applied to other viral proteins such as matrix proteins or ribonucleoproteins.

Modification of host proteins:

Since ISGylation has been shown to target newly translated proteins, ISGs would be predicted to be a population of proteins rife with targets for ISG15 conjugation following IFN stimulation. In one of the first high throughput studies identifying ISGylated proteins, both Jak1 and STAT1 were shown to be ISGylated in human thymus tissue⁶¹. In subsequent proteomic studies, many ISGs have been identified as ISG15 targets^{33; 34}. Among these, three antiviral

effectors, interferon regulatory factor 3 (IRF3), retinoic acid inducible gene 1 (RIG-I), and protein kinase R (PKR) have been analyzed in significant detail.

ISGylation of IRF3 has been reported to stabilize activated IRF3, thus positively regulating the type I IFN response^{62; 63}. Shi *et al.* showed that after SeV infection, HERC5 can bind to and ISGylate IRF3 on multiple lysine residues. ISGylation of IRF3 inhibits the interaction of IRF3 with PIN1 thus inhibiting the ubiquitination and degradation of IRF3, resulting in a more robust IFN response⁶³. This study went on to show that siRNA knock down of HERC5 or ISG15 resulted in increased replication of VSV, SeV, and NDV. However, it is unclear from these studies whether inhibition of virus replication was dependent on ISGylation of IRF3 or if ISGylation of other target proteins mediated these antiviral effects.

RIG-I was found to be ISGylated after transfection of COS-7 cells with ISG15, Ube1L and UbcH8 expression plasmids⁶⁴. Overexpression of the ISG15 conjugation system also resulted in decreased levels of non-ISGylated RIG-I, though this decrease was not dependent on proteasome activity. This reduction of RIG-I levels was not seen in Ube1L^{-/-} MEFS further implicating the importance of ISG15 conjugation to mediate this phenomenon. The reduction of RIG-I protein levels correlated with a reduction in the intensity of the IFN response triggered by NDV⁶⁴. In this study the residues modified by ISG15 were not identified and mutated, so it could not be ruled out that the decrease in RIG-I expression was an indirect result of the ISGylation of another protein. Whether directly a result of RIG-I ISGylation or not, this study suggests that ISG15 might not always engender a more intense IFN response, but rather it may act to dampen the IFN response down to an appropriate level in certain scenarios.

PKR was also identified in proteomic analysis as being a target of ISGylation^{33;34}. Okumura *et al.* recently verified that PKR is ISGylated after IFN or LPS stimulation⁶⁵. Mutational analysis revealed that PKR is ISGylated at K69 and K159. In lung fibroblasts PKR was found to be activated even in the absence of viral RNA, however this activation was dependent on ISG15. A non-ISGylatable K69R, K159R PKR mutant did not exhibit constitutive activation demonstrating that this RNA independent activation of PKR was due to ISGylation of PKR. This increased activation of PKR was also observed when ISG15 was fused to the N-terminus of PKR resulting in increased phosphorylation of eIF2 α and decreased protein synthesis. These findings suggest ISG15 may have a broader impact on protein translation prior to viral infection.

While the ISG15 mediated regulation of antiviral effectors has received much attention, it is also important to understand how ISGylation of other “non-antiviral effector” proteins might affect virus replication and pathogenesis. For example, as previously discussed, ISGylation of CHMP5 has been correlated with the ISG15-dependent inhibition of HIV-1 budding⁵⁵. ISG15 has also been implicated in the regulation of IFN induced apoptosis through modification of filamin B⁶⁶. In addition to cross-linking actin filaments, filamin B also serves as a scaffold protein for the Jun N-terminal kinase (JNK) signaling pathway. Jeon *et al.* has shown that ISGylation of filamin B disrupts its ability to bind to RAC-1, MEKK1, and MEKK4, thereby inhibiting the signaling cascade leading to JNK mediated apoptosis⁶⁶. In this study coexpression of UbcH8 and filamin B resulted in co-localization of the two proteins in actin rich membrane ruffles. Thus while only a small fraction of total filamin B is ISGylated, the fraction of ISGylated filamin B within the local microenvironment of a membrane ruffle might be quite

high. This might explain how ISGylation of a seemingly small fraction of filamin B can have a large impact on JNK signaling.

It is important to note that despite the number of studies evaluating the regulation of ISGs by ISG15, no studies in ISG15^{-/-} mice or ISG15^{-/-} cells have demonstrated ISG15 conjugation as having a role in the regulation of the type I IFN response. Analysis of cells from ISG15^{-/-} and Ube1L^{-/-} mice did not reveal any misregulation of STAT1 activation or ISG induction after stimulation with IFN beta, LPS, or combinations of both stimuli^{14; 39}. PolyI:C injections of mice had no effect on cell proliferation, and Ube1L^{-/-} cells were found to undergo similar levels of apoptosis after IFN stimulation. There could be several explanations for these discrepancies including 1) the differences in utilization of overexpression, knockdown, and knockout systems, 2) differences between the function of ISGylation in humans and mice, or 3) differences in experimental conditions and types of stimulations. Additional studies will be required to better understand these discrepancies.

Unconjugated ISG15

In addition to existing in its conjugated form, ISG15 is present in an unconjugated form both intracellularly and released into the extracellular space. Recent evidence in both murine and human models has indicated that unconjugated ISG15 may also play an important role in the host response to infections.

A recent study by Werneke *et al.* was the first *in vivo* study to suggest that unconjugated ISG15 has a biologically relevant role during infection⁴³. In this study, ISG15^{-/-} neonatal mice were found to be highly susceptible to infection with the re-emerging viral pathogen, CHIKV.

However Ube1L^{-/-} mice did not display increase lethality, indicating that the expression of unconjugated ISG15 was sufficient to protect these mice from CHIKV induced lethality. The protective mechanism of ISG15 in this model was distinct from previous models that have been studied, in that ISG15 did not appear to function as an antiviral molecule. Viral loads in all organs examined were the same in WT, Ube1L^{-/-} and ISG15^{-/-} mice. Instead the ISG15^{-/-} mice had significantly higher levels of multiple cytokines in their serum, and death of the animals occurred in a manner consistent with a cytokine storm. Together these data suggested that unconjugated ISG15 protected these neonatal mice from CHIKV induced lethality through its ability to regulate the production of proinflammatory cytokines and chemokines. The mechanism through which ISG15 regulates these responses and the cell types responsible for the increased cytokine production in this model are not known. A recombinant CHIKV engineered to express ISG15 was no less virulent than the WT virus in ISG15^{-/-} mice. This suggests that unconjugated ISG15 may need to be expressed by non-infected cells, or expressed before virus infection in order to mediate protection. It is also not certain whether intracellular unconjugated ISG15 or extracellular unconjugated ISG15 is responsible for the regulation of cytokines in this model. Future studies will be needed to address these important questions.

ISG15 has long been implicated as having a role as a cytokine-like molecule. Though ISG15 has no canonical signal peptide for release, T-cells, B-cells, monocytes, and epithelial cells have all been shown to release ISG15 after IFN stimulation *in vitro*⁶⁷. In studying the potential role for this released ISG15, it was found that treatment of peripheral blood lymphocytes with recombinant ISG15 resulted in specific proliferation of natural killer (NK) cells⁶⁸. This expansion of NK cells was found to be due to the induction of IFN gamma by T-cells. Recently, a study by Bogunovic *et al.* confirmed a role for unconjugated ISG15 in the

stimulation of IFN gamma production and correlated this function with increased disease susceptibility in humans⁶⁹. In this study ISG15 deficiency was identified as a potential predisposition for Mendelian susceptibility to mycobacterial disease. These authors found that recombinant ISG15 induced IFN gamma production by both NK cells and other lymphocytes. They went on to show that the levels of IFN gamma produced after stimulation with recombinant ISG15 was greatly enhanced by co-stimulation of cells with ISG15 and IL-12. Whole blood cells from ISG15 deficient individuals produced decreased levels of IFN gamma compared to cells from ISG15 sufficient individuals after stimulation with either mycobacteria alone or in combination with IL-12. Treatment of ISG15 deficient cells with recombinant ISG15 in addition to mycobacteria and IL-12 enhanced their ability to produce IFN gamma to levels near ISG15 sufficient cells. This data indicates that released ISG15 may play an important role in IFN gamma production during mycobacterial infection.

Together these studies suggest that ISG15 contributes to the host response to infection not only through its modification of target proteins, but also through the actions of unconjugated ISG15, perhaps functioning as a cytokine. Many questions still remain, including the identity of a receptor that can mediate these biological properties. Given the therapeutic potential for administration or inhibition of cytokines during viral infection, it is of great interest to further define the role of ISG15 in cytokine regulation.

Viral countermeasures:

Viral antagonism of antiviral effectors is a phenomenon so frequent and inevitable that the study of mutant viruses is routinely a means by which novel host biology is elucidated.

Discoveries of viral antagonism of ISG15 have further highlighted the importance of ISG15 as a part of the host antiviral response. Before the antiviral activity of ISG15 had been demonstrated, a role for ISG15 during influenza B virus infection was eluded to by the discovery of the interaction between ISG15 and the influenza B virus NS1 protein (B/NS1)¹¹. Influenza B/NS1, but not influenza A/NS1, was found to bind ISG15 and inhibit it from interacting with Ube1L, thereby preventing the formation of ISG15 conjugates. A detailed review covering the interaction between B/NS1 and ISG15 has recently been published⁷⁰. Since this discovery of B/NS1 interacting with ISG15, several other viruses have also been identified that encode proteins that can interact with and potentially antagonize ISG15.

The vaccinia E3L protein initially masked the sensitivity of vaccinia virus to ISG15⁴⁶. A WT vaccinia strain replicated to similar levels in ISG15^{-/-} and WT mouse embryonic fibroblasts (MEF) after 48 hours of infection, and ISG15^{-/-} mice did not exhibit increased lethality compared to WT mice. However, after infection with WT vaccinia virus, it was noted that ISG15 was induced but did not form conjugates. Infection of cells with a Δ E3L mutant vaccinia virus did result in ISG15 conjugate formation. The E3L protein was shown to bind to ISG15, suggesting that the E3L protein directly antagonizes ISG15 conjugation, though the exact mechanism by which this occurs is not known. ISG15^{-/-} mice exhibited increased lethality compared to WT mice when infected with this Δ E3L mutant vaccinia virus, and the mutant virus exhibited a ~25 fold increase in virus replication in ISG15^{-/-} MEFs compared to WT MEFs. Therefore, similar to influenza B virus, vaccinia virus appears to have evolved a mechanism to disrupt ISG15 conjugation and its antiviral activity.

Multiple viruses have evolved deubiquitinating enzymes capable of antagonizing host cell biology. Several of these viral proteins are capable of deconjugating ISG15 from ISGylated

target proteins. Crimean-Congo hemorrhagic fever virus (CCHFV) and equine arteritis virus encode L proteins containing ovarian tumor (OTU) domains. In host proteins OTU domains can contain ubiquitin deconjugation activity³². When transfected into cells, these viral L proteins were able to reduce the total pool of both ubiquitin and ISG15 conjugates⁷¹. Expression of the CCHFV L protein OTU domain by recombinant Sindbis virus in parallel with expression of ISG15 abolished the protection provided by ISG15 during infection of IFNAR^{-/-} mice⁷¹. Similarly, SARS-Coronavirus encodes a papain-like protease that has been shown to cleave K48 linked ubiquitin chains as well as ISG15 fusion proteins^{72; 73; 74}. While these examples highlight another potential mechanism of circumventing ISG15, direct evidence for ISG15 antagonism by these proteins remains to be demonstrated during viral infection.

The convergent evolution of viral proteins antagonizing the ISG15 conjugation system demonstrates the broad antiviral activity of ISG15. It will be interesting to investigate whether the lack of a role for ISG15 during infections with certain viruses, such as VSV and LCMV, might also be due to viral antagonism of ISG15 that has yet to be discovered.

THESIS GOALS

ISG15 was the first ubiquitin-like modifier to be identified, yet over 25 years after its discovery remarkably little is known about the molecular functions of ISG15 and ISG15 conjugation. Studies of ISG15 deficient mice have clearly established that ISG15 can mediate protection from virus induced lethality, however the molecular mechanisms mediating this protection are still not well understood.

Hundreds of host proteins have been identified as targets of ISGylation by mass spectrometry. Historically, the predominant strategy for studying ISG15 function has been a reverse genetics style of approach by verifying ISGylation of a target of interest, identifying the modified lysine residue in the target protein, and generating a non-ISGylatable mutant version of the protein to study the effects of ISGylation. Studying the effects of ISG15 conjugation through this approach has proved to be difficult for several reasons. Firstly, a number of proteins have been shown to be capable of being ISGylated on multiple lysine residues. It is unclear whether the targets are normally modified on multiple residues, or if ISG15 simply targets new lysine residues after one residue is mutated. In the case of the influenza A virus NS1 protein, one study found that seven lysine residues had to be mutated before a non-ISGylatable mutant was obtained⁶⁰. Mutating large numbers of lysines risks affecting the function of the target and thus confounding subsequent studies of the impact of ISG15 on the target protein. Secondly, while some studies have identified consequences of ISGylation, typically only ~5% of the total pool of a target protein is ISGylated. Most reported effects of ISGylation have been attributed to the disruption of interactions between the ISGylated protein and its normal binding partners. However, most studies fail to demonstrate how ISGylation of such a small fraction of the target protein might lead to a biologically relevant phenotype. Thirdly, one study has suggested that ISGylation through the E3 ligase HERC5 targets newly translated proteins with no apparent sequence specificity driving the conjugation of ISG15 to target proteins²⁵. This finding raises the question of whether exogenous overexpression of the ISG15 conjugation system or target proteins will faithfully recapitulate the effects of ISGylation on the endogenous target protein after interferon stimulation.

While ISGylation of viral proteins has been reported, and in at least some systems may contribute to the antiviral activity of ISG15, virus replication has not been altered in several models where ISG15 is known to play a role during virus infection *in vivo*. For example, ISG15^{-/-} mice display increased lethality following Sindbis virus infection, however, no defect in virus replication was observed when WT and ISG15^{-/-} MEFs were infected with Sindbis virus⁴⁰. Similarly, ISG15^{-/-} mice are more susceptible to HSV-1 infection, however no difference in HSV-1 replication has been observed in ISG15^{-/-} MEFs or in fibroblasts from human patients deficient for ISG15^{40, 69}. Discrepancies between *in vivo* protection and cell culture phenotypes might be a result of the particular cell types chosen for study. However, it is also possible that ISG15 mediated protection from lethality might not be a result of direct antagonism of virus replication, as has been demonstrated for CHIKV infection⁴³.

To date, the most profound and consistent phenotypes demonstrated for ISG15 has been the increased susceptibility of ISG15^{-/-} mice to viral infections *in vivo*. Therefore, we have chosen to take a forward genetics style of approach to investigating the function of ISG15 by dissecting the mechanisms behind the susceptibility of ISG15^{-/-} mice to viral infection.

Arguably the most robust *in vivo* phenotype in ISG15^{-/-} and Ube1L^{-/-} mice is their susceptibility to influenza B virus infection. While ISG15 mediated inhibition of virus replication has been demonstrated in tissue culture for a number of viruses, the reported effects have been modest, ~5-10 fold. Given the dramatic inhibition of influenza B virus replication by ISG15 *in vivo*, I set out to use influenza B virus infection as a model for studying the effects of ISG15 on the virus life cycle. I aimed to answer three main questions: 1.) Can ISG15 directly inhibit influenza B virus replication in primary trachea epithelial cell (mTEC) cultures *in vitro*?, 2.) Does increasing ISG15 conjugation provide increased protection against influenza B virus

infection?, and 3.) Are influenza B virus proteins targets of ISGylation, and if so what effect does ISGylation have on the virus life cycle?

The hypothesis that ISG15 protects mice from viral infection by inhibiting virus replication largely stems from two observations. First, the type I interferon system has a well established role of antagonizing virus replication, and ISG15 is one of the most rapidly and strongly induced genes after type I interferon stimulation. And second, influenza B virus replicates to levels ~100 fold greater in ISG15^{-/-} mice compared to WT mice. However, the recent evaluation of CHKV pathogenesis in ISG15^{-/-} mice demonstrates that ISG15 can confer resistance to viral infection without affecting virus burden, demonstrating that further evaluation of the role of ISG15 during other *in vivo* infection models is warranted. Therefore I chose to characterize the role of ISG15 and ISG15 conjugation during infection with two other respiratory viruses, influenza A virus and Sendai virus.

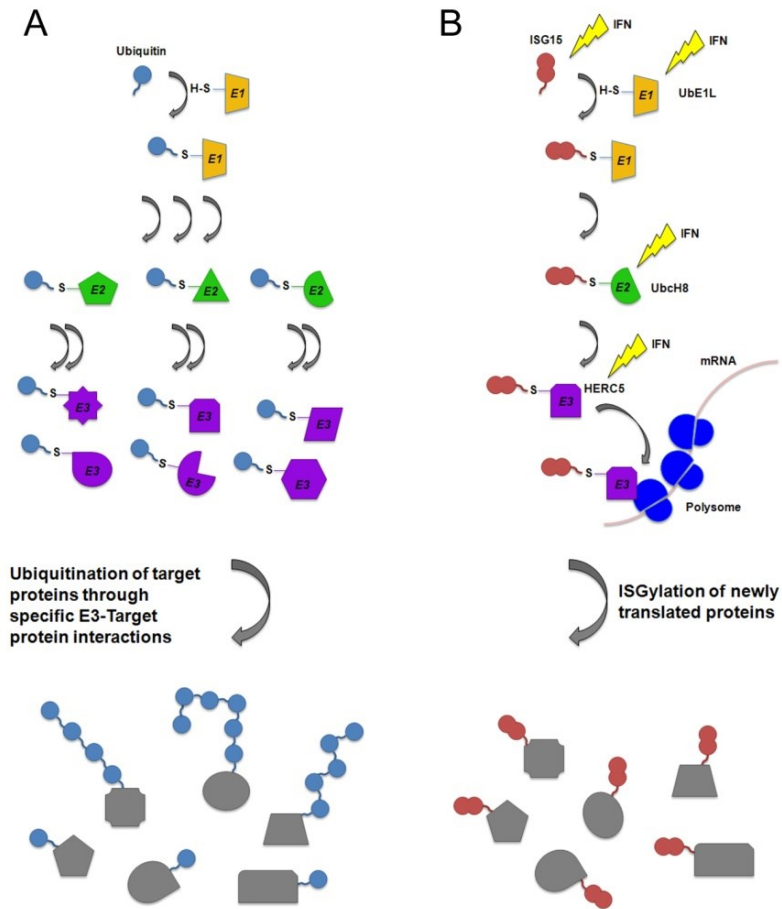


Figure 1.1 A comparison between the ubiquitin and ISG15 conjugation pathways.

Both ubiquitin and ISG15 are conjugated to target proteins by utilizing enzymatic cascades composed of E1, E2, and E3 enzymes. A) In the case of ubiquitin, it achieves specificity in target protein modification through the use of multiple E2 and E3 enzymes, which can orchestrate a broad range of specific ubiquitin modifications. Ubiquitin can also conjugate to itself on multiple lysine residues to form polyubiquitin chains on target proteins which result in different downstream functional consequences for the targeted protein. B) The ISG15

conjugation cascade is an IFN induced cascade in which the vast majority of ISG15 conjugation utilizes Ube1L, UbcH8, and HERC5. Interaction between HERC5 and polysomes leads to the preferential ISGylation of newly translated proteins. Unlike ubiquitin, there is no evidence that ISG15 forms poly-ISG15 chains or targets proteins for degradation.

REFERENCES

1. Hershko, A. & Ciechanover, A. (1998). The ubiquitin system. *Annu Rev Biochem* **67**, 425-79.
2. Ciechanover, A. (2009). Tracing the history of the ubiquitin proteolytic system: the pioneering article. *Biochem Biophys Res Commun* **387**, 1-10.
3. Komander, D. & Rape, M. (2012). The ubiquitin code. *Annu Rev Biochem* **81**, 203-29.
4. van der Veen, A. G. & Ploegh, H. L. (2012). Ubiquitin-like proteins. *Annu Rev Biochem* **81**, 323-57.
5. Korant, B. D., Blomstrom, D. C., Jonak, G. J. & Knight, E., Jr. (1984). Interferon-induced proteins. Purification and characterization of a 15,000-dalton protein from human and bovine cells induced by interferon. *J Biol Chem* **259**, 14835-9.
6. Haas, A. L., Ahrens, P., Bright, P. M. & Ankel, H. (1987). Interferon induces a 15-kilodalton protein exhibiting marked homology to ubiquitin. *J Biol Chem* **262**, 11315-23.
7. Blomstrom, D. C., Fahey, D., Kutny, R., Korant, B. D. & Knight, E., Jr. (1986). Molecular characterization of the interferon-induced 15-kDa protein. Molecular cloning and nucleotide and amino acid sequence. *J Biol Chem* **261**, 8811-6.
8. Dao, C. T. & Zhang, D. E. (2005). ISG15: a ubiquitin-like enigma. *Front Biosci* **10**, 2701-22.
9. Narasimhan, J., Wang, M., Fu, Z., Klein, J. M., Haas, A. L. & Kim, J. J. (2005). Crystal structure of the interferon-induced ubiquitin-like protein ISG15. *J Biol Chem* **280**, 27356-65.
10. Potter, J. L., Narasimhan, J., Mende-Mueller, L. & Haas, A. L. (1999). Precursor processing of pro-ISG15/UCRP, an interferon-beta-induced ubiquitin-like protein. *J Biol Chem* **274**, 25061-8.
11. Yuan, W. & Krug, R. M. (2001). Influenza B virus NS1 protein inhibits conjugation of the interferon (IFN)-induced ubiquitin-like ISG15 protein. *EMBO J* **20**, 362-71.
12. Krug, R. M., Zhao, C. & Beaudenon, S. (2005). Properties of the ISG15 E1 enzyme Ube1L. *Methods Enzymol* **398**, 32-40.
13. Chiu, Y. H., Sun, Q. & Chen, Z. J. (2007). E1-L2 activates both ubiquitin and FAT10. *Mol Cell* **27**, 1014-23.
14. Kim, K. I., Yan, M., Malakhova, O., Luo, J. K., Shen, M. F., Zou, W., de la Torre, J. C. & Zhang, D. E. (2006). Ube1L and protein ISGylation are not essential for alpha/beta interferon signaling. *Mol Cell Biol* **26**, 472-9.
15. Zhao, C., Beaudenon, S. L., Kelley, M. L., Waddell, M. B., Yuan, W., Schulman, B. A., Huibregtse, J. M. & Krug, R. M. (2004). The UbcH8 ubiquitin E2 enzyme is also the E2 enzyme for ISG15, an IFN-alpha/beta-induced ubiquitin-like protein. *Proc Natl Acad Sci U S A* **101**, 7578-82.
16. Kim, K. I., Giannakopoulos, N. V., Virgin, H. W. & Zhang, D. E. (2004). Interferon-inducible ubiquitin E2, Ubc8, is a conjugating enzyme for protein ISGylation. *Mol Cell Biol* **24**, 9592-600.
17. Durfee, L. A., Kelley, M. L. & Huibregtse, J. M. (2008). The basis for selective E1-E2 interactions in the ISG15 conjugation system. *J Biol Chem* **283**, 23895-902.
18. Zou, W. & Zhang, D. E. (2006). The interferon-inducible ubiquitin-protein isopeptide ligase (E3) EFP also functions as an ISG15 E3 ligase. *J Biol Chem* **281**, 3989-94.

19. Dastur, A., Beaudenon, S., Kelley, M., Krug, R. M. & Huibregtse, J. M. (2006). Herc5, an interferon-induced HECT E3 enzyme, is required for conjugation of ISG15 in human cells. *J Biol Chem* **281**, 4334-8.
20. Wong, J. J., Pung, Y. F., Sze, N. S. & Chin, K. C. (2006). HERC5 is an IFN-induced HECT-type E3 protein ligase that mediates type I IFN-induced ISGylation of protein targets. *Proc Natl Acad Sci U S A* **103**, 10735-40.
21. Okumura, F., Zou, W. & Zhang, D. E. (2007). ISG15 modification of the eIF4E cognate 4EHP enhances cap structure-binding activity of 4EHP. *Genes Dev* **21**, 255-60.
22. Ketscher, L., Basters, A., Prinz, M. & Knobeloch, K. P. (2012). mHERC6 is the essential ISG15 E3 ligase in the murine system. *Biochem Biophys Res Commun* **417**, 135-40.
23. Oudshoorn, D., van Boheemen, S., Sanchez-Aparicio, M. T., Rajsbaum, R., Garcia-Sastre, A. & Versteeg, G. A. (2012). HERC6 is the main E3 ligase for global ISG15 conjugation in mouse cells. *PLoS One* **7**, e29870.
24. Versteeg, G. A., Hale, B. G., van Boheemen, S., Wolff, T., Lenschow, D. J. & Garcia-Sastre, A. (2010). Species-specific antagonism of host ISGylation by the influenza B virus NS1 protein. *J Virol* **84**, 5423-30.
25. Durfee, L. A., Lyon, N., Seo, K. & Huibregtse, J. M. (2010). The ISG15 conjugation system broadly targets newly synthesized proteins: implications for the antiviral function of ISG15. *Mol Cell* **38**, 722-32.
26. Malakhov, M. P., Malakhova, O. A., Kim, K. I., Ritchie, K. J. & Zhang, D. E. (2002). UBP43 (USP18) specifically removes ISG15 from conjugated proteins. *J Biol Chem* **277**, 9976-81.
27. Ritchie, K. J., Hahn, C. S., Kim, K. I., Yan, M., Rosario, D., Li, L., de la Torre, J. C. & Zhang, D. E. (2004). Role of ISG15 protease UBP43 (USP18) in innate immunity to viral infection. *Nat Med* **10**, 1374-8.
28. Malakhova, O. A., Yan, M., Malakhov, M. P., Yuan, Y., Ritchie, K. J., Kim, K. I., Peterson, L. F., Shuai, K. & Zhang, D. E. (2003). Protein ISGylation modulates the JAK-STAT signaling pathway. *Genes Dev* **17**, 455-60.
29. Knobeloch, K. P., Utermohlen, O., Kissler, A., Prinz, M. & Horak, I. (2005). Reexamination of the role of ubiquitin-like modifier ISG15 in the phenotype of UBP43-deficient mice. *Mol Cell Biol* **25**, 11030-4.
30. Malakhova, O. A., Kim, K. I., Luo, J. K., Zou, W., Kumar, K. G., Fuchs, S. Y., Shuai, K. & Zhang, D. E. (2006). UBP43 is a novel regulator of interferon signaling independent of its ISG15 isopeptidase activity. *EMBO J* **25**, 2358-67.
31. Catic, A., Fiebiger, E., Korbel, G. A., Blom, D., Galardy, P. J. & Ploegh, H. L. (2007). Screen for ISG15-crossreactive deubiquitinases. *PLoS One* **2**, e679.
32. Reyes-Turcu, F. E., Ventii, K. H. & Wilkinson, K. D. (2009). Regulation and cellular roles of ubiquitin-specific deubiquitinating enzymes. *Annu Rev Biochem* **78**, 363-97.
33. Giannakopoulos, N. V., Luo, J. K., Papov, V., Zou, W., Lenschow, D. J., Jacobs, B. S., Borden, E. C., Li, J., Virgin, H. W. & Zhang, D. E. (2005). Proteomic identification of proteins conjugated to ISG15 in mouse and human cells. *Biochem Biophys Res Commun* **336**, 496-506.
34. Zhao, C., Denison, C., Huibregtse, J. M., Gygi, S. & Krug, R. M. (2005). Human ISG15 conjugation targets both IFN-induced and constitutively expressed proteins functioning in diverse cellular pathways. *Proc Natl Acad Sci U S A* **102**, 10200-5.

35. Liu, M., Li, X. L. & Hassel, B. A. (2003). Proteasomes modulate conjugation to the ubiquitin-like protein, ISG15. *J Biol Chem* **278**, 1594-602.
36. Geiss-Friedlander, R. & Melchior, F. (2007). Concepts in sumoylation: a decade on. *Nat Rev Mol Cell Biol* **8**, 947-56.
37. Lenschow, D. J., Giannakopoulos, N. V., Gunn, L. J., Johnston, C., O'Guin, A. K., Schmidt, R. E., Levine, B. & Virgin, H. W. t. (2005). Identification of interferon-stimulated gene 15 as an antiviral molecule during Sindbis virus infection in vivo. *J Virol* **79**, 13974-83.
38. Hsiang, T. Y., Zhao, C. & Krug, R. M. (2009). Interferon-induced ISG15 conjugation inhibits influenza A virus gene expression and replication in human cells. *J Virol* **83**, 5971-7.
39. Osiak, A., Utermohlen, O., Niendorf, S., Horak, I. & Knobloch, K. P. (2005). ISG15, an interferon-stimulated ubiquitin-like protein, is not essential for STAT1 signaling and responses against vesicular stomatitis and lymphocytic choriomeningitis virus. *Mol Cell Biol* **25**, 6338-45.
40. Lenschow, D. J., Lai, C., Frias-Staheli, N., Giannakopoulos, N. V., Lutz, A., Wolff, T., Osiak, A., Levine, B., Schmidt, R. E., Garcia-Sastre, A., Leib, D. A., Pekosz, A., Knobloch, K. P., Horak, I. & Virgin, H. W. t. (2007). IFN-stimulated gene 15 functions as a critical antiviral molecule against influenza, herpes, and Sindbis viruses. *Proc Natl Acad Sci U S A* **104**, 1371-6.
41. Giannakopoulos, N. V., Arutyunova, E., Lai, C., Lenschow, D. J., Haas, A. L. & Virgin, H. W. (2009). ISG15 Arg151 and the ISG15-conjugating enzyme UBE1L are important for innate immune control of Sindbis virus. *J Virol* **83**, 1602-10.
42. Lai, C., Struckhoff, J. J., Schneider, J., Martinez-Sobrido, L., Wolff, T., Garcia-Sastre, A., Zhang, D. E. & Lenschow, D. J. (2009). Mice lacking the ISG15 E1 enzyme UBE1L demonstrate increased susceptibility to both mouse-adapted and non-mouse-adapted influenza B virus infection. *J Virol* **83**, 1147-51.
43. Werneke, S. W., Schilte, C., Rohatgi, A., Monte, K. J., Michault, A., Arenzana-Seisdedos, F., Vanlandingham, D. L., Higgs, S., Fontanet, A., Albert, M. L. & Lenschow, D. J. (2011). ISG15 is critical in the control of Chikungunya virus infection independent of UBE1L mediated conjugation. *PLoS Pathog* **7**, e1002322.
44. Okumura, A., Lu, G., Pitha-Rowe, I. & Pitha, P. M. (2006). Innate antiviral response targets HIV-1 release by the induction of ubiquitin-like protein ISG15. *Proc Natl Acad Sci U S A* **103**, 1440-5.
45. Pincetic, A., Kuang, Z., Seo, E. J. & Leis, J. (2010). The interferon-induced gene ISG15 blocks retrovirus release from cells late in the budding process. *J Virol* **84**, 4725-36.
46. Guerra, S., Caceres, A., Knobloch, K. P., Horak, I. & Esteban, M. (2008). Vaccinia virus E3 protein prevents the antiviral action of ISG15. *PLoS Pathog* **4**, e1000096.
47. Pincetic, A. & Leis, J. (2009). The Mechanism of Budding of Retroviruses From Cell Membranes. *Adv Virol* **2009**, 6239691-6239699.
48. Woods, M. W., Kelly, J. N., Hattmann, C. J., Tong, J. G., Xu, L. S., Coleman, M. D., Quest, G. R., Smiley, J. R. & Barr, S. D. (2011). Human HERC5 restricts an early stage of HIV-1 assembly by a mechanism correlating with the ISGylation of Gag. *Retrovirology* **8**, 95.
49. Timmins, J., Scianimanico, S., Schoehn, G. & Weissenhorn, W. (2001). Vesicular release of ebola virus matrix protein VP40. *Virology* **283**, 1-6.

50. Yasuda, J., Nakao, M., Kawaoka, Y. & Shida, H. (2003). Nedd4 regulates egress of Ebola virus-like particles from host cells. *J Virol* **77**, 9987-92.
51. Malakhova, O. A. & Zhang, D. E. (2008). ISG15 inhibits Nedd4 ubiquitin E3 activity and enhances the innate antiviral response. *J Biol Chem* **283**, 8783-7.
52. Okumura, A., Pitha, P. M. & Harty, R. N. (2008). ISG15 inhibits Ebola VP40 VLP budding in an L-domain-dependent manner by blocking Nedd4 ligase activity. *Proc Natl Acad Sci U S A* **105**, 3974-9.
53. Zou, W., Papov, V., Malakhova, O., Kim, K. I., Dao, C., Li, J. & Zhang, D. E. (2005). ISG15 modification of ubiquitin E2 Ubc13 disrupts its ability to form thioester bond with ubiquitin. *Biochem Biophys Res Commun* **336**, 61-8.
54. Takeuchi, T. & Yokosawa, H. (2005). ISG15 modification of Ubc13 suppresses its ubiquitin-conjugating activity. *Biochem Biophys Res Commun* **336**, 9-13.
55. Kuang, Z., Seo, E. J. & Leis, J. (2011). Mechanism of inhibition of retrovirus release from cells by interferon-induced gene ISG15. *J Virol* **85**, 7153-61.
56. Perez, M., Craven, R. C. & de la Torre, J. C. (2003). The small RING finger protein Z drives arenavirus budding: implications for antiviral strategies. *Proc Natl Acad Sci U S A* **100**, 12978-83.
57. Crump, C. M., Yates, C. & Minson, T. (2007). Herpes simplex virus type 1 cytoplasmic envelopment requires functional Vps4. *J Virol* **81**, 7380-7.
58. Pawliczek, T. & Crump, C. M. (2009). Herpes simplex virus type 1 production requires a functional ESCRT-III complex but is independent of TSG101 and ALIX expression. *J Virol* **83**, 11254-64.
59. Zhao, C., Hsiang, T. Y., Kuo, R. L. & Krug, R. M. (2010). ISG15 conjugation system targets the viral NS1 protein in influenza A virus-infected cells. *Proc Natl Acad Sci U S A* **107**, 2253-8.
60. Tang, Y., Zhong, G., Zhu, L., Liu, X., Shan, Y., Feng, H., Bu, Z., Chen, H. & Wang, C. (2010). Herc5 attenuates influenza A virus by catalyzing ISGylation of viral NS1 protein. *J Immunol* **184**, 5777-90.
61. Malakhov, M. P., Kim, K. I., Malakhova, O. A., Jacobs, B. S., Borden, E. C. & Zhang, D. E. (2003). High-throughput immunoblotting. Ubiquitin-like protein ISG15 modifies key regulators of signal transduction. *J Biol Chem* **278**, 16608-13.
62. Lu, G., Reinert, J. T., Pitha-Rowe, I., Okumura, A., Kellum, M., Knobeloch, K. P., Hassel, B. & Pitha, P. M. (2006). ISG15 enhances the innate antiviral response by inhibition of IRF-3 degradation. *Cell Mol Biol (Noisy-le-grand)* **52**, 29-41.
63. Shi, H. X., Yang, K., Liu, X., Liu, X. Y., Wei, B., Shan, Y. F., Zhu, L. H. & Wang, C. (2010). Positive regulation of interferon regulatory factor 3 activation by Herc5 via ISG15 modification. *Mol Cell Biol* **30**, 2424-36.
64. Kim, M. J., Hwang, S. Y., Imaizumi, T. & Yoo, J. Y. (2008). Negative feedback regulation of RIG-I-mediated antiviral signaling by interferon-induced ISG15 conjugation. *J Virol* **82**, 1474-83.
65. Okumura, F., Okumura, A. J., Uematsu, K., Hatakeyama, S., Zhang, D. E. & Kamura, T. (2013). Activation of double-stranded RNA-activated protein kinase (PKR) by interferon-stimulated gene 15 (ISG15) modification down-regulates protein translation. *J Biol Chem* **288**, 2839-47.
66. Jeon, Y. J., Choi, J. S., Lee, J. Y., Yu, K. R., Kim, S. M., Ka, S. H., Oh, K. H., Kim, K. I., Zhang, D. E., Bang, O. S. & Chung, C. H. (2009). ISG15 modification of filamin B

- negatively regulates the type I interferon-induced JNK signalling pathway. *EMBO Rep* **10**, 374-80.
67. D'Cunha, J., Ramanujam, S., Wagner, R. J., Witt, P. L., Knight, E., Jr. & Borden, E. C. (1996). In vitro and in vivo secretion of human ISG15, an IFN-induced immunomodulatory cytokine. *J Immunol* **157**, 4100-8.
 68. D'Cunha, J., Knight, E., Jr., Haas, A. L., Truitt, R. L. & Borden, E. C. (1996). Immunoregulatory properties of ISG15, an interferon-induced cytokine. *Proc Natl Acad Sci USA* **93**, 211-5.
 69. Bogunovic, D., Byun, M., Durfee, L. A., Abhyankar, A., Sanal, O., Mansouri, D., Salem, S., Radovanovic, I., Grant, A. V., Adimi, P., Mansouri, N., Okada, S., Bryant, V. L., Kong, X. F., Kreins, A., Velez, M. M., Boisson, B., Khalilzadeh, S., Ozelik, U., Darazam, I. A., Schoggins, J. W., Rice, C. M., Al-Muhsen, S., Behr, M., Vogt, G., Puel, A., Bustamante, J., Gros, P., Huibregtse, J. M., Abel, L., Boisson-Dupuis, S. & Casanova, J. L. (2012). Mycobacterial disease and impaired IFN-gamma immunity in humans with inherited ISG15 deficiency. *Science* **337**, 1684-8.
 70. Zhao, C., Collins, M. N., Hsiang, T. Y. & Krug, R. M. (2013). Interferon-induced ISG15 pathway: an ongoing virus-host battle. *Trends Microbiol* **21**, 181-6.
 71. Frias-Staheli, N., Giannakopoulos, N. V., Kikkert, M., Taylor, S. L., Bridgen, A., Paragas, J., Richt, J. A., Rowland, R. R., Schmaljohn, C. S., Lenschow, D. J., Snijder, E. J., Garcia-Sastre, A. & Virgin, H. W. t. (2007). Ovarian tumor domain-containing viral proteases evade ubiquitin- and ISG15-dependent innate immune responses. *Cell Host Microbe* **2**, 404-16.
 72. Lindner, H. A., Lytvyn, V., Qi, H., Lachance, P., Ziomek, E. & Menard, R. (2007). Selectivity in ISG15 and ubiquitin recognition by the SARS coronavirus papain-like protease. *Arch Biochem Biophys* **466**, 8-14.
 73. Clementz, M. A., Chen, Z., Banach, B. S., Wang, Y., Sun, L., Ratia, K., Baez-Santos, Y. M., Wang, J., Takayama, J., Ghosh, A. K., Li, K., Mesecar, A. D. & Baker, S. C. (2010). Deubiquitinating and interferon antagonism activities of coronavirus papain-like proteases. *J Virol* **84**, 4619-29.
 74. Lindner, H. A., Fotouhi-Ardakani, N., Lytvyn, V., Lachance, P., Sulea, T. & Menard, R. (2005). The papain-like protease from the severe acute respiratory syndrome coronavirus is a deubiquitinating enzyme. *J Virol* **79**, 15199-208.
 75. Dai, J., Pan, W. & Wang, P. (2011). ISG15 facilitates cellular antiviral response to dengue and west nile virus infection in vitro. *Virol J* **8**, 468.
 76. Hsiao, N. W., Chen, J. W., Yang, T. C., Orloff, G. M., Wu, Y. Y., Lai, C. H., Lan, Y. C. & Lin, C. W. (2010). ISG15 over-expression inhibits replication of the Japanese encephalitis virus in human medulloblastoma cells. *Antiviral Res* **85**, 504-11.
 77. Broering, R., Zhang, X., Kottlilil, S., Trippler, M., Jiang, M., Lu, M., Gerken, G. & Schlaak, J. F. (2010). The interferon stimulated gene 15 functions as a proviral factor for the hepatitis C virus and as a regulator of the IFN response. *Gut* **59**, 1111-9.
 78. Kim, J. H., Luo, J. K. & Zhang, D. E. (2008). The level of hepatitis B virus replication is not affected by protein ISG15 modification but is reduced by inhibition of UBP43 (USP18) expression. *J Immunol* **181**, 6467-72.
 79. Zhang, Y., Burke, C. W., Ryman, K. D. & Klimstra, W. B. (2007). Identification and characterization of interferon-induced proteins that inhibit alphavirus replication. *J Virol* **81**, 11246-55.

80. Kim, M. J. & Yoo, J. Y. (2010). Inhibition of hepatitis C virus replication by IFN-mediated ISGylation of HCV-NS5A. *J Immunol* **185**, 4311-8.

Chapter 2

The Effects of Increased ISG15 Conjugation on Influenza B Virus Replication

(Figure 2.3 was generated by Dr. Klaus-Peter Knobeloch (University of Freiburg). Portions of Chapter 2 figures are being submitted for publication in a joint manuscript with Dr. Knobeloch.)

INTRODUCTION

The history of the ISG15 field is intimately tied to influenza B virus (IBV). ISG15 was first identified as an interferon stimulated gene in 1984 in a study evaluating proteins induced after type I interferon stimulation ¹. Soon afterwards ISG15 was found to be induced upon infection of cells with encephalomyocarditis virus ². While these observations associated the expression of ISG15 with the type I interferon response and virus infection, the first indication that ISG15 might have a role in modulating the virus life cycle came from a study showing that IBV inhibits ISG15 conjugation ³. This study used a yeast two-hybrid assay to screen a cDNA library for genes encoding proteins that interacted with the influenza B virus NS1 protein (B/NS1), but not the influenza A virus NS1 protein. B/NS1 was found to bind to ISG15 and inhibit it from forming the ISG15-activating thioester bond with its E1 activating enzyme, UBE1L, thus inhibiting ISG15 conjugation. Since then it has been shown that this effect is species specific, as B/NS1 can bind to human ISG15 but not murine ISG15, and that coexpression of B/NS1 with ISG15 results in a relocalization of ISG15 from the cytoplasm to the nucleus ⁴.

The inhibition of ISGylation by B/NS1 suggested an important role for ISG15 during IBV infection, and the generation of ISG15^{-/-} mice ultimately validated this hypothesis. ISG15^{-/-} mice are dramatically more susceptible than WT mice to IBV infection, as ~80% of ISG15^{-/-} mice succumb to infection when given a dose that causes ~5% weight loss and virtually no lethality in WT mice⁵. Evaluation of lung viral loads over the course of infection found that the

increased disease in ISG15^{-/-} mice is associated with increased viral loads that reach ~100-1000 fold greater levels in ISG15^{-/-} mice than in WT mice.

In addition to the induction of intracellular ISG15 and ISG15 conjugates, non-conjugated (“free”) ISG15 was also observed in the serum of mice after IBV infection⁵. While ISG15 exists in these three different forms, the specific inhibition of ISG15 conjugation by B/NS1 suggested that ISGylation, and not expression of free ISG15 alone, mediated the protective effects against IBV. Supporting this hypothesis, Ube1L^{-/-} mice, which express ISG15 but cannot form ISG15 conjugates, were found to also exhibit increased lethality and increased virus burden compared to WT mice after influenza B virus infection⁶. This sensitivity of IBV to ISG15 conjugation, and the general susceptibility of ISG15^{-/-} mice to viral infection, suggests that exogenous manipulation of the ISG15 conjugation pathway to increase ISGylation might serve as a novel antiviral strategy.

The level of ISG15 conjugation in a cell depends on three factors: 1.) the expression level of ISG15, 2.) the enzymatic rate of forming ISG15 conjugates, and 3.) the rate at which ISG15 is deconjugated from targeted proteins. Previous studies have demonstrated that UBP43(USP18) can act as an ISG15 specific deconjugating enzyme⁷. Therefore one approach to increase ISG15 conjugation would be to inhibit the activity of UBP43. In fact, this strategy of increasing ISGylation to study the effects of ISG15 modification was the logic behind the generation and characterization of UBP43^{-/-} mice. Interestingly, while UBP43^{-/-} mice could be generated on a mixed genetic background, it was found that backcrossing UBP43^{-/-} mice to an inbred C57BL/6 background resulted in embryonic lethality (data not shown)⁸. Though viable, these UBP43^{-/-} mice developed hydrocephalous and did not survive past 20 weeks of age. While UBP43^{-/-} mice displayed increased protection against both viral and bacterial infections, they also exhibited

hypersensitivity to poly(I:C) as they display increased lethality compared to WT mice after intraperitoneal injection of poly(I:C) ^{9; 10; 11}. Microarray analysis of UBP43^{-/-} cells showed that these cells had a global increase in the expression of IFN stimulated genes compared to WT cells ¹². Taken together, these data were originally interpreted as demonstrating that ISG15 conjugation augments the IFN response.

However, a careful re-evaluation of UBP43^{-/-} mice revealed that UBP43 has a second function that confounds the interpretation of the initial UBP43^{-/-} mouse characterization. When UBP43^{-/-} mice were bred onto the ISG15^{-/-} background, it was discovered that UBP43^{-/-} xISG15^{-/-} mice retained a hypersensitive interferon response compared to WT mice, and still developed hydrocephalus ¹¹. Further re-evaluation of UBP43 function found that UBP43 can compete with JAK1 for binding to the type I interferon receptor 2 (IFNAR2), and thus inhibit IFN signaling ¹³. This inhibition of IFN signaling was shown to occur independent of the deconjugating activity of UBP43. Consequently, the upregulation of ISG expression, and even the increased level of ISG15 conjugates, observed in the UBP43^{-/-} mice cannot be directly attributed to the absence of UBP43 deconjugation activity. Therefore it remains to be determined whether enzymatic inhibition of UBP43 would increase protection against virus infection.

To date, increased susceptibility to IBV is one of the strongest phenotypes that has been observed in ISG15^{-/-} mice. While the increased viral loads observed in ISG15^{-/-} mice suggests that ISG15 acts by inhibiting virus replication, no difference in IBV replication was observed in WT and ISG15^{-/-} murine embryonic fibroblasts (MEF) ⁵. This discrepancy between the effects of ISG15 on IBV replication *in vivo* and *in vitro* could be explained if the *in vivo* inhibition of virus replication is not cell intrinsic but, rather, is mediated by ISG15 regulation of the innate

immune response. However, previous evaluation of IBV replication in WT and ISG15^{-/-} bone marrow chimeric mice suggested that ISG15 expression within the radio-resistant compartment mediated the important function of ISG15 during infection. Only irradiated/reconstituted WT mice were able to control virus replication and they could do so irrespective of the genotype of the bone marrow with which they were reconstituted⁶. While this does not rule out ISG15 regulation of the immune response as the key mediator for inhibition of IBV replication, we hypothesized that ISG15 was directly antagonizing virus replication in infected cells. Influenza virus replicates both in the bronchiolar epithelium and in alveolar epithelial cells *in vivo*. While our lab previously reported no difference in IBV replication in ISG15^{-/-} MEFs, these cells are not an ideal cell line for studying influenza virus as they did not support robust replication⁵.

Thus we set out to determine whether ISG15 can directly antagonize IBV replication *in vitro* and whether manipulation of the ISG15 conjugation pathway to increase ISG15 conjugation will provide increased protection from IBV infection. To address these questions we evaluated the effects of ISG15 on IBV replication in primary murine trachea epithelial cell cultures (mTEC). Additionally, we evaluated the effects of manipulating ISG15 levels by evaluating influenza B virus infection both in ISG15 heterozygous mice and in a novel mouse, produced in the lab of Dr. Klaus-Peter Knobeloch, that expresses an enzymatically dead mutant version of UBP43.

RESULTS

ISG15 directly antagonizes IBV replication

Previous studies have determined conditions for culturing primary murine trachea epithelial cells at air-liquid interface *in vitro* to yield differentiated heterogeneous cell cultures. These cultures closely resemble the heterogeneous population of cells that make up the trachea epithelium seen *in vivo* and have been demonstrated to support robust influenza A virus replication^{14; 15}. In order to evaluate the effects of ISG15 on IBV replication in a permissive cell type, we generated mTEC cultures from WT and ISG15^{-/-} mice. We observed no difference in the ability of ISG15^{-/-} cultures to proliferate, to form tight junctions capable of maintaining air-liquid interface, or to differentiate into ciliated cells (data not shown). These cultures are responsive to type I interferon as both WT and ISG15^{-/-} cultures induced the expression of ISG54 after interferon β stimulation. Importantly, WT cultures also expressed ISG15 after interferon β stimulation (Figure 2.1A,B). Both WT and ISG15^{-/-} mTEC cultures supported robust IBV replication. In non-manipulated cultures, while no difference in virus replication was observed at early times after infection, a small but statistically significant increase in IBV levels was observed in ISG15^{-/-} cultures at late time points after infection (Figure 2.1B). Pre-treatment of cultures with interferon β for 24 hours prior to infection amplified this difference, resulting in an ~8 fold increase in virus replication in ISG15^{-/-} cultures compared to WT cultures at 48 hours post infection, and an ~30 fold increase at 72 hours post infection (Figure 2.1C). This data shows that in a biologically relevant cell culture system, ISG15 can restrict IBV replication *in vitro*.

ISG15 heterozygous mice display increased susceptibility to IBV infection

As our mTEC data suggested that ISG15 can directly antagonize IBV replication, we next wanted to evaluate whether the expression level of ISG15 affects its capacity to function as an antiviral protein. To do this we evaluated the susceptibility of ISG15 heterozygous (ISG15^{+/-}) mice to IBV infection. We infected WT, ISG15^{-/-}, and ISG15^{+/-} mice with 1.24×10^4 PFU of influenza B/Yamagata/88 and either monitored mice for weight loss or sacrificed mice three days post infection to evaluate virus titers in the lungs. We found that virus burden in ISG15^{+/-} mice at three days post infection fell at an intermediate level, ~10 fold greater than the viral burden of WT mice but ~10 fold lower than the viral burden of ISG15^{-/-} mice (Figure 2.2A). The ISG15^{+/-} mice also displayed an intermediate degree of weight loss after infection as compared to WT and ISG15^{-/-} mice (Figure 2.2B). WT mice did not lose any weight over the course of infection. ISG15^{-/-} mice began losing weight around 4-5 days post infection and lost ~25-30% body weight by day 8 post infection. Whereas ISG15^{+/-} mice did not start losing weight until 5-6 days post infection and only lost ~5-10% body weight before regaining weight on day 8. These data strongly suggest that the extent of antiviral activity provided by ISG15 is directly correlated to its expression level.

USP43^{C61A/C61A} mouse

The ability of ISG15 to inhibit virus replication in a dose dependent manner suggests that manipulation of ISG15 expression levels could be a viable antiviral therapeutic strategy. Our lab has previously demonstrated that the antiviral activity of ISG15 against IBV is dependent on its ability to form conjugates with other proteins, as Ube1L^{-/-} mice also display increased lethality compared to WT mice after IBV infection ⁶. Given these observations it stands to reason that

specifically increasing the amount of ISG15 conjugates might provide increased protection against IBV and possibly other viruses. Thus we wanted to test whether inhibiting ISG15 deconjugation through the inhibition of UBP43 would provide increased protection against IBV infection.

In order to test this hypothesis, Dr. Klaus-Peter Knobeloch created a novel mouse expressing an enzymatically dead version of UBP43. To generate this mouse, a targeting vector was designed to undergo homologous recombination with the endogenous UBP43 gene such that the nucleotide sequence coding for the catalytic cysteine residue (amino acid number 61) was replaced with a nucleotide sequence encoding an alanine residue (Figure 2.3A). The vector was electroporated into embryonic stem cells, and cells that underwent homologous recombination were injected into C57BL/6 embryos. Germline transmission of the c61a mutation and subsequent breeding achieved homozygous UBP43^{C61A/C61A} mice expressing an enzymatically dead version of UBP43 from the endogenous UBP43 locus (Figure 2.3B,C). The UBP43c61a mutant appeared to retain its ability to inhibit IFN signaling as indicated both by the lack of interferon hypersensitivity observed after poly(I:C) infection and by the development of interferon refractoriness after interferon α injection in UBP43^{C61A/C61A} mice (**Figure 2.3D,E**).

Susceptibility of UBP43^{C61A/C61A} mouse to influenza B virus

To evaluate whether increasing the levels of ISG15 conjugates by UBP43 protease inactivation can increase antiviral protection, UBP43^{C61A/C61A} mice were infected with influenza B/Yamagata/88 virus. As WT mice do not develop severe disease symptoms after IBV infection, we evaluated lung viral loads to assess resistance to IBV infection. We found that three days

post infection the UBP43^{C61A/C61A} mice had a ~10-fold decrease in viral loads as compared to WT mice (Figure 2.4), suggesting that UBP43^{C61A/C61A} mice do exhibit increased resistance to infection

To determine whether increasing ISGylation directly affects IBV replication in infected cells, we evaluated viral growth in UBP43^{C61A/C61A} mTECs. In non-stimulated mTEC virus growth kinetics was similar in WT and UBP43^{C61A/C61A} mTECs though we detected a small decrease in virus replication at 72 hours post infection in UBP43^{C61A/C61A} mTEC (Figure 2.1C). When mTEC were pretreated with interferon β for 24 hours prior to infection, we observed an increase in the resistance of UBP43^{C61A/C61A} cultures to IBV replication as compared to WT cultures, suggesting that increasing ISG15 conjugation through the inhibition of UBP43 enzymatic activity provides increased antiviral activity (Figure 2.1D).

To verify that UBP43^{C61A/C61A} mTECs produce elevated ISG15 conjugates after type I interferon stimulation, interferon β stimulated mTEC lysates were evaluated for ISG15 expression by western blot (Figure 2.5A). Both WT and UBP43^{C61A/C61A} cultures expressed ISG15 and formed ISG15 conjugates after interferon stimulation. Densitometry analysis showed that the ratio ISG15 conjugates to free ISG15 was greater in UBP43^{C61A/C61A} lysates than in WT lysates, suggesting that loss of UBP43 enzymatic activity does result in an accumulation of the pool of ISG15 conjugates (Figure 2.5B). Interestingly, however, we observed that in addition to producing more ISG15 conjugates UBP43^{C61A/C61A} cultures expressed a higher level of total ISG15 protein than WT cultures. Both the increased accumulation of ISG15 conjugates and the increased total expression of ISG15 was also observed between unstimulated WT and unstimulated UBP43^{C61A/C61A} mTEC cultures. To evaluate whether this increase in ISG15 expression in UBP43^{C61A/C61A} mTEC was specific for ISG15 or might be reflective of a general

misregulation of interferon stimulated genes (ISG), we evaluated the expression levels of ISG56 and ISG54 by western blot. We found that both ISG56 and ISG54 were also elevated in UBP43^{C61A/C61A} mTEC compared to WT mTEC (Figure 2.5 A,B,C).

We next wanted to evaluate whether there was an increase in ISG transcript levels, or whether this increased accumulation of ISG proteins might be a result of post-translational regulation of ISG protein stability. mTEC cultures were stimulated with interferon β for 24 hours at which point RNA was harvested from these cultures and analyzed by RT-qPCR. UBP43^{C61A/C61A} cultures had increased levels of ISG15 transcripts compared to WT cultures both at baseline and after interferon stimulation (Figure 2.6 A,B,C). Again, this phenotype was not specific for ISG15, as both ISG54 and ISG56 transcript levels were also elevated in UBP43^{C61A/C61A} cultures compared to WT cultures.

Elevated expression of ISGs and increased antiviral activity in UBP43^{C61A/C61A} mice and cells is dependent on ISG15 expression

UBP43 has previously been shown to regulate interferon signalling independent of its ISG15 deconjugation activity¹³. Therefore, we wanted to determine whether or not the elevated ISG expression in UBP43^{C61A/C61A} mTEC was dependent on the expression of ISG15. To test this, we bred UBP43^{C61A/C61A} mice onto the ISG15^{-/-} background and analyzed mTEC from these UBP43^{C61A/C61A} X ISG15^{-/-} mice for ISG production after interferon stimulation. We found that both the transcript and protein levels of ISG56, and ISG54 were not elevated as seen in the UBP43^{C61A/C61A} cells (Figure 2.5,2.6). This suggests that the increased ISG expression in

UBP43^{C61A/C61A} mTEC is dependent on ISG15 and not a result of a misregulation of interferon signalling due to an effect of the c61a mutation on another function of UBP43.

We next evaluated the resistance of UBP43^{C61A/C61A} X ISG15^{-/-} mice and mTEC cultures to IBV infection. Three days post infection with IBV, UBP43^{C61A/C61A} X ISG15^{-/-} mice exhibited elevated viral titers in their lungs compared to WT mice (Figure 2.4). The virus burdens in these mice were comparable to the viral loads observed in ISG15^{-/-} mice. Similarly, after interferon pretreatment, UBP43^{C61A/C61A} X ISG15^{-/-} mTEC cultures supported IBV replication to similar levels as observed in ISG15^{-/-} mTEC cultures (Figure 2.7). These results show that the increased protection from IBV observed in UBP43^{C61A/C61A} mice is dependent on ISG15.

DISCUSSION

Here we have shown that in a biologically relevant cell type, ISG15 can restrict influenza B virus replication in cell culture, suggesting that ISG15 does act as an anti-viral molecule to directly affect some step in the virus life cycle. These results are consistent with our lab's previous bone marrow chimera data suggesting that ISG15 expression in the radio-resistant compartment confers protection against IBV⁶. While we believe that this inhibition of IBV replication observed in cell culture is biologically relevant and occurs during infection *in vivo*, it is not clear whether the ~30-fold increase in virus replication in ISG15^{-/-} mTEC completely accounts for the ~100- to 1000-fold increase in virus burden that is observed in ISG15^{-/-} mice. Our results do not rule out a role for the immune response in contributing to the ISG15-mediated protection observed *in vivo*.

The intermediate levels of viral burden and weight loss observed after IBV infection in ISG15^{+/-} mice relative to WT and ISG15^{-/-} mice suggest that ISG15 protects against IBV in a dose dependent manner. As far as we are aware, this is the first evidence to date to suggest that the level of ISG15 expression *in vivo* is directly correlated to the level of protection conferred against virus infection. This observation has important real world implications as a study looking for genetic determinants of Mendelian susceptibility to mycobacterial disease discovered three patients who had mutations rendering them ISG15 deficient¹⁶. It is unclear whether these ISG15 deficient individuals exhibit increased susceptibility to viral infections. It was determined based on the presence of serum antibodies that these patients had been previously infected with influenza A virus and other common childhood viruses, and the authors suggested that this seropositivity demonstrated that ISG15 deficiency did not render these patients more susceptible to viral infection. The discovery of these ISG15 deficient individuals shows that, as in mice, ISG15 is not an essential gene in humans, and ISG15 deficiency does not critically immunocompromise an individual. However it is not clear what “dose” of virus these individuals were exposed to, or whether these individuals exhibited increased disease during the acute infection. ISG15^{-/-} mice are by no means immunocompromised, and while ISG15^{-/-} mice exhibit increased lethality after viral infection, a sufficient dose of virus must be given before this susceptibility can be observed. Knowing that ISG15 deficiency can occur in humans, our results suggest that in addition to ISG15 deficiency, ISG15 heterozygosity, or *trans* mutations affecting ISG15 expression levels might also underlie increased disease susceptibility to viral infection.

Ubiquitin deconjugases play an important role in controlling the ubiquitin-mediated regulation of biological pathways¹⁷. These deconjugating enzymes can fine-tune the specificity

of ubiquitination through their own specificity for target protein deconjugation. In addition to displaying specificity for particular conjugated target proteins, these deconjugating enzymes also can display specificity for particular ubiquitin-like modifiers. UBP43 was recently shown to have negligible affinity for ubiquitin compared to ISG15¹⁸. This specificity supports the possibility that small molecule inhibitors could potentially be developed to specifically inhibit UBP43. The UBP43^{C61A/C61A} mouse represents the first insight into the effects of specifically inhibiting ISG15 deconjugation *in vivo*.

The viability of UBP43^{C61A/C61A} mice and their lack of hydrocephalous development suggests that the regulation of interferon signaling through the binding of UBP43 to IFNAR2 is largely unaffected by the c61a mutation. UBP43^{C61A/C61A} mice displayed decreased viral loads compared to WT mice 3 days after infection with IBV, and IBV replication was inhibited in UBP43^{C61A/C61A} mTEC compared to in WT mTEC. These data show that increasing ISG15 conjugation through the inhibition of UBP43 does provide increased protection against IBV. However, we found that in addition to increasing the ratio of ISG15 conjugates to free ISG15, the UBP43^{C61A/C61A} mTEC also displayed increased levels of total ISG15 compared to WT mTEC. After further evaluation we found that at least a subset of other ISGs were also upregulated in UBP43^{C61A/C61A} mTEC. Evaluation of UBP43^{C61A/C61A} XISG15^{-/-} mice and mTEC showed that this increased ISG expression and the increased protection from viral infection was dependent on ISG15. As a result of the dual effects of the UBP43c61a mutation, we cannot determine whether the ISG15 dependent protection is being mediated directly through increased ISG15 conjugation, through the increased expression of other ISGs, or through the combined effects of both. Furthermore, we also cannot determine whether the observed effects

are due to increased ISG15 conjugation as a result of increased ISG15 expression, or increased ISG15 conjugation as a result of the lack of ISG15 deconjugation.

It is important to distinguish that while the result of UBP43 inhibition is usually interpreted as increasing ISG15 conjugates, there is a fundamental difference between increasing the amount of conjugates through higher expression of ISG15 and increasing the pool of ISG15 conjugates by preventing deconjugation. The fate of an ISGylated protein is not well understood, and it is possible that the increased ISG expression observed in UBP43^{C61A/C61A} mTEC is a result of a stress response to the accumulation of ISG15 conjugates rather than a direct role for ISG15 in the regulation of ISG expression. It is interesting, however, that the two functions ascribed to UBP43, deconjugation of ISG15 and deconjugation-independent binding to IFNAR2, both have the effect of inhibiting ISG induction. While the differences we observed in ISG expression in UBP43c61a mTEC were small, our results show that the mutation results in biologically relevant phenotypes. The observed increase of both ISG15 conjugates and other ISG expression levels suggests that this UBP43 inhibition might confer increased protection against other ISG15 sensitive viruses, such as vaccinia, as well as additional viruses that are restricted by other ISGs.

Further investigation is needed to determine whether the UBP43c61a mutation's effect on ISG expression is a generalizable effect or whether this might be specific for mTEC. While we noted increased ISG15 transcript expression in UBP43^{C61A/C61A} cells after interferon stimulation, we also observed increased expression in non-stimulated UBP43^{C61A/C61A} cells. The actual fold increase in transcript expression between non-treated and interferon stimulated cultures of the same genotype was not different between WT and UBP43^{C61A/C61A} cells (Figure 2.6D). mTEC cultures are differentiated heterogenous populations of cells. Thus the increased ISG expression

could reflect an increase in the baseline expression of ISGs in all cells or an increase in the number of interferon responding cells in the UBP43^{C61A/C61A} cultures. Evaluation of the number of ISG15 expressing cells versus the intensity at which cells express ISG15 could be performed by flow cytometry analysis to address this question. It will also be important to quantitatively assess ISG15 expression in other UBP43c61a cell types to evaluate how universal this phenotype is.

Previous studies have reported no effect of ISGylation on interferon signaling or downstream ISG expression, however several aspects of these studies might have resulted in a role for ISG15 in ISG regulation being overlooked. First, these studies have all been based on non-quantitative northern blot and western blot analyses. The differences that we observed in ISG56 and ISG54 expression were small but consistent. It is possible that this effect might be missed without careful normalization and quantification of northern blot experiments. Second, previous experiment used relatively high doses of interferon β , 100U/ml. Our analyses were performed using 30U/ml. High doses of interferon stimulation may saturate ISG induction and make it harder to detect a small augmentation of ISG induction mediated by ISG15. Third, previous analyses of the effect of ISG15 on ISG expression were performed in embryonic fibroblasts. If the effects we observed in UBP43^{C61A/C61A} mTEC are cell type specific, analysis of ISG15 in MEFs could have missed a biologically important role of ISG15 in regulation of gene expression. The discrepancies between both our methods and results with those of the initial studies characterizing of the ISG15^{-/-} and Ube1L^{-/-} cells suggests that a quantitative reevaluation of the effects of ISG15 conjugation on gene expression is warranted.

METHODS

Mice

WT C57BL/6J mice originally purchased from Jackson Laboratory (Bar Harbor, ME) were bred in a mouse facility at Washington University in St. Louis. Generation of ISG15^{-/-} mice and backcrossing of ISG15^{-/-} mice to the C57BL/6J background have been previously described¹⁹.

UBP43^{C61A/C61A} mice were generated as by the laboratory of Dr. Klaus-Peter Knoblach (Freiburg University, Germany) as described below. The mice were backcrossed onto the C57BL/6J background and assessed by SNP analysis (Taconic) to be >99% C57BL/6.

UBP43^{C61A/C61A} × ISG15^{-/-} mice were generated by breeding *UBP43*^{C61A/C61A} mice to ISG15^{-/-} mice.

*Generation of *USP43*^{C61A/C61A} mice*

USP18 clone (RPCI-21 332G10) was used for construction of the targeting vector (TV). A KpnI-fragment containing the Cys61 coding region was subcloned and the codon for Cys61 5'-TGT-3' was mutated to 5'-GCT-3' encoding alanine. A 5'-homology arm and the 3'-homology with the mutation were inserted in pPNT-frt3 up- and downstream of the neomycin resistance gene (neo), respectively. The resulting TV was linearized and transfected into E14.1 ES cells. Positive ES cells were identified by Southern blotting and verified by sequencing. ES cells were injected into C57BL/6 morulae and germline chimeras were interbred with a FLP deleter strain to eliminate neo.

Poly(I:C) and Interferon- α injections

Mice were injected intraperitoneally with 5µg of poly(I:C) (Invivogen) per gram of bodyweight or 1000U interferon-α (Calbiochem) per gram of bodyweight. Mice injected with poly(I:C) were monitored for survival. Mice injected with interferon-α were given a second injection 8 hours after the first and interferon-α levels in the serum were assessed by ELISA (PBL Assay Science).

Influenza virus infections

For influenza B virus experiments 6 to 8 week old male mice were infected intranasally with 1.24×10^4 PFU of influenza B/Yamagata/88 diluted to 25 µl total volume in PBS. Mice were monitored for weight loss and disease progression daily. For the determination of viral titers, infected mice were sacrificed on day 3 post infection and the right three lobes of the mouse's lungs were collected in 1ml of PBS. Lungs were homogenized in a Roche MagNA Lyser using 1.0mm diameter zirconia/silia beads (BioSpec Products), and viral loads in lung homogenates were determined by plaque assay on MDCK cells as previously described⁵.

Murine tracheal epithelial cultures

Primary mTECs were generated from the tracheas of mice as previously described¹⁴. For viral growth curves, mTECs from WT, ISG15^{-/-}, USP18^{C61A/C61A} or ISG15^{-/-} USP18^{C61A/C61A} mice were either left untreated or pre-treated with 30U/ml of IFN-β (PBL Assay Science) in the basolateral chamber. After 24 h, the basolateral chamber was washed two times with PBS and media with no IFN-β was added back to basolateral chamber. Cells were then infected by adding 9.0×10^5 PFU of influenza B/Yamagata/88 in 0.1 ml of DMEM with 1% penicillin and 1% streptomycin (1%P/S) to the apical chamber. After 1 h the virus containing media was removed and the apical chamber was washed three times with 0.2 ml DMEM 1%P/S. Then 0.1ml of

DMEM 1% P/S was added back to apical chamber. Cells were incubated at 37° C and at various times apical media was collected assayed for viral titers, and replaced with 0.1ml fresh DMEM 1%P/S to allow infection to continue. Apical media were analyzed for virus titer by plaque assay on MDCK cells.

Western Blots

For western blot analysis, mTEC were lysed in 100-150 ul of RIPA buffer containing protease inhibitor (Sigma Aldrich P8340). Lysates were analysed for ISG15 using anti-ISG15 antiserum²⁰. Lysates were also analyzed with the following commercial antibodies, anti-ISG54 (ThermoScientific PA3-845), anti-ISG56 (ThermoScientific PA3-846), anti-β actin (Sigma AC-74). Western blots were analyzed by densitometry using Adobe Photoshop CS4 histogram analysis.

RT-qPCR

RNA was isolated from mTEC using Qiagen RNeasy Mini Kit. Transcript levels in isolated RNA was analyzed using TaqMan One-Step RT-PCR (Applied Biosystems 4309169). Reactions were run using 50 ng RNA, and the following probes were used to measure transcript levels: GAPDH (IDT, Mm.PT.39a.1), ISG15 (Applied Biosystems, Mm01705338_s1), ISG54 (Applied Biosystems, Mm00492606_m1), ISG56 (Applied Biosystems, Mm00515153_m1). Relative transcript levels were determined by normalizing to GAPDH (deltaCt). Fold differences (deltadeltaCt) were determined using the average deltaCt of the reference condition.

Statistical analysis

Statistical analyses were evaluated using the Mann-Whitney U test. Error bars in figures represent the SEM.

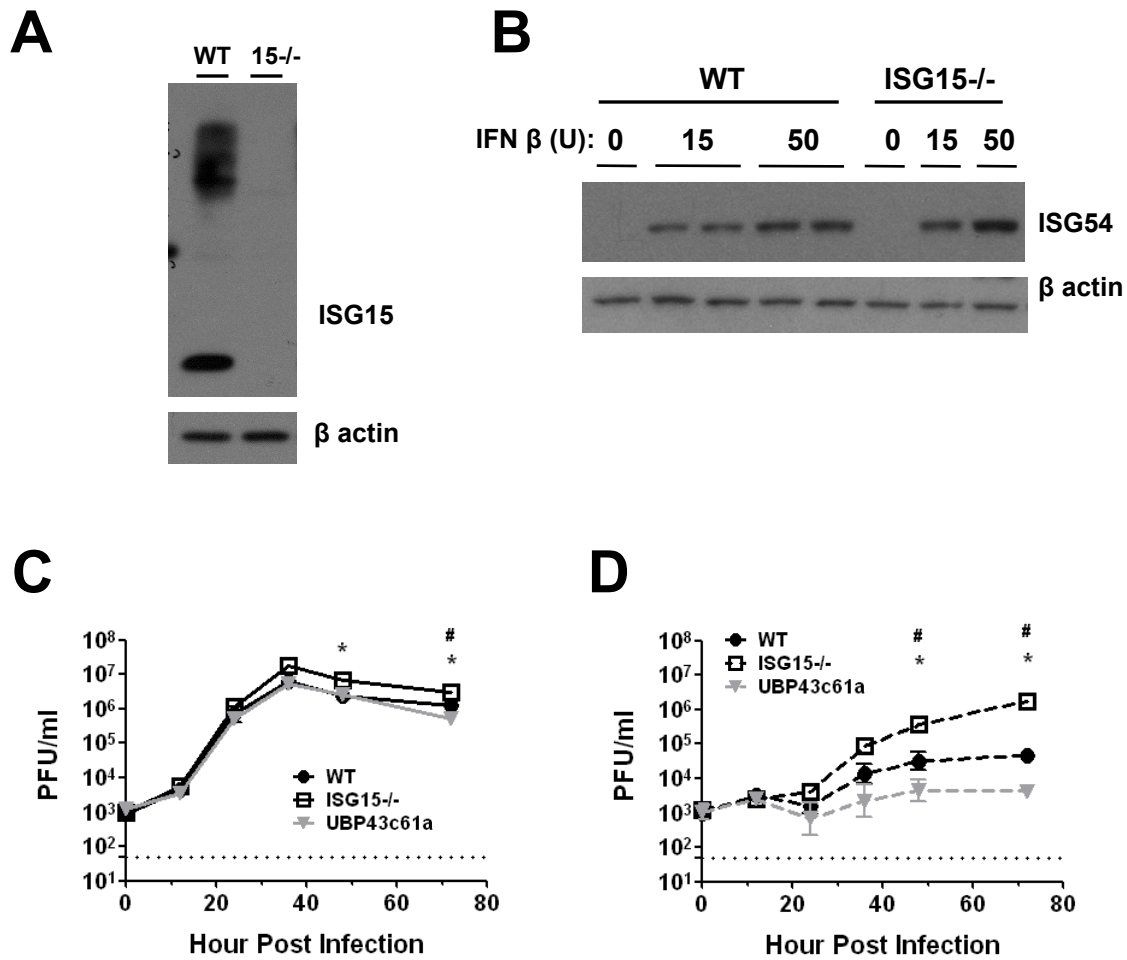


Figure 2.1. ISG15 restricts influenza B virus replication in primary mTEC cultures

(A,B) mTEC cultures generated from WT and ISG15^{-/-} mice were left untreated or treated with 100U/ml (A) or indicated concentration (B) of interferon β for 24 hours. Lysates were harvested 24 hours after interferon stimulation and protein expression was assessed by western blot. mTEC generated from WT, ISG15^{-/-}, and UBP43^{C61A/C61A} were either left untreated (C) or stimulated with 30U/ml of interferon β for 24 hours (D) prior to infection with 9×10^5 influenza B/Yamagata/88. Virus titers in the apical media were assessed over time by plaque assay on

MDCK cells. Data was generated from 2 independent infections using 2 different preparation of mTEC, 3 replicates per infection.

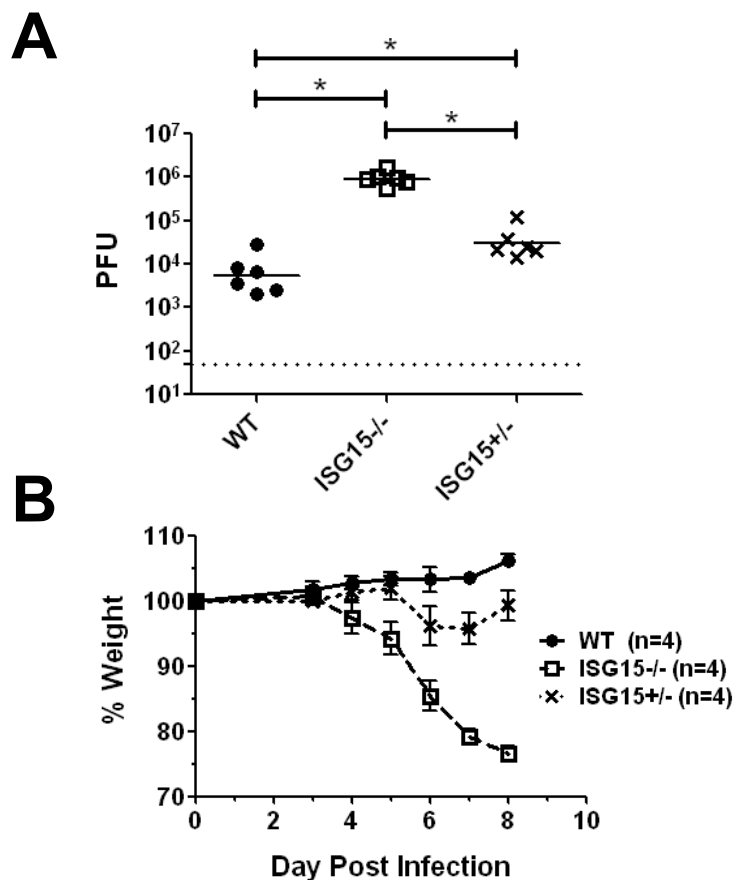


Figure 2.2. ISG15 heterozygous mice exhibit intermediate disease relative to WT and ISG15^{-/-} mice after influenza B virus infection

WT, ISG15^{-/-}, and ISG15^{+/-} were infected with 1.24×10^4 PFU of influenza B/Yamagata/88 and were either monitored for weight loss (**A**) or sacrificed 3 days post infection to assess viral loads in the lungs (**B**). Data in both (**A**) and (**B**) were generated from 2 independent infections.

* $p < 0.05$.

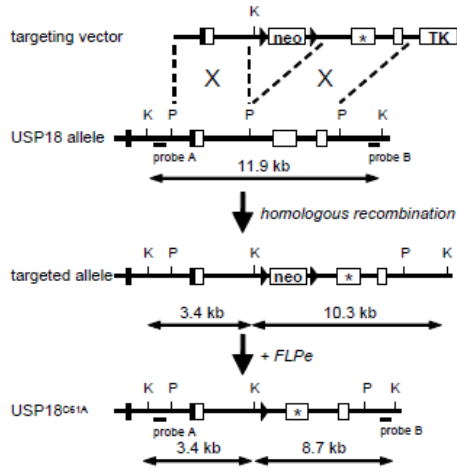
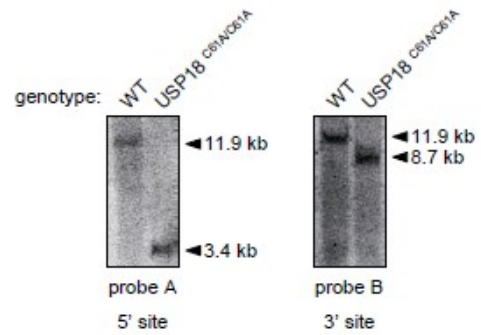
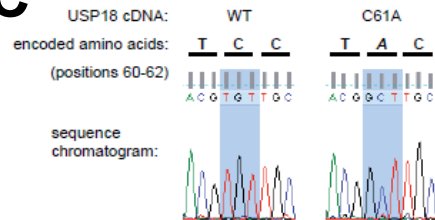
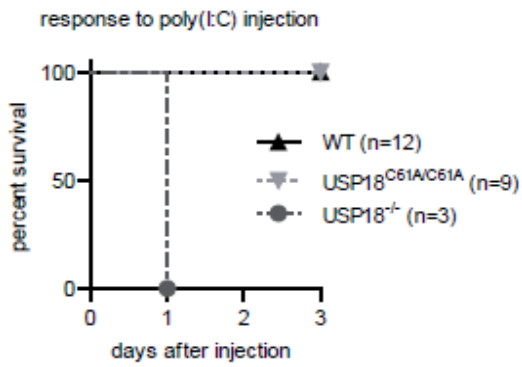
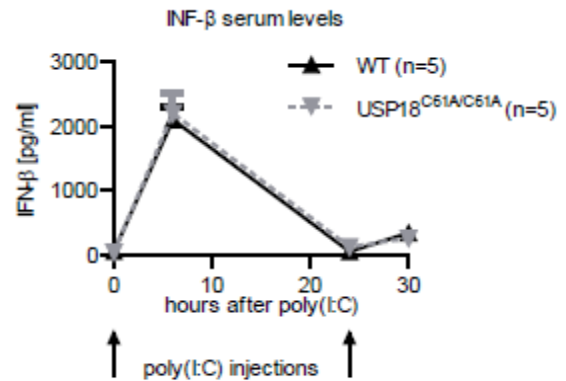
A**B****C****D****E**

Figure 2.3. UBP43^{C61A/C61A} mice are viable, retain UBP43 inhibition of interferon signaling
(A) Schematic of knock-in targeting strategy. **(B)** Southern blot analysis UBP43 locus in WT and UBP43^{C61A/C61A} mice. **(C)** Chromatogram of UBP43 locus sequencing of cDNA isolated from IFN stimulated bone marrow macrophages. **(D)** WT, UBP43^{C61A/C61A}, and UBP43^{-/-} mice were injected with poly(I:C) and monitored for lethality. **(E)** Serum interferon- α levels of mice injected with interferon- α as indicated were evaluated by ELISA. **(This data was generated in the lab of Dr. Klaus-Peter Knobeloch. Figures denotes UBP43 as USP18)**

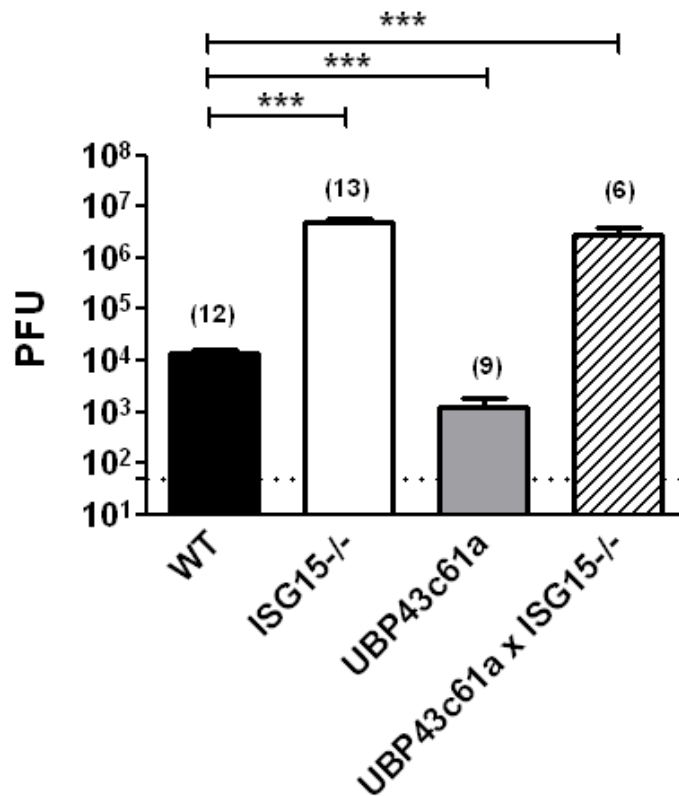


Figure 2.4. UBP43c61a mutation increases protection from influenza B virus infection in vivo in an ISG15 dependent manner

WT, ISG15^{-/-}, UBP43^{C61A/C61A}, or UBP43^{C61A/C61A} X ISG15^{-/-} mice were infected with 1.24×10^4 PFU of influenza B/Yamagata/88. Mice were sacrificed 3 days post infection and viral loads in the lungs were determined by plaque assay on MDCK cells. *** p<0.001

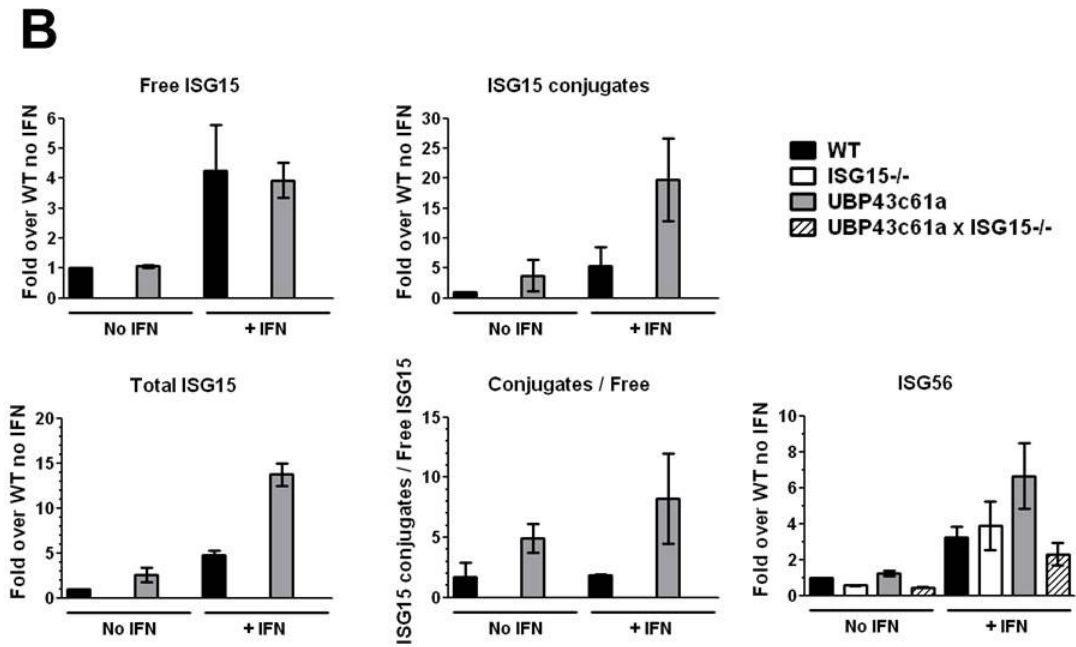
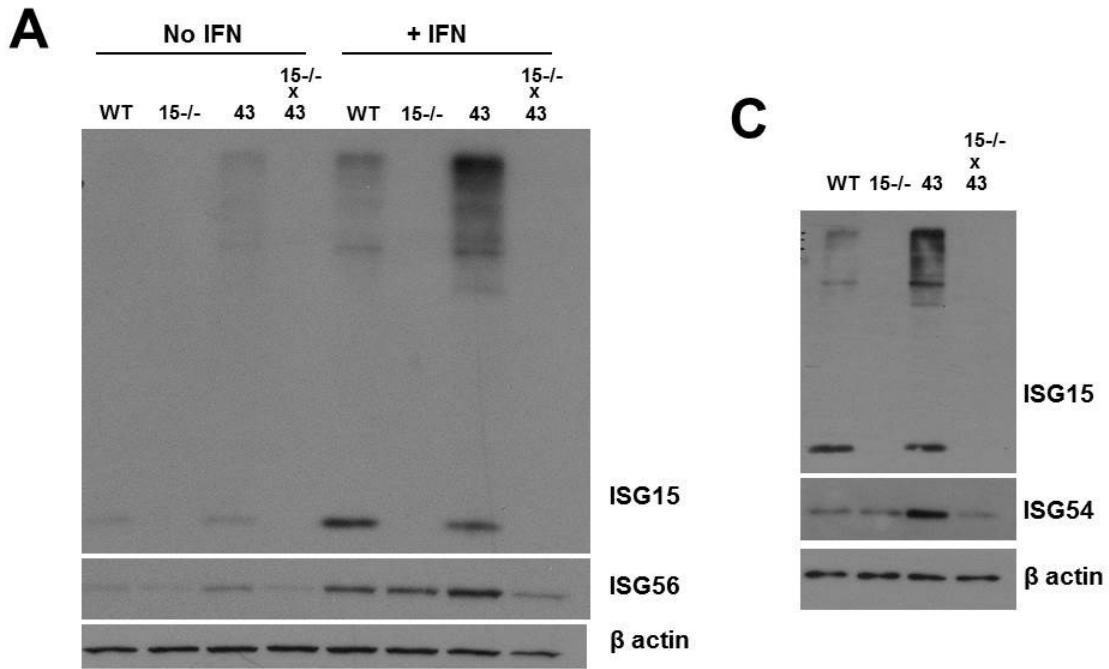


Figure 2.5. UBP43c61a mutation increases the pool of ISG15 conjugates but also increases interferon stimulated gene protein levels in a conjugation dependent manner.

mTEC generated from WT, ISG15^{-/-}, UBP43^{C61A/C61A}, or UBP43^{C61A/C61A} XISG15^{-/-} mice were either left untreated or stimulated with 30U/ml of interferon β for 24 hours and protein levels were assessed by western blot. 2 independent interferon stimulations were performed using 1 preparation of mTEC. **(A)** One representative western blot of two. **(B)** Relative protein expression in **(A)** and a duplicate experiment were assessed by densitometry analysis. **(C)** mTEC were stimulated with 100U/ml of interferon β for 24 hours and protein levels were assessed by western blot.

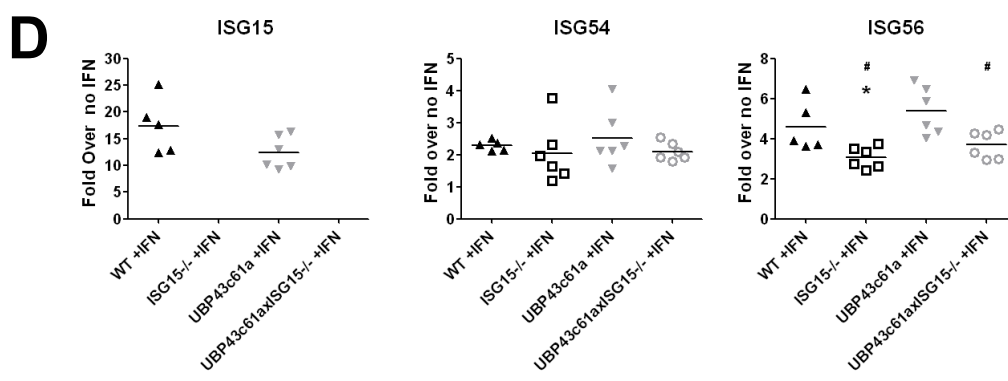
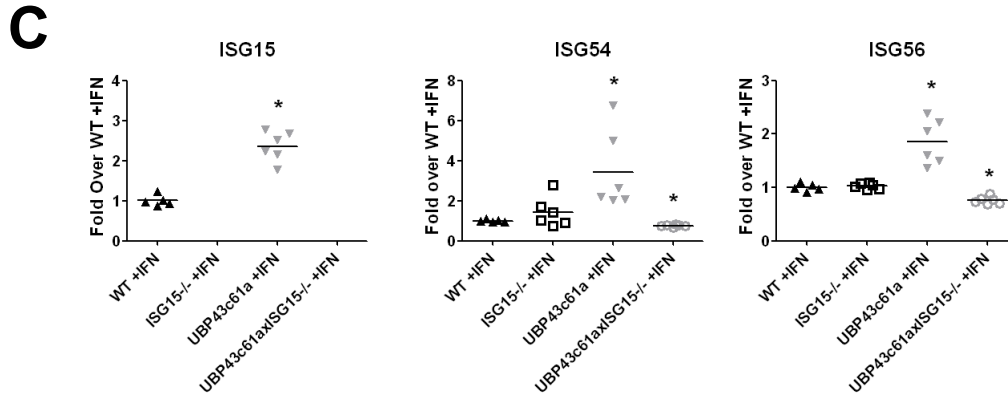
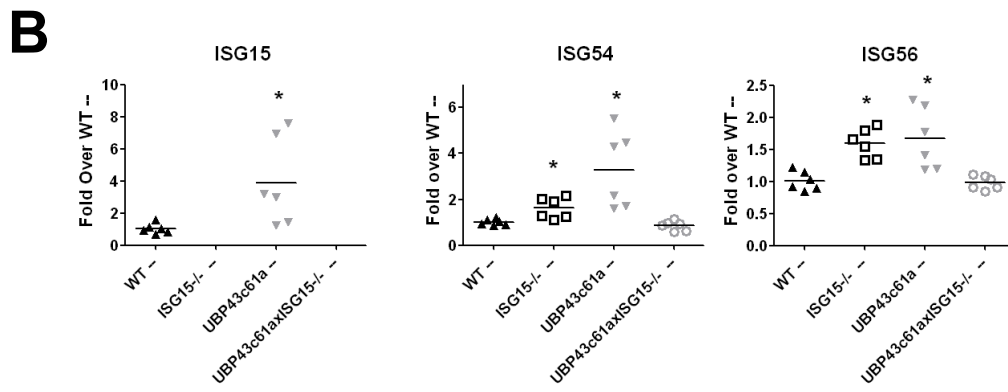
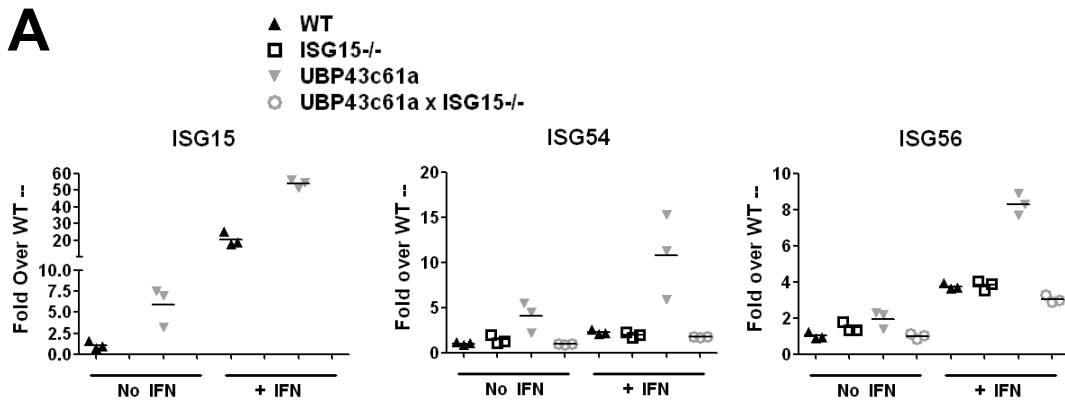


Figure 2.6. UBP43c61a mutation causes an elevation in interferon stimulated gene transcript levels in an ISG15 dependent manner.

RNA was isolated from WT, ISG15^{-/-}, UBP43^{C61A/C61A}, or UBP43^{C61A/C61A} XISG15^{-/-} mTEC that were either left untreated or stimulated with 30U/ml of interferon β for 24 hours. RNA was analyzed by RT-qPCR to assess interferon stimulated gene transcript levels. Data was generated from 2 independent interferon stimulations using 2 different preparations of mTEC, 2-3 replicates per experiment. **(A)** Transcript levels in all conditions were assessed relative to the levels in untreated WT cultures. Data in **(A)** is from one representative experiment. **(B)** Transcript levels in untreated cultures relative to WT untreated cultures. **(C)** Transcript levels of interferon stimulated cultures relative to WT interferon stimulated cultures. **(D)** Transcript levels of interferon stimulated cultures relative to levels in untreated cultures of the same genotype. Data from both stimulation experiments were pooled in **(B-D)**.

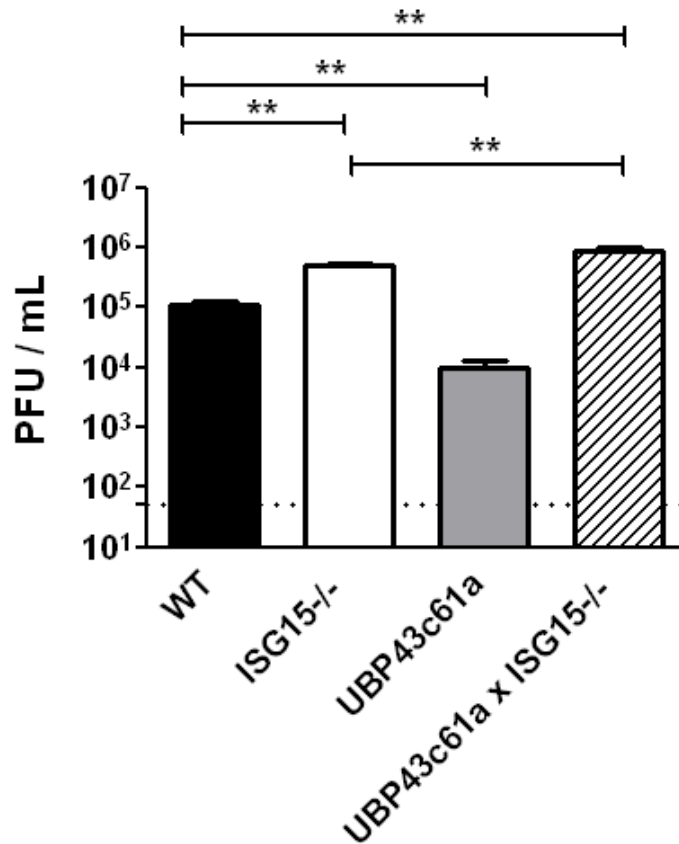


Figure 2.7. Increased protection against influenza B virus in UBP43^{C61A/C61A} mTEC is dependent on ISG15.

mTEC generated from WT, ISG15^{-/-}, UBP43^{C61A/C61A}, or UBP43^{C61A/C61A} x ISG15^{-/-} mice were treated with 30U/ml of interferon β for 24 hours and then infected with 9×10^5 PFU influenza B/Yamagata/88. Virus titers in the apical media at 48 hours post infection were assessed by plaque assay on MDCK cells. Data was generated from 3 independent infections using 2 different preparations of mTEC, 3 replicates per infection. **p<0.01

REFERENCES

1. Korant, B. D., Blomstrom, D. C., Jonak, G. J. & Knight, E., Jr. (1984). Interferon-induced proteins. Purification and characterization of a 15,000-dalton protein from human and bovine cells induced by interferon. *J Biol Chem* 259, 14835-9.
2. Haas, A. L., Ahrens, P., Bright, P. M. & Ankel, H. (1987). Interferon induces a 15-kilodalton protein exhibiting marked homology to ubiquitin. *J Biol Chem* 262, 11315-23.
3. Yuan, W. & Krug, R. M. (2001). Influenza B virus NS1 protein inhibits conjugation of the interferon (IFN)-induced ubiquitin-like ISG15 protein. *EMBO J* 20, 362-71.
4. Sridharan, H., Zhao, C. & Krug, R. M. (2010). Species specificity of the NS1 protein of influenza B virus: NS1 binds only human and non-human primate ubiquitin-like ISG15 proteins. *J Biol Chem* 285, 7852-6.
5. Lenschow, D. J., Lai, C., Frias-Staheli, N., Giannakopoulos, N. V., Lutz, A., Wolff, T., Osiak, A., Levine, B., Schmidt, R. E., Garcia-Sastre, A., Leib, D. A., Pekosz, A., Knobloch, K. P., Horak, I. & Virgin, H. W. t. (2007). IFN-stimulated gene 15 functions as a critical antiviral molecule against influenza, herpes, and Sindbis viruses. *Proc Natl Acad Sci U S A* 104, 1371-6.
6. Lai, C., Struckhoff, J. J., Schneider, J., Martinez-Sobrido, L., Wolff, T., Garcia-Sastre, A., Zhang, D. E. & Lenschow, D. J. (2009). Mice lacking the ISG15 E1 enzyme UBE1L demonstrate increased susceptibility to both mouse-adapted and non-mouse-adapted influenza B virus infection. *J Virol* 83, 1147-51.
7. Malakhov, M. P., Malakhova, O. A., Kim, K. I., Ritchie, K. J. & Zhang, D. E. (2002). UBP43 (USP18) specifically removes ISG15 from conjugated proteins. *J Biol Chem* 277, 9976-81.
8. Ritchie, K. J., Malakhov, M. P., Hetherington, C. J., Zhou, L., Little, M. T., Malakhova, O. A., Sipe, J. C., Orkin, S. H. & Zhang, D. E. (2002). Dysregulation of protein modification by ISG15 results in brain cell injury. *Genes Dev* 16, 2207-12.
9. Ritchie, K. J., Hahn, C. S., Kim, K. I., Yan, M., Rosario, D., Li, L., de la Torre, J. C. & Zhang, D. E. (2004). Role of ISG15 protease UBP43 (USP18) in innate immunity to viral infection. *Nat Med* 10, 1374-8.
10. Kim, K. I., Malakhova, O. A., Hoebe, K., Yan, M., Beutler, B. & Zhang, D. E. (2005). Enhanced antibacterial potential in UBP43-deficient mice against *Salmonella typhimurium* infection by up-regulating type I IFN signaling. *J Immunol* 175, 847-54.
11. Knobloch, K. P., Utermohlen, O., Kissler, A., Prinz, M. & Horak, I. (2005). Reexamination of the role of ubiquitin-like modifier ISG15 in the phenotype of UBP43-deficient mice. *Mol Cell Biol* 25, 11030-4.
12. Zou, W., Kim, J. H., Handidu, A., Li, X., Kim, K. I., Yan, M., Li, J. & Zhang, D. E. (2007). Microarray analysis reveals that Type I interferon strongly increases the expression of immune-response related genes in Ubp43 (Usp18) deficient macrophages. *Biochem Biophys Res Commun* 356, 193-9.
13. Malakhova, O. A., Kim, K. I., Luo, J. K., Zou, W., Kumar, K. G., Fuchs, S. Y., Shuai, K. & Zhang, D. E. (2006). UBP43 is a novel regulator of interferon signaling independent of its ISG15 isopeptidase activity. *EMBO J* 25, 2358-67.
14. You, Y., Richer, E. J., Huang, T. & Brody, S. L. (2002). Growth and differentiation of mouse tracheal epithelial cells: selection of a proliferative population. *Am J Physiol Lung Cell Mol Physiol* 283, L1315-21.

15. Ibricevic, A., Pekosz, A., Walter, M. J., Newby, C., Battaile, J. T., Brown, E. G., Holtzman, M. J. & Brody, S. L. (2006). Influenza virus receptor specificity and cell tropism in mouse and human airway epithelial cells. *J Virol* 80, 7469-80.
16. Bogunovic, D., Byun, M., Durfee, L. A., Abhyankar, A., Sanal, O., Mansouri, D., Salem, S., Radovanovic, I., Grant, A. V., Adimi, P., Mansouri, N., Okada, S., Bryant, V. L., Kong, X. F., Kreins, A., Velez, M. M., Boisson, B., Khalilzadeh, S., Ozcelik, U., Darazam, I. A., Schoggins, J. W., Rice, C. M., Al-Muhsen, S., Behr, M., Vogt, G., Puel, A., Bustamante, J., Gros, P., Huibregtse, J. M., Abel, L., Boisson-Dupuis, S. & Casanova, J. L. (2012). Mycobacterial disease and impaired IFN-gamma immunity in humans with inherited ISG15 deficiency. *Science* 337, 1684-8.
17. Reyes-Turcu, F. E., Ventii, K. H. & Wilkinson, K. D. (2009). Regulation and cellular roles of ubiquitin-specific deubiquitinating enzymes. *Annu Rev Biochem* 78, 363-97.
18. Basters, A., Geurink, P. P., El Oualid, F., Ketscher, L., Casutt, M. S., Krause, E., Ovaa, H., Knobeloch, K. P. & Fritz, G. (2014). Molecular characterization of ubiquitin-specific protease 18 reveals substrate specificity for interferon-stimulated gene 15. *FEBS J* 281, 1918-28.
19. Osiak, A., Utermohlen, O., Niendorf, S., Horak, I. & Knobeloch, K. P. (2005). ISG15, an interferon-stimulated ubiquitin-like protein, is not essential for STAT1 signaling and responses against vesicular stomatitis and lymphocytic choriomeningitis virus. *Mol Cell Biol* 25, 6338-45.
20. Lenschow, D. J., Giannakopoulos, N. V., Gunn, L. J., Johnston, C., O'Guin, A. K., Schmidt, R. E., Levine, B. & Virgin, H. W. t. (2005). Identification of interferon-stimulated gene 15 as an antiviral molecule during Sindbis virus infection in vivo. *J Virol* 79, 13974-83.

Chapter 3

A Novel Mode of ISG15 Mediated Protection from Influenza A Virus and Sendai Virus in Mice.

(Chapter 3 is being submitted, as presented here, to Journal of Virology)

INTRODUCTION

During acute infection, the survival of an organism is dependent on both its ability to inhibit pathogen replication, thus reducing pathogen burden, and its ability to tolerate the ensuing tissue damage incurred both from the pathogen itself as well as from the immune response mounted against the pathogen. Limiting pathogen replication and eventual pathogen clearance is dependent on both the innate and adaptive immune responses. Of the many genes induced after viral infection, type I interferons are among the most rapidly and robustly expressed genes, and play a critical role in modulating the immune response to viral infections.

After detection of viruses through pathogen recognition receptors, type I interferons are released from cells and subsequently bind to their cell surface receptors (IFNAR1/IFNAR2) in both an autocrine and paracrine fashion. Signaling through the type I interferon receptors induces the expression of hundreds of genes classified as interferon stimulated genes (ISG). A subset of ISGs directly inhibit different steps of virus replication, and it is through the collective action of these ISGs that type I interferons convert cells into what has classically been described as an anti-viral state ¹. Additionally, type I interferons play a role in the regulation of both innate and adaptive immune cell responses to infection ². These include their ability to induce NK cell activation, enhance antigen presentation activity by dendritic cells, and aid in the development and maintenance of CD8+ T cell memory and antibody responses. Whether type I interferons play a direct role in disease tolerance is not well understood.

Interferon stimulated gene 15 (ISG15) is one of the most rapidly and robustly induced genes upon type I interferon stimulation^{3; 4}. ISG15 is an ubiquitin-like modifier containing two ubiquitin-like domains that share approximately 30 percent amino acid sequence identity to

ubiquitin. ISG15 is expressed as a 17kD precursor protein that is proteolytically processed at its C-terminus to expose an LRLRGG amino acid motif through which it covalently conjugates to lysine residues of target proteins^{5;6}. ISGylation of target proteins occurs through an enzymatic cascade similar to that of ubiquitin conjugation, involving an E1 activating enzyme, an E2 conjugating enzyme, and an E3 ligase^{7;8;9;10;11;12}. Proteomic studies have identified hundreds of proteins as being ISGylated after interferon stimulation or capable of being ISGylated in an overexpression system^{13;14}. However, the effects of relatively few of these modifications have been studied and it remains unclear what the functional consequence of ISGylation is for most ISGylated targets.

To date, the most striking phenotype that has been described in mice deficient in ISG15 is their increased susceptibility to a number of viruses, ranging from influenza viruses to herpes simplex virus 1 (HSV-1), Chikungunya virus (CHIKV), vaccinia virus, and Sindbis virus^{15;16;17;18}. Consequently, ISG15 has been hypothesized to protect the host from virus induced lethality by acting as an anti-viral molecule and directly inhibiting viral replication. Indeed, initial studies into the mechanism by which ISG15 mediates protection supported a role for ISG15 in directly antagonizing the virus life cycle. Our lab has shown that influenza B virus (IBV) replicates to 100 fold greater levels in the lungs of ISG15^{-/-} deficient mice compared to WT mice¹⁶. This inhibition of replication was dependent on the ability of ISG15 to form conjugates as increased influenza B virus replication was also seen in mice that lack the ISG15 E1 activating enzyme, UBE1L, and thus fail to form ISG15 conjugates¹⁹. Additionally, ISG15 has been shown to inhibit the replication of vaccinia virus both *in vivo* and in tissue culture¹⁸.

Subsequent *in vitro* studies have also implicated ISG15 in having a small antagonizing effect on the replication of influenza A virus, Sendai virus, human papillomavirus, Ebola virus,

and HIV-1 in tissue culture^{20; 21; 22; 23; 24; 25; 26; 27; 28}. However, recent evidence has suggested that the role of ISG15 during infection is not limited to conjugation dependent inhibition of virus replication. ISG15^{-/-} but not UBE1L^{-/-} neonatal mice are more susceptible to CHKV induced lethality than WT mice¹⁷. This increased lethality was not due to increased viral burden as similar viral loads were detected in WT, UBE1L^{-/-}, and ISG15^{-/-} mice. Additionally, ISG15 was not found to affect CHKV replication in tissue culture. Rather, the non-conjugated (“free”) form of ISG15 protected mice against CHKV by regulating cytokine expression during infection. Supporting this role for free ISG15 *in vivo*, recent reports have confirmed that extracellular free ISG15 can activate NK cells *in vitro* and augment the expression of interferon gamma in response to mycobacterium^{29; 30; 31}. The ability of ISG15 to protect mice without having a direct effect on virus replication, and its ability to act as a cytokine, suggests that inhibition of virus replication in tissue culture is not the only measurement that should be used to determine whether ISG15 plays an important role in the host during infection. Given the newly described functions of free ISG15 *in vivo*, a more detailed characterization of the role of ISG15 in different viral infection models is warranted.

It has been previously demonstrated that during influenza B virus infection ISG15 protects the host by reducing viral burden. In this study we sought to determine if ISG15 protected mice by a similar mechanism of action during other respiratory virus infections. We found that both ISG15^{-/-} and UBE1L^{-/-} mice exhibited increased susceptibility to lethality induced by both influenza A virus and Sendai virus infections, demonstrating that this protection requires ISG15 conjugation. However, unlike influenza B virus infection, this protection did not appear to be mediated through the inhibition of virus replication. We also did not observe significant alterations in the cytokine response or the recruitment of inflammatory cells to the

lungs after infection. Together these results provide further evidence that ISG15 can protect the host from viral infection by mechanisms that extend beyond the regulation of viral replication.

RESULTS

ISG15 functions in a conjugation dependent manner to protect mice from influenza A virus induced lethality without altering viral loads.

We have previously shown that ISG15 contributes to the host response against both IAV and IBV, as mice lacking ISG15 exhibit increased lethality after infection compared to WT mice¹⁶. ISG15 mediated protection against IBV infection is dependent upon ISG15 conjugation and results in the dramatic reduction in viral loads in vivo¹⁹. To determine if the protective activity of ISG15 during IAV infection was also dependent upon conjugation we infected WT, ISG15^{-/-}, and Ube1L^{-/-} mice with 5.0×10^3 pfu influenza A/WSN/33 intranasally (i.n.) and monitored the mice for lethality. As we have seen previously, mice lacking ISG15 displayed increased lethality compared to WT mice (Figure 3.1A). This protection mediated by ISG15 appeared to be largely conjugation dependent, as Ube1L^{-/-} mice also displayed increased lethality compared to WT mice (Figure 3.1A). Interestingly, despite the large difference in survival, weight loss in both ISG15^{-/-} and Ube1L^{-/-} mice were similar to WT mice through nine days post infection, after which both the ISG15^{-/-} and Ube1L^{-/-} mice began to succumb to infection (Figure 3.1B). This observation is strikingly different from what we have previously reported for IBV infection,

where increased mortality in both the Ube1L^{-/-} and ISG15^{-/-} mice was associated with a dramatic increase in weight loss as compared to WT mice¹⁹.

The increased lethality we observed in ISG15^{-/-} mice during IBV infection was also accompanied by a 2-3 log increase in viral titers at days 3 and 6 post infection compared to WT mice, supporting the model of ISG15 acting as an antiviral molecule¹⁹. To determine if ISG15 played a similar role during IAV infection, we next evaluated viral loads within the lungs of infected mice during the course of infection. Virus could be detected in the lung 1 day post infection, with all three genotypes of mice displaying similar viral titers (Figure 3.1C). Peak viral titers were reached by 3 days post infection, but despite the increased lethality observed in both the ISG15^{-/-} and Ube1L^{-/-} mice, we observed similar viral loads in all mice at both days 3 and 6 post infection. On day 8 post infection lung titers were still similar between the three genotypes as the mice began to clear the virus. These results suggest that during IAV infection ISG15 protects the host from lethality in a conjugation dependent manner that is independent of its previously reported effects on viral replication.

ISG15 also protects mice from Sendai virus induced lethality in a conjugation dependent manner with minimal impact upon viral loads.

The observation that ISG15^{-/-} mice succumbed to influenza A virus infection despite having no differences in viral loads was an unexpected result, especially given our previous findings in the influenza B virus model. In order to determine if this observation was unique to IAV infection we wanted to evaluate the role of ISG15 conjugation in the pathogenesis of a third respiratory virus; therefore we infected WT, ISG15^{-/-}, and Ube1L^{-/-} mice i.n. with Sendai virus, a mouse

parainfluenza virus, and monitored them for weight loss and lethality. As seen during IAV and IBV infection, ISG15 protected mice from Sendai virus induced lethality in a conjugation dependent manner. In WT mice an infectious dose of 1.2×10^6 pfu induced significant disease with ~25% weight loss but rarely resulted in lethality (Figure 3.2A,B). In contrast, 70% of both the ISG15^{-/-} and Ube1L^{-/-} mice succumbed to infection by day 10 post infection. Similar to what we observed during IAV infection, there was little difference in weight loss between the different genotypes of mice during the first 10 days of infection despite the increased lethality observed in both the ISG15^{-/-} and Ube1L^{-/-} mice (Figure 3.2B). We next evaluated viral loads in the lungs of these mice during the course of Sendai virus infection. Once again, unlike the 2-3 log increases in viral replication that we observed during influenza B virus infection, we noted minimal differences in viral loads between the three genotypes during the course of Sendai virus infection. In all three genotypes of mice, peak viral loads were reached at 3 days post infection, with no differences noted between the genotypes (Figure 3.2C). At 6 days post infection there was a small, ~3-fold, increase in viral loads in the ISG15^{-/-} and Ube1L^{-/-} mice as compared to WT mice. By day 8 post infection all three genotypes of mice had started to clear the virus, and we observed no difference in viral loads between WT and ISG15^{-/-} mice, though we did detect increased viral burden in the Ube1L^{-/-} mice. Thus similar to what we observed during IAV infection, ISG15 protected mice from Sendai virus induced lethality in a conjugation dependent manner, while having a minimal impact upon viral burden over the course of infection. Therefore in both models, ISG15 appears to protect the host from lethality by a mechanism that is distinct from its role during IBV infection.

ISG15 does not affect Influenza A virus or Sendai virus replication in vitro

While we did not observe a major difference between IAV or Sendai virus burden in ISG15^{-/-} and WT mice, it has been previously reported that ISG15 conjugation can antagonize both IAV and Sendai virus replication in human cell lines. siRNA knockdown of ISG15 or HERC5 in HEK293 cells resulted in increased Sendai virus replication²³. Similarly, siRNA knockdown of ISG15 or HERC5 in A549 cells or ISG15 and Ube1L in Calu3 cells resulted in ~5-10 fold increases in IAV replication^{20;22}. Given these previous findings, and the fact that we did see a small increase in Sendai virus titers in ISG15^{-/-} mice at day 6 post infection, we wanted to more carefully evaluate whether ISG15 can directly impact viral replication in the mouse model. To this end, we generated primary murine trachea epithelial cells (mTEC) from WT, ISG15^{-/-}, and Ube1L^{-/-} mice and evaluated IAV and Sendai virus growth in these cells.

As we have previously reported that IBV replicates to higher titers in ISG15^{-/-} mice compared to WT mice, we first infected mTEC with IBV to determine if these cultures could recapitulate the virus replication phenotype observed *in vivo*. In cultures that were not pretreated with interferon, a small but statistically significant increase in IBV replication was observed at late time points in mTEC derived from ISG15^{-/-} mice (Figure 3.3A). This difference in IBV replication between ISG15^{-/-} and WT cells increased to greater than 10 fold when the cultures were treated with interferon β for 24 hours prior to infection in order to induce ISG15 expression and conjugation (Figure 3.3B). Next, we assessed the replication of IAV and Sendai virus in mTECs lacking ISG15 or Ube1L. In untreated mTEC both IAV and Sendai virus grew with similar kinetics in WT, ISG15^{-/-} and Ube1L^{-/-} cells (Figure 3.3C,E). We then pretreated the mTEC cultures with a dose of interferon β that induced ISG15 conjugation and resulted in ~100 fold inhibition of virus replication at 24 and 36 hours post infection in WT mTEC. However,

even after interferon stimulation we observed no difference in replication of either IAV or Sendai virus in any of the three genotypes of mTECs (Figure 3.3D,F). These results, together with our *in vivo* viral titer data, suggest that unlike IBV infection in which ISG15 directly inhibits viral replication, during both IAV and Sendai virus infection ISG15 does not directly inhibit virus replication within infected cells.

The loss of ISG15 does not alter the cytokine response during influenza A virus or Sendai virus infection.

We have recently reported that ISG15 protects neonatal mice from Chikungunya virus induced lethality¹⁷. In this model ISG15 downregulates the host cytokine response without affecting CHKV titers. CHKV infected ISG15^{-/-} pups exhibit a global increase in serum inflammatory cytokines and appear to die in a manner consistent with death by cytokine storm. We therefore wanted to evaluate whether ISG15 regulation of the cytokine response to infection might be responsible for the increased lethality in ISG15^{-/-} mice after IAV or Sendai virus infection.

We infected WT, ISG15^{-/-} and Ube1L^{-/-} mice with IAV and at days 3, 6, and 8 post infection mice were sacrificed to collect bronchoalveolar lavage fluid (BALF). We then evaluated a panel of 10 proinflammatory cytokines in the BALF. The levels of all cytokines evaluated peaked at 6 days post infection and were either not detectable or were greatly reduced by day 8 post infection (Figure 3.4A). In a few cases there were statistically significant changes in cytokines levels (IL-6, RANTES, IL-12p40) however these differences were less than 2 fold changes between genotypes and were not seen in both the ISG15^{-/-} and Ube1L^{-/-} mice. Overall,

no dramatic differences were observed in any BALF cytokines between WT, ISG15^{-/-}, or Ube1L^{-/-} mice at any time after IAV infection (Figure 3.4A).

We performed a similar analysis of BALF cytokines during Sendai virus infection. Once again all cytokines analyzed were induced above mock levels in all three genotypes of mice. For some analytes (IL-1B, IL-6, RANTES, and IL-13) the peak response occurred at day 3, while the remaining cytokines peaked at day 6 post infection. Similar to what we observed during influenza A virus infection, no dramatic differences were seen in any BALF cytokines between WT, ISG15^{-/-}, or Ube1L^{-/-} mice after Sendai virus infection. Once again, in the few circumstances where there were statistically significant differences between groups the differences were less than 2 fold (Figure 3.4B). Finally, we also evaluated interferon alpha levels in BALF of Sendai virus infected mice by ELISA. The interferon alpha levels peaked at 3 days post infection, similar to the viral titers in the lungs, and diminished over the course of infection. We observed no difference in interferon alpha production in WT, ISG15^{-/-}, or Ube1L^{-/-} mice at any time after Sendai virus infection (Figure 3.4C). Overall, the ISG15^{-/-} and Ube1L^{-/-} mice appear to produce a normal interferon and cytokine response during both influenza A and Sendai virus infection, unlike the global cytokine misregulation observed in ISG15^{-/-} mice during CHKV infection.

Similar immune cell populations are recruited to the lungs in WT, ISG15^{-/-}, and Ube1L^{-/-} mice during Sendai virus infection.

Much of the tissue damage incurred after respiratory virus infection is believed to be a result of immunopathology induced in response to the virus^{32; 33}. Characterization of highly

pathogenic pandemic strains of IAV have noted increased neutrophil and macrophage infiltration in the lungs^{34; 35}. Additionally, a study of gene expression differences in the lung after sub-lethal and lethal IAV infection also found that one of the strongest correlations to lethal IAV infection was increased neutrophil recruitment and subsequent tissue damage³⁶. While neutrophils and inflammatory macrophages are necessary for control of virus replication, it is thought that excessive recruitment can lead to excessive damage of the lung resulting in death^{36; 37}. We therefore next evaluated the cellular recruitment to the lungs of ISG15^{-/-} mice during Sendai virus infection.

An analysis of gross lung histopathology from infected mice revealed no obvious difference in the degree of inflammation between all three genotypes of mice following either IAV or Sendai virus infection (data not shown). To evaluate this more carefully we first assessed the total number of cells that were recruited to the lung. We infected mice with Sendai virus and at various times post infection we analyzed the total number of cells recovered from lung parenchyma digests and BALF. We observed no difference in the total number of cells collected from the lung parenchyma or BALF of WT and ISG15^{-/-} mice at any time point after infection, though we did find increased total cellularity in Ube1L^{-/-} mice compared to WT mice at certain times (Figure 3.5A,B). We also observed no difference in total cell numbers recruited to the lungs of WT and ISG15^{-/-} mice after influenza A virus infection (data not shown).

To more carefully analyze the makeup of the cells recruited to the lung during infection we performed flow cytometry on the cells isolated from the BALF and lung parenchyma during Sendai virus infection. We saw an elevation of neutrophils, inflammatory monocytes, and NK cells over mock infected levels by day 3 post infection, but no significant differences were observed between WT, ISG15^{-/-}, or Ube1L^{-/-} mice at 3 or 6 days post infection (Figure 3.5C).

At day 8 post infection we did observe an increase in inflammatory monocytes in ISG15^{-/-} lungs compared to WT and UBE1L^{-/-} mice. We observed T-cell recruitment above mock infected levels starting at day 6 post infection, but observed no differences in CD8⁺ or CD4⁺ T-cell numbers between genotypes (Figure 3.5D). We also observed similar percentages of cell types in BALF from WT, ISG15^{-/-}, and UBE1L^{-/-} mice infected with Sendai virus (data not shown). Overall, we observed no major differences between the three genotypes in the number or composition of inflammatory cells recruited to the lung after infection.

During recovery from infection mice lacking ISG15 display increased pulmonary damage.

While previous studies of respiratory virus pathogenesis have revealed that immunodeficiency can lead to spread of virus outside of the lung, we were unable to detect either IAV or Sendai virus by plaque assay in the kidney, spleen, liver, heart or brain at day 8 post infection (data not shown)³⁸. Histological analysis of these organs revealed no pathology outside of the lung (data not shown). Furthermore, histological evaluation of the lung epithelium at day 8 post infection revealed similar damage in both the ISG15^{-/-} and UBE1L^{-/-} mice compared to WT mice (data not shown). During both IAV and Sendai virus infection the ISG15^{-/-} and UBE1L^{-/-} mice succumb to infection around days 9-10 post infection (Figures 3.1 and 3.2). Previous characterization of the lung histopathology during IAV and Sendai virus infection have shown that at this time the airway epithelium is beginning to repair itself from the damage induced during the infection^{39; 40; 41}. We therefore hypothesized that ISG15 may play a role in lung repair after infection.

In order to evaluate the lung pathology during this healing phase we decreased the infectious dose of Sendai virus in order to increase the survival of ISG15^{-/-} mice. This reduced dose of Sendai virus resulted in increased survival of both the ISG15^{-/-} and UbE1L^{-/-} mice, with only 20% of the mice succumbing to the infection, while none of the WT mice died (Figure 3.6A). Interestingly, at this lower dose, while WT mice began to regain body weight at day 8 post infection, the ISG15^{-/-} and UbE1L^{-/-} mice were delayed in initiating weight recovery (Figure 3.6B). At day 11 post infection both the ISG15^{-/-} and UbE1L^{-/-} mice had recovered only 80% of their initial body weight as compared to the 90% weight recovery observed in the WT mice. An analysis of viral loads in the lungs revealed that, similar to the higher dose of infection peak, viral titers were observed at days 3 and 6 post infection in all genotypes, and by day 11 post infection all three genotypes of mice had cleared replicating virus (Figure 3.6C). At both days 3 and 6 post infection we did note a small increase in viral loads (~3 fold) in ISG15^{-/-} mice compared to WT mice. The biological significance of this is unclear. Histological evaluation of lungs harvested from these mice at day 11 post infection showed increased numbers of diseased small terminal airways in the ISG15^{-/-} mice compared to WT mice (Figure 3.5 D-H). This increased disease presentation was a combination of small airways that were denuded of epithelium and small airways where the epithelial recovery resulted in epithelial hyperplasia and alveolar epithelialization.

DISCUSSION

Due to its robust expression after type I interferon stimulation, ISG15 has long been hypothesized to contribute to the interferon mediated intracellular anti-viral response. Supporting this hypothesis, ISG15^{-/-} mice have been shown to be more susceptible to viral infections, and a number of reports have been published showing the ability of ISG15 to antagonize replication of viruses in tissue culture. One way that this inhibition has been shown to occur is through the ISGylation of viral and host proteins. ISGylation of human papillomavirus capsid protein has been shown to inhibit the infectivity of virus that incorporates ISGylated capsid, and ISGylation of the influenza A virus NS1 protein has been shown to both inhibit its ability to associate with importin α and to affect its ability to antagonize the interferon response^{21; 22; 24}. Additionally, hundreds of host proteins are also ISGylated and these modifications likely contribute to antagonizing the virus life cycle. In the case of Ebola virus, ISG15 can inhibit VLP release by inhibiting the ubiquitin E3 ligase activity of Nedd4^{27; 28}. It is not currently well understood what role ISG15 plays in the regulation of the type I interferon response. Although it has been reported that ISG15 can modulate the antiviral response by regulating the stability of IRF3 and RIG-I after virus infection in tissue culture, evaluation of ISG15^{-/-} and UBE1L^{-/-} mice has not uncovered a role for ISGylation in the regulation of downstream ISG expression after type I interferon or polyI:C stimulation^{23; 42; 43; 44}.

While there is now evidence that ISG15 can act as a protective factor during CHKV infection by a mechanism that does not involve inhibition of virus replication, this observation was found to be mediated by the unconjugated form of ISG15¹⁷. Here we report a novel mode of ISG15 mediated protection from virus infection. We have shown that similar to its role during

IBV infection, ISG15 protects mice from IAV in a conjugation dependent manner. However while ISG15 is important for protecting mice from IAV induced lethality, we observed no difference in virus burden, suggesting that ISG15 protects mice from IAV and IBV by two distinct mechanisms. And unlike its role during CHKV infection, ISG15 had no effect on cytokine regulation after IAV infection. We have also shown that this mode of ISG15 mediated protection does not appear to be unique to IAV infection. Through the evaluation of Sendai virus pathogenesis in ISG15^{-/-} and Ube1L^{-/-} mice, we found that ISG15 conjugation protects mice from Sendai virus by a mechanism that closely resembles the characteristics of ISG15-mediated protection against IAV infection.

While in the Sendai virus model we did detect a small increase in viral loads in ISG15^{-/-} and Ube1L^{-/-} mice compared to WT mice, these differences paled in comparison to the magnitude by which ISG15 restricts IBV replication. Additionally, we observed no difference in IAV or Sendai virus replication in mTEC. We believe that these results together suggest that ISG15 does not directly antagonize IAV or Sendai virus replication within infected cells. Rather, differences in the host response may contribute to the small viral load differences observed during Sendai virus infection. For example, it has been shown that ISG15 inhibits apoptosis through ISGylation of filamin B and that ISG15^{-/-} peritoneal macrophages have a reduced phagocytic capacity^{45; 46}. A number of viruses have been reported to induce apoptosis, and it is thought that in some cases this might facilitate virus spread⁴⁷. Either increased apoptosis or a decreased capacity to clear apoptotic bodies could then facilitate increase virus spread *in vivo*, and thus increased virus titers, without directly affecting the virus replication within infected cells.

It has previously been reported that ISG15 inhibits the replication of both IAV and Sendai virus in tissue culture^{20; 21; 22; 23}. The discrepancies between our findings and previously published data could reflect a difference between a primary heterogenous culture of cells and immortalized cell lines. There is precedent for cell type specific effects of ISG15 on IAV replication, which is further supported by the fact that we did not initially detect a difference in IBV replication in ISG15^{-/-} embryonic fibroblasts^{16; 20}. It is also possible that these discrepancies reflect a difference in the function or specificity of human and murine ISG15. Such species specificity has been reported with respect to the IBV NS1 protein, which can bind to and inhibit conjugation of human ISG15 but not mouse ISG15^{48; 49}. It is possible that Sendai virus and IAV may have some capacity to inhibit anti-viral functions of murine ISG15 but not human ISG15. Further studies will be needed to explain these discrepancies.

In both IAV and Sendai virus infected mice we observed lethality at around 9 to 10 days post infection, a time when mice are clearing the acute viral infection, beginning to regain weight, and beginning to repair the airway epithelium. By lowering the infectious dose of virus and allowing a significant number of the ISG15^{-/-} mice to survive infection, we observed a difference in the ability of the ISG15^{-/-} mice to recover weight, and histological examination of the lungs revealed increased disease in the smaller airways of the lung in the ISG15^{-/-} mice. It is not clear whether this increase in diseased airways is a result of increased damage, a defect in the wound repair response of ISG15^{-/-} mice, or some combination of both. A previous report evaluating disease susceptibility of different mouse strains to Sendai virus found that while resistant and susceptible mouse strains have dramatically different LD₅₀ titers, little difference in viral loads or viral clearance were observed between mice over the course of infection⁵⁰. This

study reported that increased susceptibility to Sendai virus induced lethality seemed to correlate with increased damage and delayed re-epithelialization in the lung.

Recent studies have also highlighted the importance of maintaining proper airway epithelial integrity in surviving IAV infection. Mice lacking cellular inhibitor of apoptosis 2 (cIAP2) were recently shown to exhibit increased lethality after IAV infection without any detected difference in virus burden or in the immune response to infection⁵¹. Rather these cIAP2 mice displayed increased necroptosis in the airway epithelium. Innate lymphoid cells have also been reported to protect mice from IAV infection by a manner that is independent of controlling virus replication. These cells secrete amphiregulin which helps to promote survival by increasing airway epithelial integrity⁵². And, increased damage to the airway epithelium was reported to be the main histological difference observed during lethal IAV and Streptococcus co-infection compared to infection with either IAV or Streptococcus alone⁵³.

Bronchiolar epithelial healing after Sendai virus infection involves the loss of epithelial differentiation markers on cells, cell proliferation and migration repopulate the damaged airways, followed by differentiation of cells into the proper epithelial cell types³⁹. We are currently investigating how ISG15 might affect this process within the lung after viral infection, but there is precedent for ISG15 playing a role in the process of epithelial-to-mesenchymal transition (EMT), an important dedifferentiation process during development and tissue wound repair. EMT involves a reprogramming of cellular gene expression resulting in, amongst other changes, a dramatic reorganization of the actin cytoskeleton and increased cell motility⁵⁴. A recent proteomic study identified ISG15 as a protein enriched during hepatocyte growth factor induced EMT and while it is not clear what role ISG15 plays in this process, several studies have discovered functions for ISG15 that could be consistent with a role in EMT⁵⁵. Epidermal

growth factor receptor, a protein known to be associated with EMT, is down regulated by overexpression of UBE1L⁵⁶. Additionally, knockdown of ISG15 or UbCH8 in a breast cancer cell line resulted in a reorganization of the actin cytoskeleton and the decreased ability of a cell monolayer to close a scratch wound in tissue culture⁵⁷. Consistent with a potential role in either mitigating tissue damage or promoting tissue healing, ISG15 has also been reported to be induced in the brains of mice during both mechanical and genetic tissue damage recovery models, as well as in the brains of squirrels during periods of hibernation induced ischemia^{58; 59}. Ischemia induced by middle cerebral artery occlusion was found to induce ISG15 in the brains of mice, and both ISG15^{-/-} and UBE1L^{-/-} mice developed increased brain tissue damage and more severe neurological defects compared to WT mice as a consequence of experimentally induced ischemia⁶⁰. Together these studies provide insight into potential pathways outside of immune modulation that could be regulated by ISGylation and contribute to the increased lethality we observe in the ISG15^{-/-} mice during IAV and Sendai virus infection.

ISG15 is strongly upregulated after type I interferon stimulation and viral infection, and, in many cases, it protects the host from viral induced morbidity and mortality. While early studies demonstrated its ability to function as a direct antiviral molecule and inhibit virus replication, more recent studies, including this one, have revealed that ISG15 can also regulate additional host responses that impact upon survival. Interestingly, while ISG15 did not inhibit IAV or Sendai virus replication in mice, the function of ISG15 conjugation does appear to correlate with the function of the type I interferons *in vivo*. IFNAR^{-/-} mice display dramatically elevated viral loads compared to WT mice during IBV infection¹⁹. However, a number of studies have found either no difference or only small differences in virus replication and virus clearance in IFNAR^{-/-} or STAT1^{-/-} mice during IAV, Sendai virus, or RSV infection^{19; 61; 62; 63}.

^{64; 65; 66}. Type I interferons have clearly been demonstrated to inhibit virus replication in tissue culture. However the role of type I interferons during respiratory virus infections *in vivo* is less well understood, and recent findings suggest that the more important role of type I interferon function during these infections might be to modulate the immune response to regulate tissue damage and morbidity. Similarly, our results suggest that ISG15 conjugation plays a role in some aspect of disease tolerance against IAV and Sendai virus infection. It will be important in the future to more thoroughly evaluate how ISG15 conjugation of host proteins alters the basic biology of the cell, what physiological roles it plays in non-infected mice, and how these functions might affect disease in mice after viral infection.

METHODS

Mice

Mice were bred and maintained at Washington University School of Medicine in accordance with all federal and University guidelines, under specific-pathogen-free conditions. WT C57BL/6J mice were purchased from Jackson Laboratory (Bar Harbor, ME), bred and maintained in our facilities. ISG15^{-/-} mice (provided by Dr. Klaus-Peter Knobeloch, University Clinic Freiburg, Germany) and UbE1L^{-/-} mice (provided by Dr. Dong-Er Zhang, University of California, San Diego) were generated as previously described⁴³. ISG15^{-/-} and UbE1L^{-/-} mice were fully backcrossed (>99.72% and 99.93% respectively to C57BL/6 by congenic SNP analysis through Taconic Laboratories (Hudson, NY)).

Viruses

Influenza A virus. Recombinant influenza A/WSN/33 (rWSN) virus was generated from cDNA as previously described⁶⁷. The virus was grown on MDCK cells using DMEM containing 1 ug/ml N-acetyltrypsin (Sigma Chemicals, St. Louis, MO), 100 units/ml penicillin, and 100 ug/ml streptomycin (Invitrogen, Carlsbad, CA). The cells were infected at a multiplicity of infection of 0.01 pfu per cell, harvested 48 hrs postinfection and titered by plaque assay in MDCK cells.

Influenza B virus. Recombinant WT influenza B/Yamagata/88 virus was grown in 10 day old embryonated chicken eggs and titered by plaque assay in MDCK cells.

Sendai virus. Sendai/52 Fushimi strain virus was purchased from ATCC. Virus was plaque purified after infection of Vero cells to isolate a single clone that was then propagated in 11 day

old embryonated chicken eggs. Virus from allantoic fluid was diluted in PBS and stored at -80 degrees Celcius.

Viral stocks were titered by plaque assay on MDCK cells for influenza virus and Vero cells for Sendai virus.

Virus growth curves

Murine tracheal epithelial cultures were generated from the different genotypes of mice as previously described⁶⁸. Cells were harvest from tracheas of female mice (5 to 12-weeks old) and grown under media in transwells (Corning) for 7 days. Apical media was then removed and the cells were grown at air-liquid interface for 2-3 weeks prior to experimentation. For viral growth curves, virus was diluted in DMEM supplemented with 1% Penicillin/1% Streptomycin (1%P/S) to concentrations such that indicated number of pfu were administered in volumes of 100ul. Infections were performed by adding 100ul of virus to the apical chamber and incubating at 37 degrees C for 1 hour. Virus was removed and the apical chamber was washed 3 times with 200ul of DMEM(1%P/S). After washing 100ul of DMEM(1%P/S) was added back to apical chamber. At indicated times apical media was collected and replaced with 100ul of DMEM(1%P/S). Virus titers in apical media were assessed by plaque assay on MDCK cells. For interferon β pretreatment conditions, indicated concentrations of interferon β (PBL Assay Science) were added to basolateral media. After 24 hours, immediately prior to infection, basolateral media was removed and basolateral chambers were washed 2 times with PBS and then replaced with media containing no interferon.

In vivo infections

Mice were anesthetized using an intraperitoneal injection of a ketamine/xylazine cocktail prior to infection. For IAV infections, 6-8 week old female mice were infected with 5000 pfu of influenza A/WSN/33 virus in 25 μ l PBS i.n. For Sendai virus infections, 8-10 week old male mice were infected with 1.2×10^6 pfu Sendai virus in a total volume of 30 μ l of PBS i.n. for figures 3.2-3.5. For experiments performed in figure 3.6 to assess lung repair mice were infected with a dose ($0.6-1.0 \times 10^6$ PFU) that reduced lethality to ~20% in the infected ISG15^{-/-} mice. Weight loss was monitored by cage average for IAV infection and by individual mice for Sendai virus infection.

Lung viral load assessment

To assess lung titers, the right superior, middle, and inferior lobes were collected in 1 mL of PBS. Lungs were homogenized in a Roche MagNA Lyser using 1.0 mm diameter zirconia/silica beads (BioSpec Products). Titers of lung homogenates were assessed by plaque assay using MDCK cells for influenza A virus and Vero cells for Sendai virus.

Infiltrating cells analysis

Bronchoalveolar lavage analysis: BALF was collected by inserting a catheter into the trachea and flushing 800 μ l of PBS into and out of the lungs 3 times (~600 μ l recovered). Lavages were centrifuged at 250g for 5 minutes to pellet cells. Supernatant was collected and analyzed for cytokine and chemokine analysis. Cells collected from lavages were resuspended in FACS

buffer (PBS, 3%BSA, 0.1% sodium azide) and cells from mice of the same genotype were pooled for further analysis. Red blood cells were lysed in 200ul of RBC lysis buffer (Sigma) for 5 minutes at room temperature. Cells were then washed in FACS buffer, and incubated in FcR block for 30 minutes. Cells were then stained in different mixes of antibodies against cell surface markers for 30 minutes, washed 3 times in FACS buffer, fixed in 1% formaldehyde and analyzed by flow cytometry (BD FACSCanto).

Lung digests: For analysis of infiltrating cells in the lung parenchyma, the left lung was collected from a lavaged mouse. The lung was minced with scissors and incubated in DMEM with 350U/mL Collagenase Type I (Worthington) and 50U/mL DNase (Worthington) for 1 hour at 37 degrees. Remaining tissue after digestions was crushed between the rough edge of frosted microscope slides. Cells were passed through a cell strainer. Red blood cells were lysed in 1 mL of RBC lysis buffer (Sigma) for 5 minutes at room temperature. Cells were then washed with FACS buffer, blocked, stained and analyzed as described above for BALF cells.

Antibodies

The following antibodies were purchased from eBioscience- FITC-anti-MCH II (M5/114.15.2), APC-anti-B220 (RA3-682), PERCP-Cy5.5-anti-CD11b (M1/70), PERCP-Cy5.5-anti-CD3ε (145-2C11). The following antibodies were purchased from BioLegend- FITC-anti-CD8 (53-6.7), PE-anti-Ly6G (1A8), PE-anti-CD19 (6D5), APC-anti-CD11c (N418), Pacific Blue-anti-Ly6c (HK1.4). The following antibodies were purchased from BD Biosciences- PE-anti-CD4 (GK1.5), APC-anti-NK1.1 (PK136).

Cytokine analysis

BALF was collected as described above and analyzed using Bio-Rad Bio-Plex analysis according to manufacturer's instructions. Quantification of interferon alpha in BALF was performed using a pan-interferon alpha ELISA (PBL Assay Science). For Sendai virus infection cytokine analysis, data from all time points was generated from a total of 6-8 mice collected from 3 separate infections, except for UbE1L^{-/-} day 3 data which was generated from 5 mice over 2 infections. Cytokine analysis of mock infected mice was generated from 2 mice of each genotype for days 3 and 6 post mock infection (intranasal PBS instillation), and one mouse from each genotype for day 8 post mock infection. Analytes in mock infected BALF did not vary between genotype or day post mock infection, thus all mock values were pooled together. For influenza A virus infection cytokine analysis WT and ISG15^{-/-} data was generated from 5-6 mice from 1-2 experiments. UbE1L^{-/-} data was generated from 3-4 mice from one experiment. Mock infection data was generated from 4-6 mice from 2-3 experiments. No difference was detected between any genotype at any time points, thus all mock values were pooled together.

Histology

For lung histological analysis, mice were infected as described above and sacrificed at the indicated time post infection. The right lobes were tied off with suture and excised. The left lobe was inflated with 500ul formalin, or all lobes were inflated with 1.0ml of formalin. Lungs were then incubated in a 50ml conical tube containing 15mL formalin. After 36-48 hours in formalin, lungs were washed for at least 15 minutes in serial washes of PBS, 30% ethanol, 50%

ethanol, and then stored in 70% ethanol until processed for paraffin embedding, sectioning and staining. Lung sections were stained with hemotoxylin and eosin and were scored blindly by a pathologist.

Statistics

All data were analyzed with Prism software (GraphPad, San Diego, CA). Statistical analyses for viral titers, weight loss, and cytokines were performed using Mann-Whitney U test. Survival data were analyzed by the Mantel-Cox test, with death as the primary variable. Error bars in figures represent the SEM.

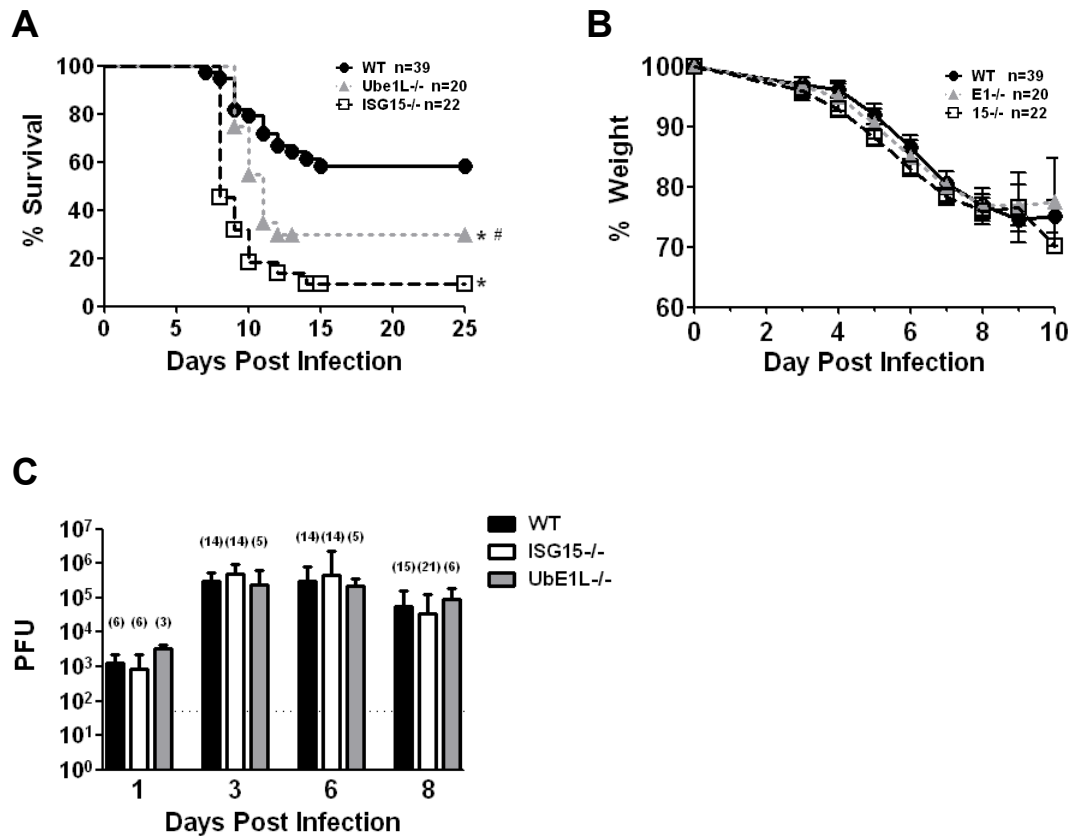


Figure 3.1. ISG15 protection against influenza A virus is conjugation dependent, but not anti-viral.

WT, ISG15^{-/-}, and UBE1L^{-/-} mice were infected with 5.0×10^3 pfu influenza A/WSN/33 i.n. Mice were monitored for (A) lethality and (B) weight loss, or (C) sacrificed at the indicated times post infection and viral loads in the lungs were assessed by plaque assay. For viral load assessment, the numbers of mice analyzed per genotype at each time point are indicated in parentheses. Samples were collected from 1-6 independent experiments. In (A), * $p < 0.05$, vs WT; # $p < 0.05$ vs ISG15^{-/-}.

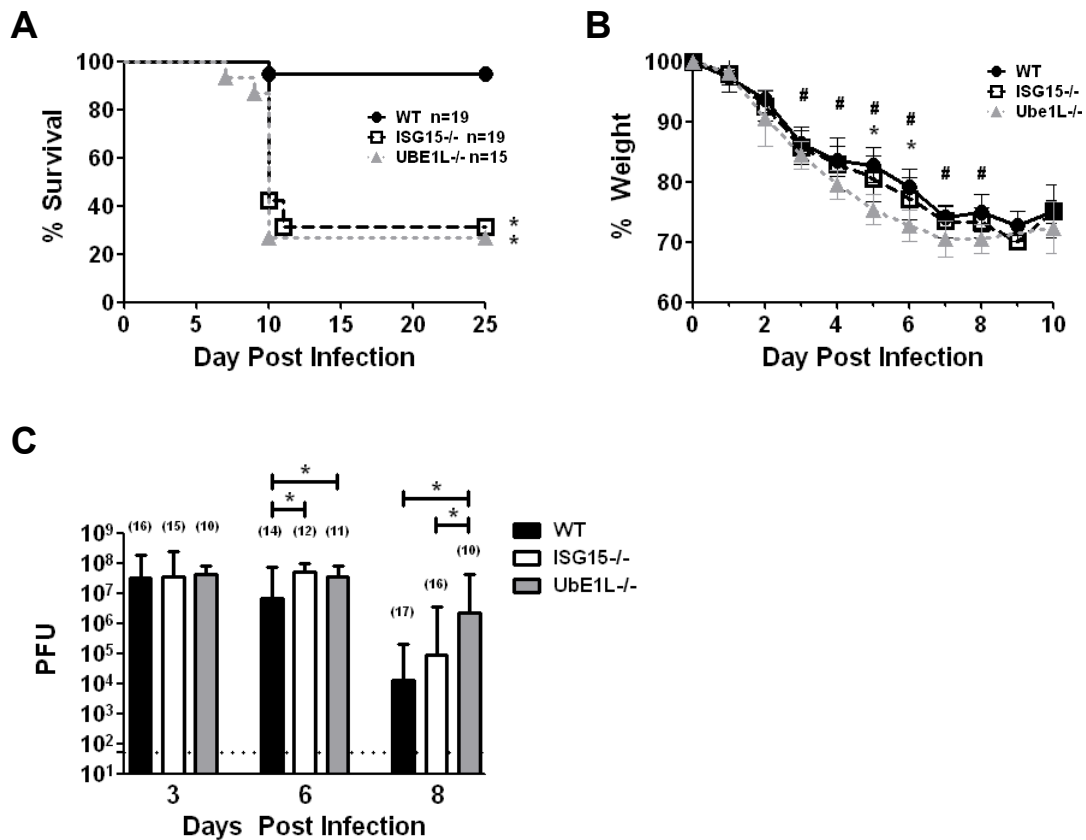


Figure 3.2. ISG15 protects against Sendai virus induced lethality by a conjugation dependent mechanism, but has no major effect on virus loads.

WT, ISG15^{-/-}, and UBE1L^{-/-} mice were infected with 1.2×10^6 pfu Sendai virus i.n. and monitored for (A) lethality (B) weight loss or (C) sacrificed at the indicated times post infection and viral loads in the lungs were assessed by plaque assay. For viral load assessment, the numbers of mice analyzed per genotype at each time point are indicated in parentheses. Samples were collected from 2-6 experiments. In (A) * $p < 0.05$, vs WT. In (B), * $p < 0.05$, WT vs ISG15^{-/-}; # $p < 0.05$ WT vs Ube1L^{-/-}.

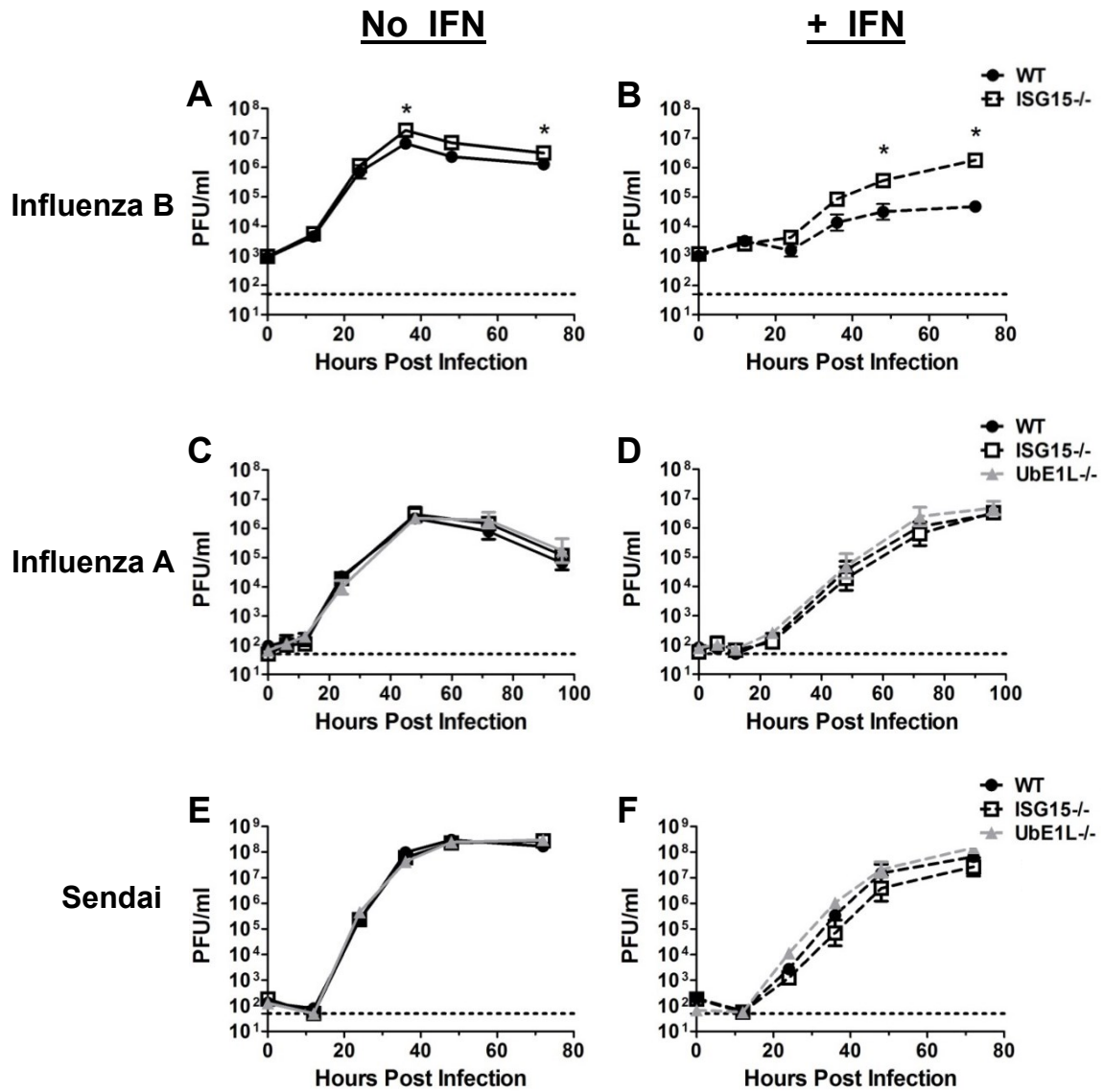


Figure 3.3. Influenza A and Sendai virus replication is not altered in primary tracheal epithelial cultures lacking ISG15 or ISG15 conjugates.

Primary murine trachea epithelial cell cultures (mTECs) were generated from WT, ISG15^{-/-}, or UBE1L^{-/-} mice. Cultures were either left untreated (**A,C,E**) or stimulated with interferon β for 24 hours (**B,D,F**) before infecting with influenza B/Yamagata/88 (**A,B**), influenza A/WSN/33 (**C,D**), or Sendai virus (**E,F**). Apical media was titered by plaque assay at various times after infection to evaluate virus replication. Doses of interferon β and viral infectious doses were different for each virus: *IAV*: 100U/ml interferon β ; 9×10^4 pfu. *Sendai virus*: 30U/ml interferon β ; 9×10^5 pfu. *IBV*: 30U/ml interferon β ; 9×10^5 pfu. Virus growth curves were generated from 2 independent infections performed on 2 different mTEC preparations with a total of 5-6 total replicates between the two infections. * $p < 0.05$.

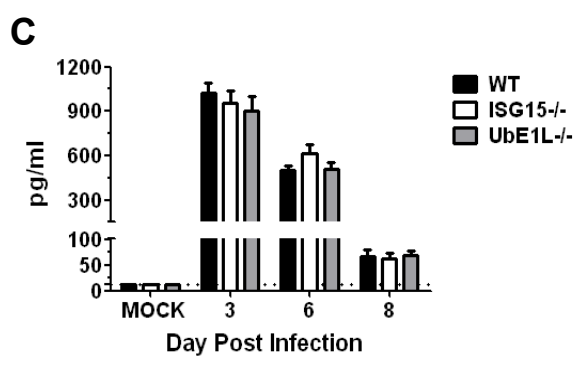
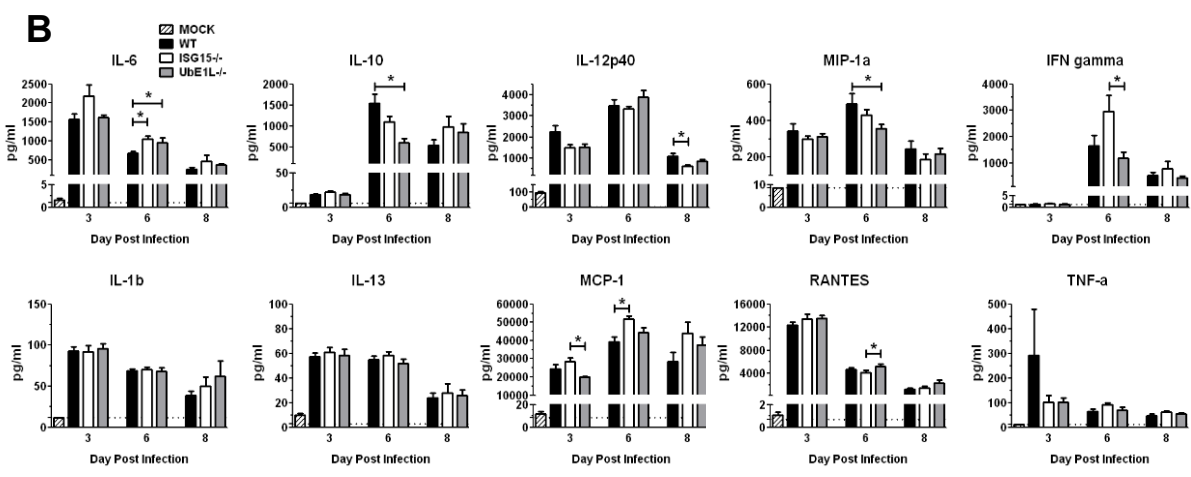
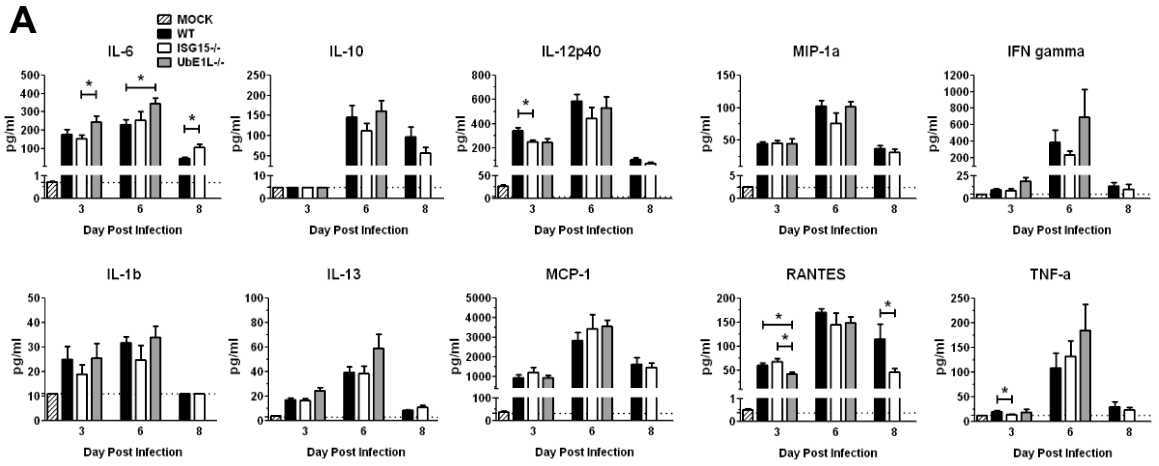


Figure 3.4. ISG15 does not affect cytokine production after influenza A or Sendai virus infection.

WT, ISG15^{-/-} and UBE1L^{-/-} mice were infected with **(A)** 5.0×10^3 pfu influenza A/WSN/33 or **(B)** 1.2×10^6 pfu Sendai virus. **(A, B)** At days 3, 6 and 8 post infection mice were sacrificed bronchoalveolar lavage fluid was analyzed for cytokines by BioRad multiplex analysis. **(C)** Interferon- α levels in BAL fluid from Sendai virus infected mice were analyzed by ELISA. * $p < 0.05$.

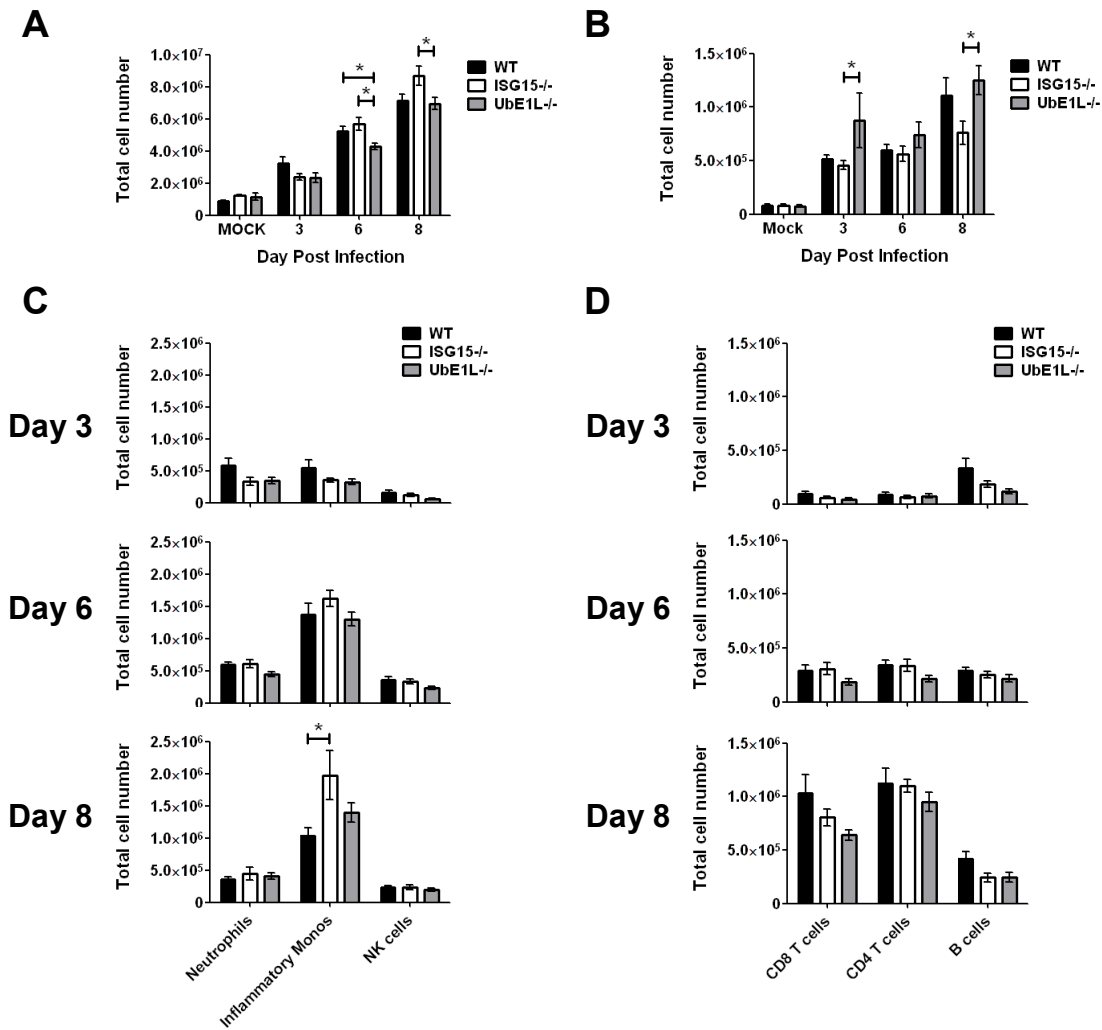


Figure 3.5. Similar numbers and cell populations are recruited to the lungs during Sendai virus infection in the presence and absence of ISG15 conjugation.

(A-C) WT, ISG15^{-/-}, and UBE1L^{-/-} mice were infected with 1.2×10^6 pfu Sendai virus i.n. Mice were sacrificed at 3, 6, or 8 days post infection. Lungs were lavaged and subsequently processed into single cell suspensions. Single cell suspensions of digested lungs (A) and cells recovered from BALF (B) were analyzed for total cell number by hemocytometer count. Cell populations recovered from lung digests were stained for cell surface markers and analyzed by FACS (C, D).

* $p < 0.05$.

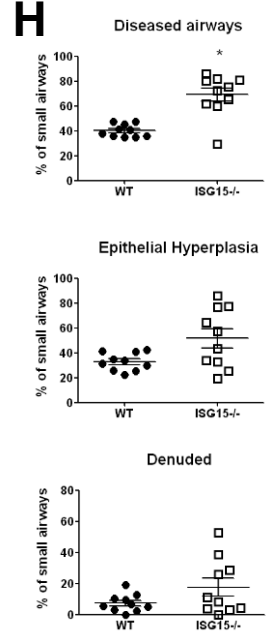
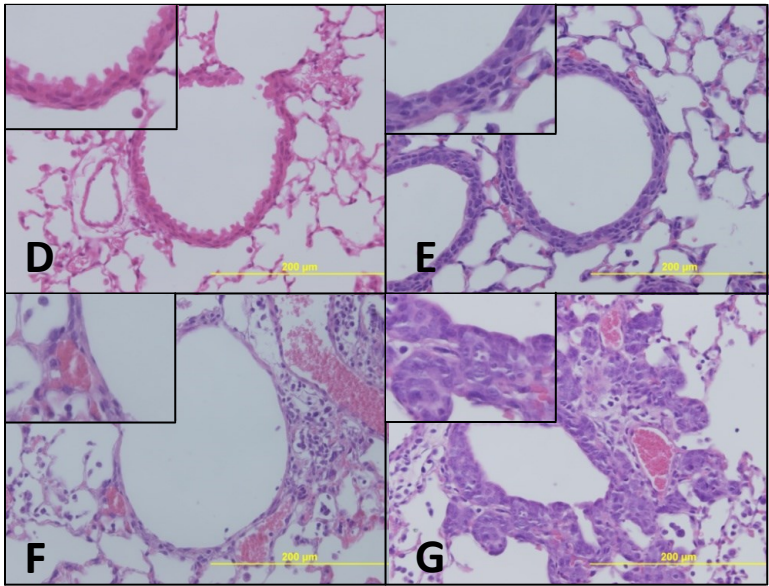
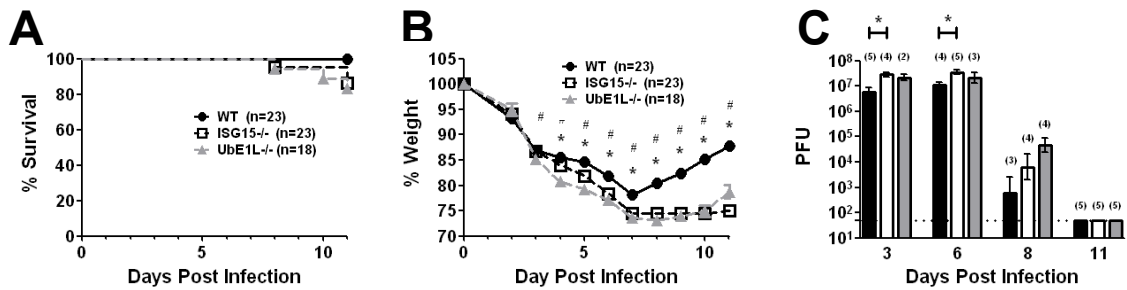


Figure 3.6. Infection with Sendai virus at a lower dose reveals increased weight loss and distal airway damage in ISG15^{-/-} mice.

WT, ISG15^{-/-}, and UBE1L^{-/-} mice were infected with 0.6-1.0x10⁶ pfu Sendai virus and were monitored for **(A)** lethality and **(B)** weight loss (*p<0.05 WT vs ISG15^{-/-}, #p<0.05 WT vs UBE1L^{-/-}). **(C)** Viral loads in the lungs of mice were analyzed at days 3, 6, 8, and 11 post infection by plaque assay. **(D-H)** Lungs harvested from mice infected with Sendai virus for 11 days were fixed, sectioned, and stained with hematoxylin and eosin. **(D)** Representative image of a small airway from a mock infected mouse. **(E-G)** Representative images of small airways from a mouse infected with Sendai virus for 11 days. Small airways were categorized into 3 principle states: **(E)** Airways exhibiting no aberrant disease, **(F)** airways denuded of epithelium, and **(G)** airways with epithelial hyperplasia. **(H)** Stained sections were scored blindly by a pathologist by categorizing small airway disease status into those describe in **(E-F)**. An average of 52.8 small airways were scored per mouse (Min. 33, Max. 89, Median 46). * p<0.05.

REFERENCES

1. Schoggins, J. W. & Rice, C. M. (2011). Interferon-stimulated genes and their antiviral effector functions. *Curr Opin Virol* **1**, 519-25.
2. Goodbourn, S., Didcock, L. & Randall, R. E. (2000). Interferons: cell signalling, immune modulation, antiviral response and virus countermeasures. *J Gen Virol* **81**, 2341-64.
3. Korant, B. D., Blomstrom, D. C., Jonak, G. J. & Knight, E., Jr. (1984). Interferon-induced proteins. Purification and characterization of a 15,000-dalton protein from human and bovine cells induced by interferon. *J Biol Chem* **259**, 14835-9.
4. Der, S. D., Zhou, A., Williams, B. R. & Silverman, R. H. (1998). Identification of genes differentially regulated by interferon alpha, beta, or gamma using oligonucleotide arrays. *Proc Natl Acad Sci U S A* **95**, 15623-8.
5. Knight, E., Jr., Fahey, D., Cordova, B., Hillman, M., Kutny, R., Reich, N. & Blomstrom, D. (1988). A 15-kDa interferon-induced protein is derived by COOH-terminal processing of a 17-kDa precursor. *J Biol Chem* **263**, 4520-2.
6. Loeb, K. R. & Haas, A. L. (1992). The interferon-inducible 15-kDa ubiquitin homolog conjugates to intracellular proteins. *J Biol Chem* **267**, 7806-13.
7. Krug, R. M., Zhao, C. & Beaudenon, S. (2005). Properties of the ISG15 E1 enzyme Ube1L. *Methods Enzymol* **398**, 32-40.
8. Zhao, C., Beaudenon, S. L., Kelley, M. L., Waddell, M. B., Yuan, W., Schulman, B. A., Huibregtse, J. M. & Krug, R. M. (2004). The UbcH8 ubiquitin E2 enzyme is also the E2 enzyme for ISG15, an IFN-alpha/beta-induced ubiquitin-like protein. *Proc Natl Acad Sci U S A* **101**, 7578-82.
9. Dastur, A., Beaudenon, S., Kelley, M., Krug, R. M. & Huibregtse, J. M. (2006). Herc5, an interferon-induced HECT E3 enzyme, is required for conjugation of ISG15 in human cells. *J Biol Chem* **281**, 4334-8.
10. Kim, K. I., Giannakopoulos, N. V., Virgin, H. W. & Zhang, D. E. (2004). Interferon-inducible ubiquitin E2, Ubc8, is a conjugating enzyme for protein ISGylation. *Mol Cell Biol* **24**, 9592-600.
11. Oudshoorn, D., van Boheemen, S., Sanchez-Aparicio, M. T., Rajsbaum, R., Garcia-Sastre, A. & Versteeg, G. A. (2012). HERC6 is the main E3 ligase for global ISG15 conjugation in mouse cells. *PLoS One* **7**, e29870.
12. Ketscher, L., Basters, A., Prinz, M. & Knobeloch, K. P. (2012). mHERC6 is the essential ISG15 E3 ligase in the murine system. *Biochem Biophys Res Commun* **417**, 135-40.
13. Zhao, C., Denison, C., Huibregtse, J. M., Gygi, S. & Krug, R. M. (2005). Human ISG15 conjugation targets both IFN-induced and constitutively expressed proteins functioning in diverse cellular pathways. *Proc Natl Acad Sci U S A* **102**, 10200-5.
14. Giannakopoulos, N. V., Luo, J. K., Papov, V., Zou, W., Lenschow, D. J., Jacobs, B. S., Borden, E. C., Li, J., Virgin, H. W. & Zhang, D. E. (2005). Proteomic identification of proteins conjugated to ISG15 in mouse and human cells. *Biochem Biophys Res Commun* **336**, 496-506.
15. Lenschow, D. J., Giannakopoulos, N. V., Gunn, L. J., Johnston, C., O'Guin, A. K., Schmidt, R. E., Levine, B. & Virgin, H. W. t. (2005). Identification of interferon-stimulated gene 15 as an antiviral molecule during Sindbis virus infection in vivo. *J Virol* **79**, 13974-83.

16. Lenschow, D. J., Lai, C., Frias-Staheli, N., Giannakopoulos, N. V., Lutz, A., Wolff, T., Osiak, A., Levine, B., Schmidt, R. E., Garcia-Sastre, A., Leib, D. A., Pekosz, A., Knobeloch, K. P., Horak, I. & Virgin, H. W. t. (2007). IFN-stimulated gene 15 functions as a critical antiviral molecule against influenza, herpes, and Sindbis viruses. *Proc Natl Acad Sci U S A* **104**, 1371-6.
17. Werneke, S. W., Schilte, C., Rohatgi, A., Monte, K. J., Michault, A., Arenzana-Seisdedos, F., Vanlandingham, D. L., Higgs, S., Fontanet, A., Albert, M. L. & Lenschow, D. J. (2011). ISG15 is critical in the control of Chikungunya virus infection independent of UbE1L mediated conjugation. *PLoS Pathog* **7**, e1002322.
18. Guerra, S., Caceres, A., Knobeloch, K. P., Horak, I. & Esteban, M. (2008). Vaccinia virus E3 protein prevents the antiviral action of ISG15. *PLoS Pathog* **4**, e1000096.
19. Lai, C., Struckhoff, J. J., Schneider, J., Martinez-Sobrido, L., Wolff, T., Garcia-Sastre, A., Zhang, D. E. & Lenschow, D. J. (2009). Mice lacking the ISG15 E1 enzyme UbE1L demonstrate increased susceptibility to both mouse-adapted and non-mouse-adapted influenza B virus infection. *J Virol* **83**, 1147-51.
20. Hsiang, T. Y., Zhao, C. & Krug, R. M. (2009). Interferon-induced ISG15 conjugation inhibits influenza A virus gene expression and replication in human cells. *J Virol* **83**, 5971-7.
21. Zhao, C., Hsiang, T. Y., Kuo, R. L. & Krug, R. M. (2010). ISG15 conjugation system targets the viral NS1 protein in influenza A virus-infected cells. *Proc Natl Acad Sci U S A* **107**, 2253-8.
22. Tang, Y., Zhong, G., Zhu, L., Liu, X., Shan, Y., Feng, H., Bu, Z., Chen, H. & Wang, C. (2010). Herc5 attenuates influenza A virus by catalyzing ISGylation of viral NS1 protein. *J Immunol* **184**, 5777-90.
23. Shi, H. X., Yang, K., Liu, X., Liu, X. Y., Wei, B., Shan, Y. F., Zhu, L. H. & Wang, C. (2010). Positive regulation of interferon regulatory factor 3 activation by Herc5 via ISG15 modification. *Mol Cell Biol* **30**, 2424-36.
24. Durfee, L. A., Lyon, N., Seo, K. & Huibregtse, J. M. (2010). The ISG15 conjugation system broadly targets newly synthesized proteins: implications for the antiviral function of ISG15. *Mol Cell* **38**, 722-32.
25. Okumura, A., Lu, G., Pitha-Rowe, I. & Pitha, P. M. (2006). Innate antiviral response targets HIV-1 release by the induction of ubiquitin-like protein ISG15. *Proc Natl Acad Sci U S A* **103**, 1440-5.
26. Woods, M. W., Kelly, J. N., Hattlmann, C. J., Tong, J. G., Xu, L. S., Coleman, M. D., Quest, G. R., Smiley, J. R. & Barr, S. D. (2011). Human HERC5 restricts an early stage of HIV-1 assembly by a mechanism correlating with the ISGylation of Gag. *Retrovirology* **8**, 95.
27. Okumura, A., Pitha, P. M. & Harty, R. N. (2008). ISG15 inhibits Ebola VP40 VLP budding in an L-domain-dependent manner by blocking Nedd4 ligase activity. *Proc Natl Acad Sci U S A* **105**, 3974-9.
28. Malakhova, O. A. & Zhang, D. E. (2008). ISG15 inhibits Nedd4 ubiquitin E3 activity and enhances the innate antiviral response. *J Biol Chem* **283**, 8783-7.
29. D'Cunha, J., Knight, E., Jr., Haas, A. L., Truitt, R. L. & Borden, E. C. (1996). Immunoregulatory properties of ISG15, an interferon-induced cytokine. *Proc Natl Acad Sci U S A* **93**, 211-5.

30. D'Cunha, J., Ramanujam, S., Wagner, R. J., Witt, P. L., Knight, E., Jr. & Borden, E. C. (1996). In vitro and in vivo secretion of human ISG15, an IFN-induced immunomodulatory cytokine. *J Immunol* **157**, 4100-8.
31. Bogunovic, D., Byun, M., Durfee, L. A., Abhyankar, A., Sanal, O., Mansouri, D., Salem, S., Radovanovic, I., Grant, A. V., Adimi, P., Mansouri, N., Okada, S., Bryant, V. L., Kong, X. F., Kreins, A., Velez, M. M., Boisson, B., Khalilzadeh, S., Ozcelik, U., Darazam, I. A., Schoggins, J. W., Rice, C. M., Al-Muhsen, S., Behr, M., Vogt, G., Puel, A., Bustamante, J., Gros, P., Huibregtse, J. M., Abel, L., Boisson-Dupuis, S. & Casanova, J. L. (2012). Mycobacterial disease and impaired IFN-gamma immunity in humans with inherited ISG15 deficiency. *Science* **337**, 1684-8.
32. Damjanovic, D., Small, C. L., Jeyanathan, M., McCormick, S. & Xing, Z. (2012). Immunopathology in influenza virus infection: uncoupling the friend from foe. *Clin Immunol* **144**, 57-69.
33. La Gruta, N. L., Kedzierska, K., Stambas, J. & Doherty, P. C. (2007). A question of self-preservation: immunopathology in influenza virus infection. *Immunol Cell Biol* **85**, 85-92.
34. Perrone, L. A., Plowden, J. K., Garcia-Sastre, A., Katz, J. M. & Tumpey, T. M. (2008). H5N1 and 1918 pandemic influenza virus infection results in early and excessive infiltration of macrophages and neutrophils in the lungs of mice. *PLoS Pathog* **4**, e1000115.
35. Kobasa, D., Takada, A., Shinya, K., Hatta, M., Halfmann, P., Theriault, S., Suzuki, H., Nishimura, H., Mitamura, K., Sugaya, N., Usui, T., Murata, T., Maeda, Y., Watanabe, S., Suresh, M., Suzuki, T., Suzuki, Y., Feldmann, H. & Kawaoka, Y. (2004). Enhanced virulence of influenza A viruses with the haemagglutinin of the 1918 pandemic virus. *Nature* **431**, 703-7.
36. Brandes, M., Klauschen, F., Kuchen, S. & Germain, R. N. (2013). A systems analysis identifies a feedforward inflammatory circuit leading to lethal influenza infection. *Cell* **154**, 197-212.
37. Tumpey, T. M., Garcia-Sastre, A., Taubenberger, J. K., Palese, P., Swayne, D. E., Pantin-Jackwood, M. J., Schultz-Cherry, S., Solorzano, A., Van Rooijen, N., Katz, J. M. & Basler, C. F. (2005). Pathogenicity of influenza viruses with genes from the 1918 pandemic virus: functional roles of alveolar macrophages and neutrophils in limiting virus replication and mortality in mice. *J Virol* **79**, 14933-44.
38. Garcia-Sastre, A., Durbin, R. K., Zheng, H., Palese, P., Gertner, R., Levy, D. E. & Durbin, J. E. (1998). The role of interferon in influenza virus tissue tropism. *J Virol* **72**, 8550-8.
39. Look, D. C., Walter, M. J., Williamson, M. R., Pang, L., You, Y., Sreshta, J. N., Johnson, J. E., Zander, D. S. & Brody, S. L. (2001). Effects of paramyxoviral infection on airway epithelial cell Foxj1 expression, ciliogenesis, and mucociliary function. *Am J Pathol* **159**, 2055-69.
40. Buchweitz, J. P., Harkema, J. R. & Kaminski, N. E. (2007). Time-dependent airway epithelial and inflammatory cell responses induced by influenza virus A/PR/8/34 in C57BL/6 mice. *Toxicol Pathol* **35**, 424-35.
41. Ibricevic, A., Pekosz, A., Walter, M. J., Newby, C., Battaile, J. T., Brown, E. G., Holtzman, M. J. & Brody, S. L. (2006). Influenza virus receptor specificity and cell tropism in mouse and human airway epithelial cells. *J Virol* **80**, 7469-80.

42. Osiak, A., Utermohlen, O., Niendorf, S., Horak, I. & Knobeloch, K. P. (2005). ISG15, an interferon-stimulated ubiquitin-like protein, is not essential for STAT1 signaling and responses against vesicular stomatitis and lymphocytic choriomeningitis virus. *Mol Cell Biol* **25**, 6338-45.
43. Kim, K. I., Yan, M., Malakhova, O., Luo, J. K., Shen, M. F., Zou, W., de la Torre, J. C. & Zhang, D. E. (2006). Ube1L and protein ISGylation are not essential for alpha/beta interferon signaling. *Mol Cell Biol* **26**, 472-9.
44. Kim, M. J., Hwang, S. Y., Imaizumi, T. & Yoo, J. Y. (2008). Negative feedback regulation of RIG-I-mediated antiviral signaling by interferon-induced ISG15 conjugation. *J Virol* **82**, 1474-83.
45. Jeon, Y. J., Choi, J. S., Lee, J. Y., Yu, K. R., Kim, S. M., Ka, S. H., Oh, K. H., Kim, K. I., Zhang, D. E., Bang, O. S. & Chung, C. H. (2009). ISG15 modification of filamin B negatively regulates the type I interferon-induced JNK signalling pathway. *EMBO Rep* **10**, 374-80.
46. Yanguéz, E., Garcia-Culebras, A., Frau, A., Llompart, C., Knobeloch, K. P., Gutierrez-Erlandsson, S., Garcia-Sastre, A., Esteban, M., Nieto, A. & Guerra, S. (2013). ISG15 regulates peritoneal macrophages functionality against viral infection. *PLoS Pathog* **9**, e1003632.
47. Roulston, A., Marcellus, R. C. & Branton, P. E. (1999). Viruses and apoptosis. *Annu Rev Microbiol* **53**, 577-628.
48. Yuan, W. & Krug, R. M. (2001). Influenza B virus NS1 protein inhibits conjugation of the interferon (IFN)-induced ubiquitin-like ISG15 protein. *EMBO J* **20**, 362-71.
49. Sridharan, H., Zhao, C. & Krug, R. M. (2010). Species specificity of the NS1 protein of influenza B virus: NS1 binds only human and non-human primate ubiquitin-like ISG15 proteins. *J Biol Chem* **285**, 7852-6.
50. Parker, J. C., Whiteman, M. D. & Richter, C. B. (1978). Susceptibility of inbred and outbred mouse strains to Sendai virus and prevalence of infection in laboratory rodents. *Infect Immun* **19**, 123-30.
51. Rodrigue-Gervais, I. G., Labbe, K., Dagenais, M., Dupaul-Chicoine, J., Champagne, C., Morizot, A., Skeldon, A., Brincks, E. L., Vidal, S. M., Griffith, T. S. & Saleh, M. (2014). Cellular inhibitor of apoptosis protein cIAP2 protects against pulmonary tissue necrosis during influenza virus infection to promote host survival. *Cell Host Microbe* **15**, 23-35.
52. Monticelli, L. A., Sonnenberg, G. F., Abt, M. C., Alenghat, T., Ziegler, C. G., Doering, T. A., Angelosanto, J. M., Laidlaw, B. J., Yang, C. Y., Sathaliyawala, T., Kubota, M., Turner, D., Diamond, J. M., Goldrath, A. W., Farber, D. L., Collman, R. G., Wherry, E. J. & Artis, D. (2011). Innate lymphoid cells promote lung-tissue homeostasis after infection with influenza virus. *Nat Immunol* **12**, 1045-54.
53. Jamieson, A. M., Pasman, L., Yu, S., Gamradt, P., Homer, R. J., Decker, T. & Medzhitov, R. (2013). Role of tissue protection in lethal respiratory viral-bacterial coinfection. *Science* **340**, 1230-4.
54. Kalluri, R. & Weinberg, R. A. (2009). The basics of epithelial-mesenchymal transition. *J Clin Invest* **119**, 1420-8.
55. Farrell, J., Kelly, C., Rauch, J., Kida, K., Garcia-Munoz, A., Monsefi, N., Turriziani, B., Doherty, C., Mehta, J. P., Matallanas, D., Simpson, J. C., Kolch, W. & von Kriegsheim, A. (2014). HGF Induces Epithelial-to-Mesenchymal Transition by Modulating the Mammalian Hippo/MST2 and ISG15 Pathways. *J Proteome Res*.

56. Jiang, A. P., Zhou, D. H., Meng, X. L., Zhang, A. P., Zhang, C., Li, X. T. & Feng, Q. (2014). Down-regulation of epidermal growth factor receptor by curcumin-induced UBE1L in human bronchial epithelial cells. *J Nutr Biochem* **25**, 241-9.
57. Desai, S. D., Reed, R. E., Burks, J., Wood, L. M., Pullikuth, A. K., Haas, A. L., Liu, L. F., Breslin, J. W., Meiners, S. & Sankar, S. (2012). ISG15 disrupts cytoskeletal architecture and promotes motility in human breast cancer cells. *Exp Biol Med (Maywood)* **237**, 38-49.
58. Wang, R. G., Kaul, M. & Zhang, D. X. (2012). Interferon-stimulated gene 15 as a general marker for acute and chronic neuronal injuries. *Sheng Li Xue Bao* **64**, 577-83.
59. Lee, Y. J., Johnson, K. R. & Hallenbeck, J. M. (2012). Global protein conjugation by ubiquitin-like-modifiers during ischemic stress is regulated by microRNAs and confers robust tolerance to ischemia. *PLoS One* **7**, e47787.
60. Nakka, V. P., Lang, B. T., Lenschow, D. J., Zhang, D. E., Dempsey, R. J. & Vemuganti, R. (2011). Increased cerebral protein ISGylation after focal ischemia is neuroprotective. *J Cereb Blood Flow Metab* **31**, 2375-84.
61. Goritzka, M., Durant, L. R., Pereira, C., Salek-Ardakani, S., Openshaw, P. J. & Johansson, C. (2014). Alpha/Beta Interferon Receptor Signaling Amplifies Early Proinflammatory Cytokine Production in the Lung during Respiratory Syncytial Virus Infection. *J Virol* **88**, 6128-36.
62. Durbin, J. E., Johnson, T. R., Durbin, R. K., Mertz, S. E., Morotti, R. A., Peebles, R. S. & Graham, B. S. (2002). The role of IFN in respiratory syncytial virus pathogenesis. *J Immunol* **168**, 2944-52.
63. Lopez, C. B., Yount, J. S., Hermesh, T. & Moran, T. M. (2006). Sendai virus infection induces efficient adaptive immunity independently of type I interferons. *J Virol* **80**, 4538-45.
64. Shahangian, A., Chow, E. K., Tian, X., Kang, J. R., Ghaffari, A., Liu, S. Y., Belperio, J. A., Cheng, G. & Deng, J. C. (2009). Type I IFNs mediate development of postinfluenza bacterial pneumonia in mice. *J Clin Invest* **119**, 1910-20.
65. Seo, S. U., Kwon, H. J., Ko, H. J., Byun, Y. H., Seong, B. L., Uematsu, S., Akira, S. & Kweon, M. N. (2011). Type I interferon signaling regulates Ly6C(hi) monocytes and neutrophils during acute viral pneumonia in mice. *PLoS Pathog* **7**, e1001304.
66. Davidson, S., Crotta, S., McCabe, T. M. & Wack, A. (2014). Pathogenic potential of interferon alpha in acute influenza infection. *Nat Commun* **5**, 3864.
67. Neumann, G., Watanabe, T., Ito, H., Watanabe, S., Goto, H., Gao, P., Hughes, M., Perez, D. R., Donis, R., Hoffmann, E., Hobom, G. & Kawaoka, Y. (1999). Generation of influenza A viruses entirely from cloned cDNAs. *Proc Natl Acad Sci U S A* **96**, 9345-50.
68. You, Y., Richer, E. J., Huang, T. & Brody, S. L. (2002). Growth and differentiation of mouse tracheal epithelial cells: selection of a proliferative population. *Am J Physiol Lung Cell Mol Physiol* **283**, L1315-21.

Chapter 4

Conclusions and Future Directions

Conclusions and Future Directions

Over the course of the past 30 years, the combined efforts of many labs have characterized the expression of ISG15, the structure of ISG15, and both the components and biochemistry of the ISG15 conjugation pathway. Yet the effects of ISG15 conjugation on target proteins remains poorly understood. Most efforts to evaluate the molecular consequence of ISGylation have approached this question through the generation of non-ISGylatable mutant proteins, or through the fusion of ISG15 to the N-terminus of proteins, with minimal success. Typically, the observed phenotypes have been small, and almost all effects of ISGylation have been reported to occur through the disruption of normal protein-protein interactions. Also, while studies have observed changes in function of the ISGylated protein, most have failed to demonstrate how modification of a small fraction of the total protein would lead to any appreciable phenotype. One possible explanation for the dearth of insights into the function of ISGylation on particular proteins is that ISG15 mediates large effects on global cellular processes through the cumulative small effects on many different proteins. However, another possibility is that previous studies have not examined the effects of ISGylation in biologically relevant pathways.

In the current studies, we set out to characterize the function of ISG15 from a top-down approach of dissecting the mechanisms responsible for the largest phenotype discovered in ISG15^{-/-} mice to date: susceptibility to viral infection. First we evaluated the effect of ISG15 on influenza B virus (IBV) infection in tissue culture. We found that ISG15 can restrict IBV replication in a biologically relevant cell culture system. We then used a novel mouse expressing an enzymatically dead form of the ISG15 deconjugating enzyme, UBP43, to show that inhibiting ISG15 deconjugation increases the pool of ISG15 conjugates and increases the anti-viral protection mediated by ISG15. In a separate series of studies, we characterized the pathogenesis

of influenza A virus (IAV) and Sendai virus in ISG15^{-/-} and UbE1L^{-/-} mice to evaluate the role of ISG15 during other respiratory virus infections. Surprisingly, we found that while ISG15 protects mice from IAV and Sendai virus in a conjugation dependent manner, the mechanism by which it promotes survival of mice appears to be quite different from its role during IBV infection. Little difference in viral burden between WT and ISG15^{-/-} mice was observed *in vivo*, and no difference in IAV or Sendai virus replication was detected in tissue culture. We also observed no major differences in the acute immune response after infection in ISG15^{-/-} mice compared to WT mice. Our findings suggest that ISG15^{-/-} mice are not deficient in their ability to clear viral infection, but rather are more sensitive to disease induced by viral infection, either sustaining greater tissue damage during infection or having a decreased capacity to heal after infection.

In addition to the data presented in chapters 1 and 2, preliminary data from both of these projects have provided a number of avenues to pursue studying the function of ISG15.

ISGylation of Viral Proteins

Some previous studies showing inhibition of virus replication by ISG15 have proposed a model in which ISG15 directly disrupts the virus lifecycle through ISGylation of viral proteins. Influenza A/NS1, influenza A/M1, and HPV capsid protein have all been shown to be ISGylated, and in the case of influenza A/NS1 and HPV capsid protein, ISG15 modification has been shown to inhibit virus replication^{1;2;3}. We have also been able to demonstrate that influenza B/NS1 is ISGylated during infection of mTEC (Figure 4.1A). Additionally, we have shown that influenza B/M1 and influenza A/M1 and A/NS1 are capable of being ISGylated in 293T cells expressing

the ISG15 conjugation system (data not shown). However using brute force lysine mutagenesis, mass spectrometry, and other novel methods, we were unable to identify ISGylated lysine residues in order to generate non-ISGylatable mutant proteins. Part of this failure was likely due to the ability of ISG15 to modify individual proteins on multiple lysine residues. While ISGylated proteins often have only one modification, the modified species observed by western blot is actually a heterogeneous population of proteins modified by one ISG15 protein on different lysine residues. Two reports of A/NS1 being ISGylated both found that 7-8 lysine residues were detected as being ISGylated, and in one of the studies all 7 lysines had to be mutated before NS1 was rendered non-ISGylatable^{1;3}.

While ISGylation of NS1 and M1 have now been reported by other labs, we also discovered a novel interaction between ISG15 and the influenza virus nucleoprotein protein (NP). We found that in infected cells, both influenza A and influenza B NP co-immunoprecipitated with ISG15 in a conjugation dependent interaction (Figure 4.1A,B). Interestingly, it was predominantly non-ISGylated NP that pulled down with ISG15. While we could not detect ISGylated NP protein during infection, we were able to recapitulate this interaction in 293T cells expressing the ISG15 conjugation system and influenza virus NP (Figure 4.2A). In this overexpression system we could detect ISGylation of NP protein (Figure 4.2B). As NP is known to oligomerize when expressed independent of other viral proteins, we believe that it is likely that the non-ISGylated NP that co-immunoprecipitates with ISG15 is likely being pulled down by interacting with ISGylated NP protein⁴. However, we have not ruled out the possibility that NP coimmunoprecipitates with ISG15 because it is interacting with ISGylated host proteins.

It has been hypothesized that incorporation of ISGylated HPV capsid protein into HPV virions might affect capsid structure and thus infectivity of the virion ². In a similar model, it is possible that NP ISGylation alters the structure of NP oligomers and the ability of NP to cover and protect vRNA in vRNP complexes. This might leave the vRNP more susceptible to RNA sensors. It is not clear whether this interaction between ISG15 and NP might affect virus replication. Notably, we observe this interaction during IAV infection despite observing no difference in IAV replication in ISG15^{-/-} mTEC. However, it is possible that in the case of IAV, other proteins, such as NS1, can compensate to inhibit the downstream effects of vRNP detection. For example, A/NS1 is capable of inhibiting RIG-I, however it is not known whether B/NS1 is able to do the same ⁵. It will be interesting to determine whether vRNP isolated from WT mTEC have ISGylated NP incorporated into them, and whether there is a difference in the ability of RIG-I, PKR, and other RNA sensors to bind to vRNP isolated from WT or ISG15^{-/-} mTEC. It will also be interesting to further characterize what effects this interaction between ISG15 and NP might have on processes not directly related to intracellular virus replication, such as antigen presentation, and to evaluate whether ISG15 also interacts with the NP of other viruses.

Effects of ISG15 on Cell Transcriptome and Proteome

As a member of the ubiquitin-like modifier family of regulatory proteins, and as one of the most highly induced genes after interferon stimulation, it was thought that ISG15 would play an important role in the regulation of interferon signaling and ISG expression. However, no major differences in ISG expression were observed in ISG15^{-/-} or Ube1L^{-/-} cells ^{6;7}. Our

studies in UBP43^{C61A/C61A} cells suggest that inhibition of ISG15 deconjugation does have an effect on gene expression. This effect was small but consistent, suggesting that a similar effect in the original studies evaluating the effect of ISG15 on ISG expression might have been overlooked by non-quantitative assessments of gene expression. Furthermore, all of these previous studies have specifically focused on how ISG15 affects ISG expression. There is a complete absence of published studies evaluating the effects of ISG15 on global gene expression.

As a post-translational modifier, the potential effects of ISG15 are determined by the cellular proteome, and thus, by definition, the effects of ISG15 will be cell type specific. ISG15 inhibition of virus replication could be mediated entirely through ISGylation of viral proteins. However, hundreds of host proteins are ISGylated and ISG15 interaction with Nedd4 and proteins in the endosomal sorting complexes required for transport (ESCRT) system has been shown to inhibit release of Ebola, HIV-1, and ASLV, suggesting that manipulation of host cell biology can also inhibit virus replication ^{8; 9; 10; 11; 12}. Our IBV mTEC infection model represents a biologically relevant system where 24 hours of interferon stimulation converts cells into different states of virus permissiveness depending on the presence or absence of ISG15. Thus it will be illuminating to analyze global differences in the status of these cells that might result in this difference in virus replication. Cell transcriptomes could be analyzed by microarray analysis. Given that ISG15 is a post-translational modifier, it might have an effect on the cellular proteome independent of transcriptional regulation. Therefore it would also be informative to perform stable isotope labeling by amino acids in cell culture (SILAC) in order to determine how ISG15 might affect global protein levels in mTEC.

Role of ISG15 in cell death after Sendai virus infection

As reported in Chapter 3, we observed no difference in Sendai virus replication in WT and ISG15^{-/-} mTEC. These cultures support virus replication for days after peak virus levels are observed in the apical media. After 6.5 days of infection, we observed increased lactate dehydrogenase in the apical media of ISG15^{-/-} mTEC compared to the apical media of WT mTEC (Figure 4.3A). This indication of increased cell death was observed even though there was still no difference in virus production between WT and ISG15^{-/-} cells at this late time point (Figure 4.3B). When these cultures were stained for Sendai virus antigen, it was observed that ISG15^{-/-} cells had a more elongated fibroblast-like morphology than WT cells (Figure 4.3C). These observations appear to be mediated through an ISG15 conjugation dependent mechanism as Ube1L^{-/-} cultures phenocopied what was seen in ISG15^{-/-} cultures (Figure 4.3 A-C).

Increased cell death could potentially facilitate in increased viral spread during infection *in vivo*, which might account for the small elevation in virus burden observed ISG15^{-/-} mice at some time points. Alternatively this increased cell death might be responsible for the increased disease observed late during infection. Our mTEC model provides us with a means to evaluate the mechanism by which ISG15 conjugation prevents cell death after Sendai virus infection. We are currently working on identifying what cell death pathway is responsible for this phenotype. Once this has been evaluated we can return to our *in vivo* model to assess whether we can detect a similar process occurring in the distal airway epithelium and whether particular cell death inhibitors might protect ISG15^{-/-} mice from increased Sendai virus induced pathology. Additionally, we are evaluating whether we can detect a similar phenotype after infection of mTEC with IAV.

Role of ISG15 during Sendai virus infection *in vivo*

It remains unclear precisely why ISG15^{-/-} mice are more susceptible to Sendai virus infection. We did note slightly elevated titers in ISG15^{-/-} mice compared to WT mice at some times after infection and there was a trend of slightly delayed virus clearance in ISG15^{-/-} mice at day 8 post infection. This makes it difficult to determine whether the increased pathology observed in ISG15^{-/-} lungs is a result of increased damage from increased viral burden or a result of a defect in the repair response after clearance of the infection. While we noted increased weight loss in ISG15^{-/-} mice at our lower dose of Sendai virus infection, when we decreased the infectious dose further we observed no lethality in ISG15^{-/-} mice and no difference in weight loss or weight recovery compared to WT mice (Figure 4.4). This supports the idea that there is no defect in the ability of ISG15^{-/-} mice to control and clear infection. Rather, it appears that increased morbidity only occurs in ISG15^{-/-} mice when the damage caused by infection crosses a certain threshold.

While our morbidity experiments and histology analysis suggest that ISG15^{-/-} mice are dying from a defect that occurs late during infection, it is important to note that we did observe that ISG15^{-/-} mice exhibit ruffled fur starting at day 2-3 post infection (Figure 4.5). Neither WT nor UbE1L^{-/-} mice exhibit the ruffled fur observed in ISG15^{-/-} mice, suggesting that this phenomenon results from the lack of free ISG15. The fact that UbE1L^{-/-} mice do not exhibit ruffled fur, but are still susceptible to infection, suggests that either the reason for the ruffled fur is inconsequential in regards to infection outcome, or that UbE1L^{-/-} and ISG15^{-/-} mice might be

susceptible to Sendai virus for different reasons. Either way, the ruffled fur observed in ISG15^{-/-} mice demonstrates that ISG15 does play a role in the early response to Sendai virus infection. Further evaluation is needed to determine how the response of ISG15^{-/-} mice is different from WT mice.

We have not identified any difference in inflammatory cell recruitment to the lungs, however, this has not been an exhaustive analysis. It is possible that certain specific cell types are not recruited or functioning properly in ISG15^{-/-} mice. We saw no elevated recruitment of neutrophils or inflammatory macrophages that might suggest a mechanism for causing increased damage in the lung. We also did not see major differences in T cell recruitment. It is possible that while similar numbers and types of cells are recruited to the lungs, these cells might behave differently in the absence of ISG15. However, our BAL cytokine analysis did not detect any obvious differences that might suggest a difference in the activity of the inflammatory cell infiltrates.

Many increasingly esoteric hypotheses could be tested to determine how the response to Sendai infection in ISG15^{-/-} mice differs from that of WT mice. However, at this point it seems prudent to pursue experiments to broadly evaluate differences between WT and ISG15^{-/-} mice during infection. It has previously been reported that innate lymphoid cells can protect airway epithelium integrity in mice and promote survival after IAV infection without affecting viral burden¹³. This precedent reinforces the idea that we do not know whether the increased pathology observed in ISG15^{-/-} mice is intrinsic to the airway epithelium or is mediated in *trans* by inflammatory cells. To narrow down what cells might be conferring the ISG15-mediated protection from Sendai virus, we are currently performing bone marrow chimera experiments to

evaluate whether the radiosensitive or radioresistant compartments of cells are necessary and/or sufficient for mediating protection through ISG15 expression.

We are also performing microarray analysis on lung RNA harvested from mice infected with Sendai virus. We have isolated total lung RNA from non-manipulated mice, and mice infected with Sendai virus for 3, 6, 8, and 11 days. These samples should allow us to evaluate the effects of basal expression of ISG15 in non-infected mice, the early differences in gene expression that result in the distinct ruffled fur phenotype observed in ISG15^{-/-} mice by day 3 post infection, and the environment of the healing lung at day 11 post infection.

Concluding Remarks

Because ISG15 is one of the most strongly upregulated genes after type I interferon stimulation, it was thought that ISG15 would play an important role in mediating the anti-viral state induced by type I interferons. Surprisingly, the initial characterization of ISG15^{-/-} mice found no increase in susceptibility to LCMV and VSV infection, and no major defect in interferon signaling⁶. Interestingly, similarly unexpected observations have been reported for ISG15's sister diubiquitin-like modifier, FAT10. FAT10 is an interferon γ inducible diubiquitin-like protein¹⁴. While FAT10^{-/-} cells appeared to have elevated rates of apoptosis and FAT10^{-/-} mice were more sensitive to LPS than WT mice, the initial characterization of FAT10^{-/-} mice revealed no other major phenotypes and no obvious defect in the immune system¹⁵. A recent re-evaluation of these mice revealed that FAT10^{-/-} mice actually have a slightly extended life span and decreased adiposity compared to WT mice¹⁶. The decreased adiposity in FAT10^{-/-} mice resulted from an upregulation of fatty acid metabolism genes. This unexpected finding

demonstrates how an interferon inducible ubiquitin-like modifier can affect basic physiology outside of the context of acute infection. It will be important to further evaluate how this effect might factor into the response to acute infection.

The remarkably strong protective effect of ISG15 during IBV infection has arguably been a double-edged sword for the ISG15 field, as it has bolstered the hypothesis that the major function of ISG15 is to inhibit virus replication. However, our findings suggest that ISG15 may have a role in the regulation of the host response to infection outside of the immune response. ISG15 has been implicated in inhibiting virus budding through the regulation of a number of proteins that play a role in the ESCRT pathway. How ISG15 might affect vesicular trafficking in non-infected host cells, and what physiological effects this might have, has not been studied. ISG15 has been demonstrated to be expressed during red blood cell differentiation¹⁷. While ISG15^{-/-} mice are viable and have no general health defects, it is not clear how the effects of ISG15 on red blood cell differentiation might affect the fitness of ISG15^{-/-} mice during acute respiratory infection. ISG15 has also been reported to be expressed in the endometrium during pregnancy, and the overexpression of ISG15 and UBE1L have often been observed in cancer cells^{18;19}. As increased lethality after virus infection remains the most robust phenotype that has been observed in mice, further characterization of the role of ISG15 in these *in vivo* infection models is needed. However, to better understand the function of ISG15, it will also be important to re-evaluate the role of ISG15 in general homeostatic processes *in vivo*.

METHODS

Mice

Mice were bred and maintained at Washington University School of Medicine in accordance with all federal and University guidelines, under specific-pathogen-free conditions. WT C57BL/6J mice were purchased from Jackson Laboratory (Bar Harbor, ME), bred and maintained in our facilities. ISG15^{-/-} mice (provided by Dr. Klaus-Peter Knobeloch, University Clinic Freiburg, Germany) and Ube1L^{-/-} mice (provided by Dr. Dong-Er Zhang, University of California, San Diego) were generated as previously described. ISG15^{-/-} and Ube1L^{-/-} mice were fully backcrossed (>99.72% and 99.93% respectively to C57BL/6 by congenic SNP analysis through Taconic Laboratories (Hudson, NY).

Viruses

Influenza A virus. Recombinant influenza A/WSN/33 (rWSN) virus was generated from cDNA as previously described. The virus was grown on MDCK cells using DMEM containing 1 ug/ml N-acetyltryptin (Sigma Chemicals, St. Louis, MO), 100 units/ml penicillin, and 100 ug/ml streptomycin (Invitrogen, Carlsbad, CA). The cells were infected at a multiplicity of infection of 0.01 pfu per cell, harvested 48 hrs postinfection and titered by plaque assay in MDCK cells.

Influenza B virus. Recombinant WT influenza B/Yamagata/88 virus was grown in 10 day old embryonated chicken eggs and titered by plaque assay in MDCK cells.

Sendai virus. Sendai/52 Fushimi strain virus was purchased from ATCC. Virus was plaque purified after infection of Vero cells to isolate a single clone that was then propagated in 11 day

old embryonated chicken eggs. Virus from allantoic fluid was diluted in PBS and stored at -80 degrees Celcius.

Viral stocks were titered by plaque assay on MDCK cells for influenza virus and Vero cells for Sendai virus.

mTEC infections

Murine tracheal epithelial cultures were generated from the indicated genotypes of mice as previously described. Cells were harvest from tracheas of female mice (5 to 12-weeks old) and grown under media in transwells (Corning) for 7 days. Apical media was then removed and the cells were grown at air-liquid interface for 2-3 weeks prior to experimentation. Virus was diluted in DMEM supplemented with 1% Penicillin/1% Streptomycin (1%P/S) to concentrations of 9×10^5 pfu in 100ul of media. Infections were performed by adding 100ul of virus to the apical chamber and incubating at 37 degrees C for 1 hour. Virus was removed and the apical chamber was washed 3 times with 200ul of DMEM(1%P/S). After washing 100ul of DMEM(1%P/S) was added back to apical chamber. At indicated times apical media was collected and replaced with 100ul of DMEM(1%P/S). Virus titers in apical media were assessed by plaque assay on MDCK cells. For interferon β pretreatment, 30U/ml of interferon β (PBL Assay Science) was added to basolateral media. After 24 hours, immediately prior to infection, basolateral media was removed and basolateral chambers were washed 2 times with PBS and then replaced with media containing no interferon.

In vivo infections

Mice were anesthetized using an intraperitoneal injection of a ketamine/xylene cocktail prior to infection. 8-10 week old male mice were infected intranasally with $(0.6-1.0) \times 10^6$ pfu Sendai virus in a total volume of 30ul of PBS.

Lactate dehydrogenase assay

Lactate dehydrogenase in apical media was assessed using CytoTox 96 NonRadioactive Cytotoxicity Assay (Promega). Assay was scaled down to analyze 25 ul of sample.

mTEC immunostaining

mTEC were fixed by incubating in 4% formaldehyde diluted in PBS for 10 minutes. Cells were permeabilized for 12 minutes in PBS, 0.2% TritonX 100, 0.1% sodium citrate. Cells were blocked in PBS with 3%BSA and 3% normal goat serum for 30 minutes. Cells were stained for Sendai virus antigen using anti-Sendai virus chicken serum and Alexa Fluor 488[®] conjugated goat anti-chicken secondary antibody.

Plasmids

Expression plasmids were transfected into 293T cells using Lipofectamine 2000 (Life Technologies). 6His-ISG15(LRLRAA), 6His-ISG15(LRLRGG), HA-mUbe1L(E1), and FLAG-mUbcM8(E2)) were described previously^{20, 21}. mHERC6(E3) was described previously²². Influenza B/Lee/40 nucleoprotein and influenza A/WSN/33 nucleoprotein were cloned into pCMV2.0 expression plasmid.

Immunoprecipitations and pull-downs

ISG15 immunoprecipitations were performed using anti-ISG15(3C2) antibody. Anti-FLAG(M2) affinity resin was purchased from Sigma. Nickel affinity resin (Qiagen) was used to pull-down proteins via 6-His tag. For 293T pull-downs, 48 hours post transfection cells were lysed in RIPA buffer or NiNTA lysis buffer. Cell debris was pelleted and lysate supernatant was incubated overnight on pull-down beads/resins at 4 degrees Celsius. Pull-downs were washed 4 times using original lysis buffer. Protein was boiled off of anti-ISG15 and Nickel affinity resins in 2x sample buffer. Protein was eluted off of anti-FLAG resin using FLAG peptide. For mTEC immunoprecipitations, each well of mTEC were lysed in 150ul of RIPA buffer. Lysate from 3 wells of each condition were pooled into the same immunoprecipitation. The remainder of the mTEC immunoprecipitation protocol was identical to 293T pull-down protocol.

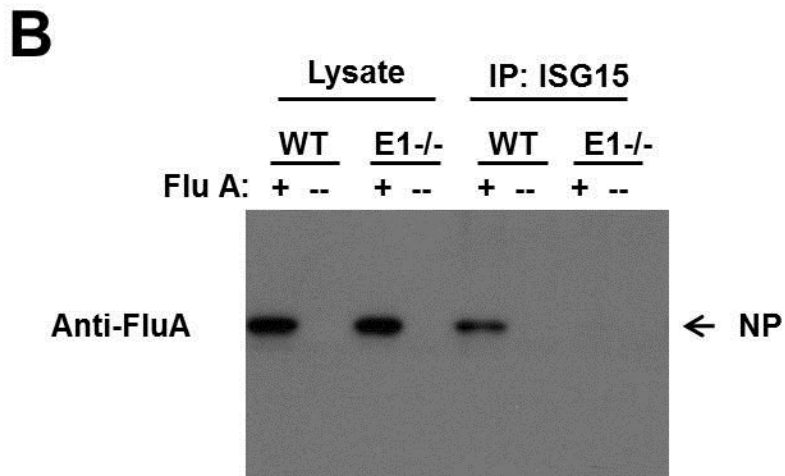
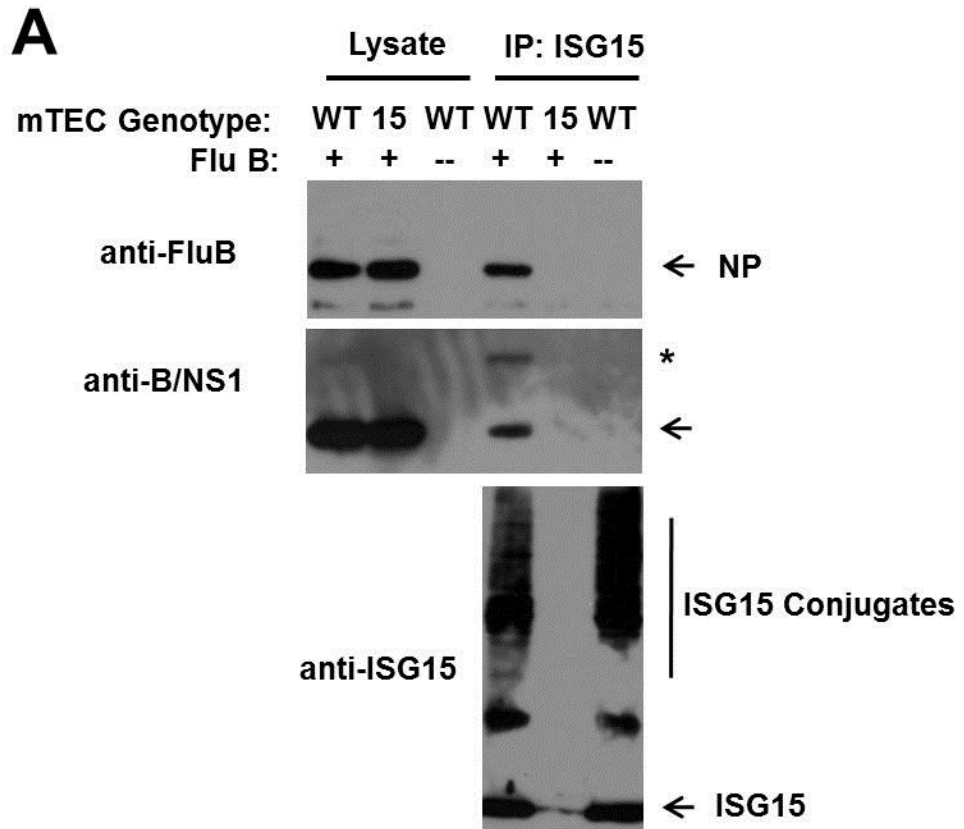


Figure 4.1. Influenza virus proteins co-immunoprecipitate with ISG15 during infection in mTEC.

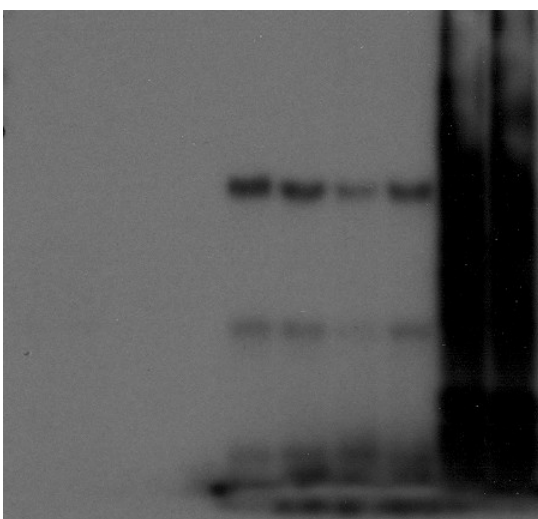
mTEC were generated from WT, ISG15^{-/-}, or Ube1L^{-/-} mice. mTEC were pretreated with interferon β for 24 hours and subsequently infected with 9×10^5 pfu of influenza B virus (**A**) or influenza A virus (**B**). 36 hours post infection mTEC lysates were harvested in RIPA buffer and ISG15 was immunoprecipitated. Lysates and immunoprecipitates were analyzed by western blot for viral protein. Arrows indicate non-modified proteins, asterisk indicates ISGylated form of protein.

A

	Lysate		IP:ISG15							
FLAG-NP of Flu:	A	B	A	B	A	B	A	B	A	B
mE1, mE2, mE3:	--	--	--	--	--	--	+	+	+	+
mISG15(LRLR??):	--	--	--	--	G	G	A	A	G	G



Anti-FLAG



Anti-ISG15

B

	IP: FLAG			IP: FLAG		
FLAG-A/NP:	+	+	+	+	+	+
6His-ISG15:	+	--	+	+	--	+
mE1,mE2,mE3:	--	+	+	--	+	+

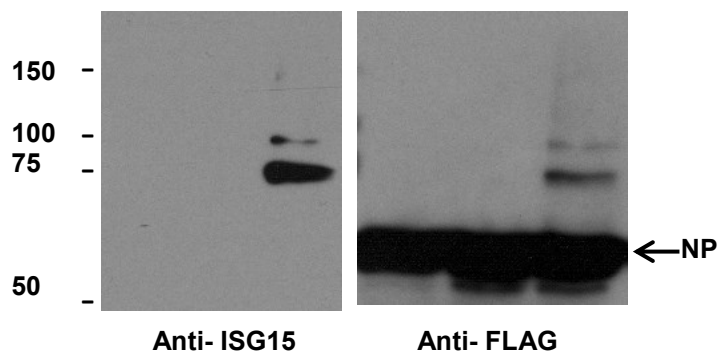


Figure 4.2. Influenza virus nucleoprotein interacts with ISG15 in a conjugation dependent manner.

(A) 293T cells were transfected with FLAG-tagged influenza A virus nucleoprotein or FLAG-tagged influenza B virus expression constructs, with or without expression plasmids encoding the ISG15 conjugation machinery (E1, E2, E3), and HIS-tagged WT ISG15(LRLRGG) or a HIS-tagged mutant of ISG15 incapable of undergoing conjugation ISG15(LRLRAA). 48 hours post transfection lysates were harvested and ISG15 was pulled down using Ni-affinity resin. Lysates and pull-downs were analyzed for ISG15 and NP by western blot.

(B) 293T cells were transfected with indicated expression constructs as in **(A)**. 48 hours post transfection lysates were immunoprecipitated using anti-FLAG affinity resin, and immunoprecipitates were analyzed by western blot.

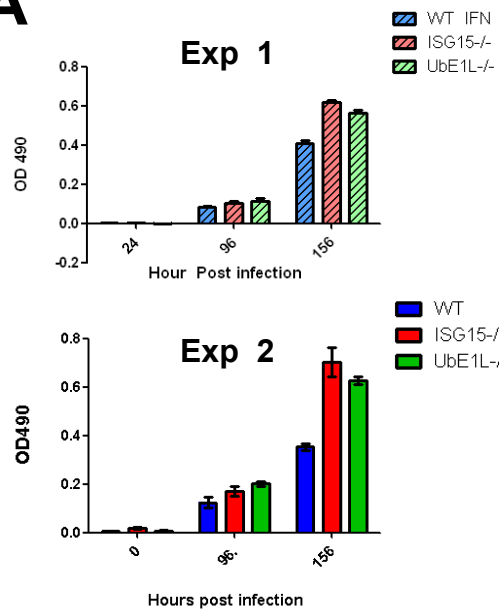
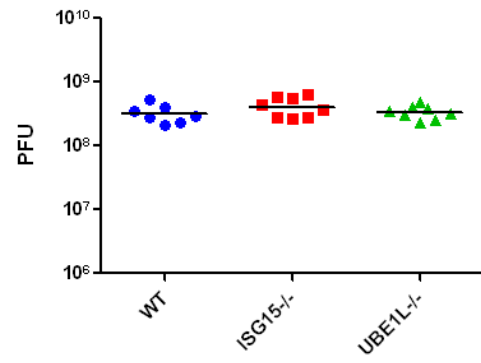
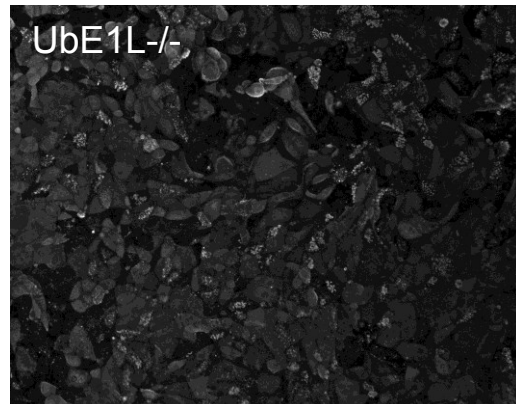
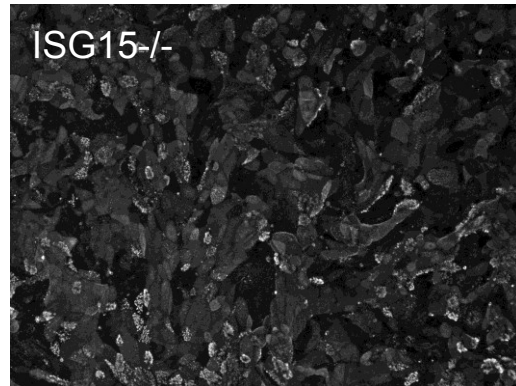
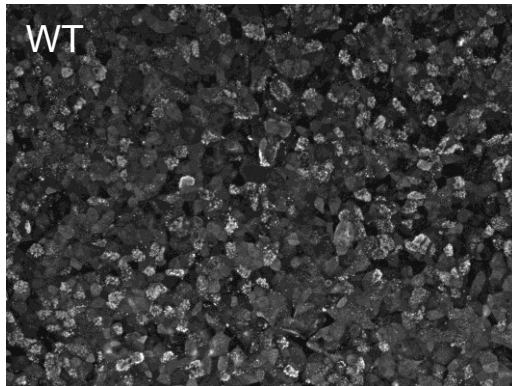
A**B****C**

Figure 4.3. ISG15 conjugation promotes cell survival in mTEC after Sendai virus infection

mTEC were generated from WT, ISG15^{-/-}, or Ube1L^{-/-} mice. Cultures were treated with 30U/ml of interferon β for 24 hours and subsequently infected with 9×10^5 pfu Sendai virus. **(A)** Lactate dehydrogenase levels in the apical media were assessed over the course of infection. **(B)** Sendai virus levels in the apical media at 6.5 days post infection were determined by plaque assay. **(C)** mTEC cultures were infected with Sendai virus for 6.5 days at which point they were fixed and stained with anti-Sendai virus serum (white).

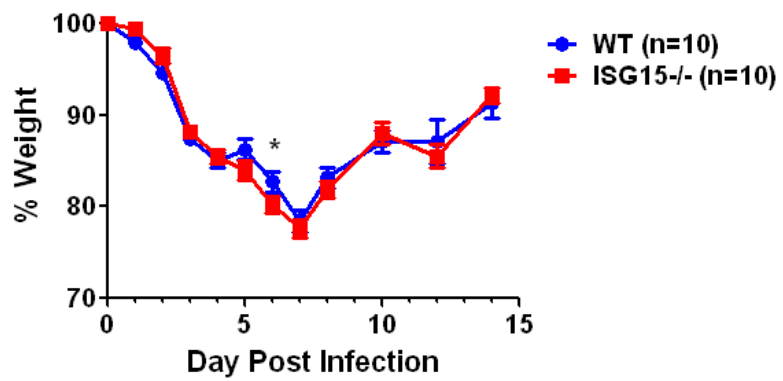


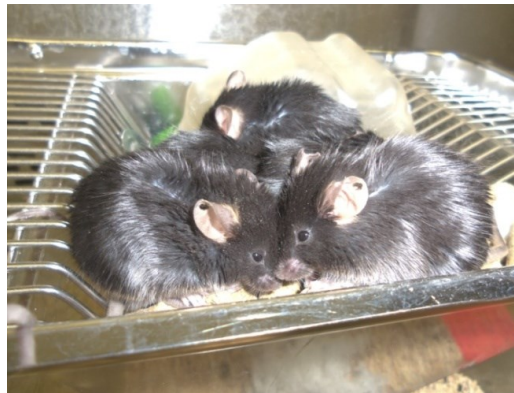
Figure 4.4. ISG15^{-/-} mice infected with sub-lethal dose of Sendai viruses exhibit no difference in weight loss compared to WT mice.

WT and ISG15^{-/-} mice were infected with 4×10^5 PFU Sendai virus and monitored for weight loss. Data was collected from 2 independent infections, 5 mice per infection.

WT



ISG15^{-/-}



UbE1L^{-/-}



Figure 4.5. ISG15^{-/-} mice exhibit ruffled fur after Sendai virus infection

WT, ISG15^{-/-}, and UbE1L^{-/-} mice were infected with 1.0×10^6 PFU Sendai and pictures were taken daily to monitor disease. ISG15^{-/-} but not WT or UbE1L^{-/-} mice exhibited a dramatic ruffling of fur. Above pictures were taken on day 7 post infection, however ruffled fur in ISG15^{-/-} mice could be observed as early as 2-3 days post infection.

REFERENCES

1. Zhao, C., Hsiang, T. Y., Kuo, R. L. & Krug, R. M. (2010). ISG15 conjugation system targets the viral NS1 protein in influenza A virus-infected cells. *Proc Natl Acad Sci U S A* **107**, 2253-8.
2. Durfee, L. A., Lyon, N., Seo, K. & Huibregtse, J. M. (2010). The ISG15 conjugation system broadly targets newly synthesized proteins: implications for the antiviral function of ISG15. *Mol Cell* **38**, 722-32.
3. Tang, Y., Zhong, G., Zhu, L., Liu, X., Shan, Y., Feng, H., Bu, Z., Chen, H. & Wang, C. (2010). Herc5 attenuates influenza A virus by catalyzing ISGylation of viral NS1 protein. *J Immunol* **184**, 5777-90.
4. Ye, Q., Krug, R. M. & Tao, Y. J. (2006). The mechanism by which influenza A virus nucleoprotein forms oligomers and binds RNA. *Nature* **444**, 1078-82.
5. Gack, M. U., Albrecht, R. A., Urano, T., Inn, K. S., Huang, I. C., Carnero, E., Farzan, M., Inoue, S., Jung, J. U. & Garcia-Sastre, A. (2009). Influenza A virus NS1 targets the ubiquitin ligase TRIM25 to evade recognition by the host viral RNA sensor RIG-I. *Cell Host Microbe* **5**, 439-49.
6. Osiak, A., Utermohlen, O., Niendorf, S., Horak, I. & Knobloch, K. P. (2005). ISG15, an interferon-stimulated ubiquitin-like protein, is not essential for STAT1 signaling and responses against vesicular stomatitis and lymphocytic choriomeningitis virus. *Mol Cell Biol* **25**, 6338-45.
7. Kim, K. I., Yan, M., Malakhova, O., Luo, J. K., Shen, M. F., Zou, W., de la Torre, J. C. & Zhang, D. E. (2006). Ube1L and protein ISGylation are not essential for alpha/beta interferon signaling. *Mol Cell Biol* **26**, 472-9.
8. Sanyal, S., Ashour, J., Maruyama, T., Altenburg, A. F., Cragolini, J. J., Bilate, A., Avalos, A. M., Kundrat, L., Garcia-Sastre, A. & Ploegh, H. L. (2013). Type I interferon imposes a TSG101/ISG15 checkpoint at the Golgi for glycoprotein trafficking during influenza virus infection. *Cell Host Microbe* **14**, 510-21.
9. Malakhova, O. A. & Zhang, D. E. (2008). ISG15 inhibits Nedd4 ubiquitin E3 activity and enhances the innate antiviral response. *J Biol Chem* **283**, 8783-7.
10. Okumura, A., Pitha, P. M. & Harty, R. N. (2008). ISG15 inhibits Ebola VP40 VLP budding in an L-domain-dependent manner by blocking Nedd4 ligase activity. *Proc Natl Acad Sci U S A* **105**, 3974-9.
11. Pincetic, A., Kuang, Z., Seo, E. J. & Leis, J. (2010). The interferon-induced gene ISG15 blocks retrovirus release from cells late in the budding process. *J Virol* **84**, 4725-36.
12. Okumura, A., Lu, G., Pitha-Rowe, I. & Pitha, P. M. (2006). Innate antiviral response targets HIV-1 release by the induction of ubiquitin-like protein ISG15. *Proc Natl Acad Sci U S A* **103**, 1440-5.
13. Monticelli, L. A., Sonnenberg, G. F., Abt, M. C., Alenghat, T., Ziegler, C. G., Doering, T. A., Angelosanto, J. M., Laidlaw, B. J., Yang, C. Y., Sathaliyawala, T., Kubota, M., Turner, D., Diamond, J. M., Goldrath, A. W., Farber, D. L., Collman, R. G., Wherry, E. J. & Artis, D. (2011). Innate lymphoid cells promote lung-tissue homeostasis after infection with influenza virus. *Nat Immunol* **12**, 1045-54.
14. Pelzer, C. & Groettrup, M. (2010). FAT10 : Activated by UBA6 and Functioning in Protein Degradation. *Subcell Biochem* **54**, 238-46.

15. Cnaan, A., Yu, X., Booth, C. J., Lian, J., Lazar, I., Gamfi, S. L., Castille, K., Kohya, N., Nakayama, Y., Liu, Y. C., Eynon, E., Flavell, R. & Weissman, S. M. (2006). FAT10/diubiquitin-like protein-deficient mice exhibit minimal phenotypic differences. *Mol Cell Biol* **26**, 5180-9.
16. Cnaan, A., DeFuria, J., Perelman, E., Schultz, V., Seay, M., Tuck, D., Flavell, R. A., Snyder, M. P., Obin, M. S. & Weissman, S. M. (2014). Extended lifespan and reduced adiposity in mice lacking the FAT10 gene. *Proc Natl Acad Sci U S A* **111**, 5313-8.
17. Maragno, A. L., Pironin, M., Alcalde, H., Cong, X., Knobloch, K. P., Tangy, F., Zhang, D. E., Ghysdael, J. & Quang, C. T. (2011). ISG15 modulates development of the erythroid lineage. *PLoS One* **6**, e26068.
18. Austin, K. J., Bany, B. M., Belden, E. L., Rempel, L. A., Cross, J. C. & Hansen, T. R. (2003). Interferon-stimulated gene-15 (Isg15) expression is up-regulated in the mouse uterus in response to the implanting conceptus. *Endocrinology* **144**, 3107-13.
19. Andersen, J. B. & Hassel, B. A. (2006). The interferon regulated ubiquitin-like protein, ISG15, in tumorigenesis: friend or foe? *Cytokine Growth Factor Rev* **17**, 411-21.
20. Giannakopoulos, N. V., Luo, J. K., Papov, V., Zou, W., Lenschow, D. J., Jacobs, B. S., Borden, E. C., Li, J., Virgin, H. W. & Zhang, D. E. (2005). Proteomic identification of proteins conjugated to ISG15 in mouse and human cells. *Biochem Biophys Res Commun* **336**, 496-506.
21. Lenschow, D. J., Giannakopoulos, N. V., Gunn, L. J., Johnston, C., O'Guin, A. K., Schmidt, R. E., Levine, B. & Virgin, H. W. t. (2005). Identification of interferon-stimulated gene 15 as an antiviral molecule during Sindbis virus infection in vivo. *J Virol* **79**, 13974-83.
22. Oudshoorn, D., van Boheemen, S., Sanchez-Aparicio, M. T., Rajsbaum, R., Garcia-Sastre, A. & Versteeg, G. A. (2012). HERC6 is the main E3 ligase for global ISG15 conjugation in mouse cells. *PLoS One* **7**, e29870.